Gas Transport in Porous Media: The Dusty-Gas Model

E.A. MASON
Brown University, Providence, Rhode Island, U.S.A.

and

A.P. MALINAUSKAS
Oak Ridge National Laboratory, Oak Ridge, Tennessee, U.S.A.

ELSEVIER – Amsterdam – Oxford – New York 1983

CONTENTS

Page

Chapter I.

INTRODUCTION AND HISTORICAL BACKGROUND

The primary purpose of this monograph is to give a detailed presentation of a theory that had been developed to describe the transport of gases through porous media. This theory is often known as the "dusty-gas model," because the porous medium is treated as one component of the gas mixture, consisting of giant molecules held fixed in space, and the highly developed kinetic theory of gases is applied to this supermixture. The physical picture involved is both simple and appealing — so much so that the model has been invented independently at least four times, starting with James Clerk Maxwell in 1860 [M25]. However, it is only in recent years that the consequences and ramifications of the model have been worked out in sufficient detail to constitute a comprehensive and consistent body of theory. This theory is now mature and developed enough to be a useful tool for engineers. It has, in fact, already been used to some extent for modeling chemical reactions in porous catalysts, as has been reviewed in a monograph by Jackson [J1]. Nevertheless, the theory does not seem to be widely known among engineers, probably because much of it has been published in journals primarily devoted to physics or physical chemistry. Furthermore, the language of kinetic theory used in the basic papers is not always familiar to engineers.

That diffusion can be an important limitation of reactivity in porous catalysts has been recognized for a long time [S1, S8, S19, T3, W4], so that one area of application of the dusty-gas model to engineering problems is fairly obvious. It is less obvious that the model has a much wider scope than just gas transport in porous media. Two examples may be mentioned at this point. First, if the forces holding the giant molecules ("dust") fixed in space are removed, so that these giant molecules are free to move in the gas, the result is an aerosol system. Thus a small change in the dusty-gas equations converts them from a description of gas transport in a porous medium to a description of aerosol motion in nonuniform gas mixtures. Put another way, in one case we rest on the particles and account for the motion of the gas, and in the other case, we sit out in the gas and account for the motion of the particles. It

is thus not so surprising that the two cases can be described by similar sets of equations.

As a second example, the model can be applied to transport in membranes by regarding the gas mixture as a solution, and the porous medium as a membrane. The model then serves as a test and a diagnostic probe of supposedly very general phenomenological theories of transport in membranes. Any difficulties or deficiencies identified in this way are usually easily remedied, either by modifying the original phenomenological equations, or by replacing specifically gas-like terms of the dusty-gas equations with terms appropriate for arbitrary fluids (e.g., partial pressures are replaced by activities). Ultimately, one may hope to learn enough about the crucial points of the problem to construct a general statistical-mechanical theory that is valid for general fluids and not just perfect gases.

The scope of this monograph is limited to a description of the dusty-gas model, with emphasis on its application to gas transport in porous media. In addition, a brief discussion of its applications in other fields is presented, and some indication of specific applications in chemical engineering is given. However, we do not try to give a complete survey of the subject of gas transport in porous media and its applications in chemical engineering; but a number of books and review articles are already available for the reader who seeks such a survey [B2, B3, C1, D12, H7, J1, S1, Y1].

In the remainder of this chapter, we present a brief review of the historical background of the dusty-gas model. The model has had an unusually long history, and its origins are intertwined with the origins of the kinetic theory of gases itself. Many crucial points, both experimental and theoretical, have been elucidated, then forgotten or misunderstood, and later rediscovered independently. In Chapter II, a systematic critical account of the theory behind the model is given, beginning with simple momentum-transfer arguments, and then proceeding to the full machinery of modern gas kinetic theory. The chapter is concluded with a summary of the final transport equations developed from the model. Chapter III is devoted to a selection of experimental tests of the model as applied to gas transport, whereas in Chapter IV it is shown how the fundamental ideas behind the model can be used to develop extensions and generalizations of the results for porous media; four examples are given — slip and creep phenomena exhibited by gases over solid surfaces, radiometer effects, aerosol motion, and membrane transport. Finally, some specific applications to chemical engineering are mentioned in Chapter V.

In retrospect, the history of gas transport in porous media can be somewhat artificially arranged into an apparently logical sequence, and can even be divided into two parts, an experimental part and a theoretical part.

On the experimental side, serious study of gas transport of any kind can reasonably be said to date from the first work of Thomas Graham, who, in 1829, studied the diffusion of various gases from a closed vessel through a small tube into the surrounding air [G2]. No diffusion coefficient values were obtained from those measurements at the time, for such coefficients were not to be defined until 26 years later, when Adolf Fick [F4] formulated his mathematical statement of the law of diffusion by analogy with Fourier's law of heat conduction. After his first work, Graham's interest in gaseous diffusion took a rather different turn, prompted by some observations by Doebereiner of the escape of hydrogen through a slight crack in a jar immersed in a pneumatic trough. The water in the trough rose into the jar, showing that hydrogen escaped faster through the crack than the air could enter. This observation prompted Graham to devise an experiment which utilized a calibrated glass tube with a porous plate at one end and with the other end immersed in a vessel of water (or mercury). The gas to be investigated was added to the tube by the displacement of water, and its volume noted. As the gas diffused out, and the air diffused in, through the porous plate, the water level tended to rise or fall in the tube, depending on whether the gas was lighter or heavier than air. Since a change in the water level would have caused a pressure difference across the porous plate, Graham kept the pressure uniform by flowing water into or out of the outer vessel to keep the water level the same as the level inside the tube. After some time, all of the gas had diffused out and had been replaced by the air that had diffused into the tube. Graham noticed that the ratio of the volume of gas that diffused out of the tube to the volume of air that diffused into it was equal to the ratio of the square root of the density (or molecular weight) of air to that of the gas. These investigations were reported in a paper read before the Royal Society of Edinburgh in 1831, and later published in three sections [G3]. It should be noted that these experiments were not carried out in the free-molecule regime; the free-molecule result is called effusion, which was also discovered by Graham, but not until about 13 years later [G4]. The statement of these diffusion results has been enshrined for many years in textbooks as "Graham's Law of Diffusion," which has been sadly misunderstood [M11, M16]. If Graham's diffusion work had been correctly remembered and understood, much effort and confusion over diffusion in porous media in recent years might have been avoided.

The reason that Graham's law of diffusion was misunderstood was that later workers lost sight of the crucial importance of keeping the pressure strictly constant during the course of the experiment. Almost all diffusion experiments were later performed in a closed container, so that a pressure difference developed within the container until the amounts of gas moving in the opposing directions became equal, to avoid a continual increase in pressure on one side of the container. This type of experiment was popularized by Loschmidt in 1870 [L7, L8], using an apparatus based on an earlier design by Graham [G6]. The pressure gradient in such an apparatus is almost immeasurably small, except in capillary tubes, but its consequences are significant. Loschmidt and subsequent workers assumed that Graham's law of diffusion was applicable to such closed-vessel experiments, and mistakenly concluded that the amounts of gases transferred in a true uniform-pressure Graham experiment should be in the ratio of the diffusion coefficients as measured in Loschmidt-type experiments. Such a result holds only within deviations of about 20%, whereas the true diffusion law holds within 1 or 2%. Graham's diffusion law thus became relegated to the scrapheap of results that are of historical interest but which are only crude approximations. Even the noted chemistry historian J. R. Partington fell victim to this misconception [P1].

In contrast, Graham's law of effusion [G4, G6] has been remembered very well, probably because its explanation is simple, and the conditions for its validity are obvious, namely, that the mean free paths of the gas molecules must be much larger than the diameter of the hole or pore through which the gas moves. In this case, it is clear that the rate of transport of the gas is proportional to the mean molecular speed, and therefore inversely proportional to the square root of the molecular mass. The diffusion law gives the same final result, but for a different and more subtle reason — here the rate of transport is inversely proportional to the mean molecular absolute momentum. It is ironic that the experiments Graham performed in establishing his effusion law probaby did not fulfill the conditions for free-molecule flow. A study of the original papers [G4, G6] by Jackson [J1] indicated that Graham probably operated in the continuum or hydrodynamic regime. Of course, Graham had no reliable way of estimating the magnitude of a mean free path, and such an estimate did not appear until 1866 [L6], several years after Graham's work was completed. A real experimental test of the effusion law did not occur until the work of Knudsen, over 40 years later [K5]. The reason for Graham's observation of a square-root dependence on mass is a purely mechanical one, not directly related to molecular behavior at all. Under suitable conditions, a

unit volume of fluid discharged from an orifice will have its potential energy, due to the pressure difference, converted almost completely into kinetic energy of flow, $(1/2)\rho V^2$; since the rate of flow is proportional to the flow speed V, it will be inversely proportional to the square root of the density ρ or molecular weight for a fixed pressure difference. This hydrodynamic result is the basis of a device for the determination of gas densities, known as a Bunsen effusiometer [M20]. However, the potential energy can be distributed in other ways, particularly among molecular internal degrees of freedom, and the results therefore will depend also on the specific heat and other quantities. Effusiometers are therefore no longer considered to be very reliable [N1].

The effusion results change markedly if the orifice is replaced by a long tube. Graham called the resulting gas flow phenomenon transpiration [G5], but it is now known as laminar viscous flow. Since the viscosity of a gas does not depend in any simple way on its molecular weight or density, Graham was not able to draw any simple conclusions about transpiration. A detailed kinetic theory, such as Maxwell worked out, was required to explain this kind of phenomenon. Graham did, however, make two experimental observations of great interest, although one of them was not recognized until much later [M12]. His observations showed that gas viscosity was independent of pressure, a result that went unnoticed at the time. He also observed that the addition of a moderate amount of a light gas to a heavy viscous gas increased, rather than decreased, the viscosity. Both of these results are readily accounted for by kinetic theory. In retrospect, they should have provided more impressive evidence for the correctness of the theory than they actually did [M12].

Although experiments on gas flow and diffusion through porous media continued at a fairly steady pace through the first half of the twentieth century [B2, C1, W5, W7, W8, W10], no particularly striking advances occurred until 1953, when Hoogschagen carried out some uniform-pressure experiments in a flow system, and measured both diffusion flows separately [H12, H13]. This sort of experiment had been done before, but it was apparently assumed erroneously that the molar flow rates would be equal and opposite, as they are in a closed-vessel experiment. Hoogschagen of course immediately rediscovered Graham's law of diffusion, but was puzzled because the correct diffusion law had been forgotten and only the effusion law remembered. Thus it seemed that the square-root law would only be found in the free-molecule region, and Hoogschagen was certain that his experiments were far from this regime. He proposed a simple momentum-transfer argument to rationalize his results, essentially along the lines of the discussion in Section A of Chapter II.

There was a short lull of a few years, and then the square-root law was independently rediscovered by a number of experimenters at about the same time [E4, R5, S5, W9]. The square-root law in the continuum regime was still considered puzzling, especially since a simple argument based on fluid dynamics indicated that the flow rate ratio in free space should vary inversely as the first power of the mass ratio, rather than as the square root [D13, E5, M29]. A flurry of theoretical work was thus initiated [D13, E5, E6, H8, M21, S6, S7, W9], and a reasonable consensus seemed eventually to be reached on a suitable set of flow equations [G8, M22]. Still, no one had recognized Graham's law of diffusion! This recognition occurred only after the problem was essentially solved, and by then was mainly of historical interest [M11, M16]. Earlier recognition might have saved a lot of concern and effort.

The importance of Graham's law of diffusion is not in what it says about diffusion coefficients (it says nothing), but in its bearing on the coupling between diffusion and flow, as will be elaborated in the next chapter. If the phenomena are divided, as Graham did, into uniform-pressure diffusion, effusion, and transpiration, they have a simple additive behavior to an excellent approximation [M15]. However, division by some other scheme (e.g., Loschmidt's equal countercurrent diffusion) spoils the simple additivity, and the problem of describing general simultaneous diffusion and flow becomes very complicated in the transition region between free-molecule and continuum behavior. Although Graham obtained no diffusion coefficients, his diffusion-tube experiment at uniform pressure can be used to determine the effective diffusion coefficient of a gas pair in a porous system, by observation of the rate of rise or fall of the water level. This is a very simple and convenient way of obtaining information concerning the internal geometries of porous media [E3].

On the theoretical side, we note that the dusty-gas model was apparently first invented by Maxwell in 1860, in connection with a discussion of Graham's law of diffusion [M25]. He obtained no definite result with this model, and its discussion occupies only a short space in a much longer paper in which Maxwell developed a theory of transport phenomena in gases by momentum-transfer and mean-free-path methods. The momentum-transfer method was independently applied to diffusion phenomena by Stefan in 1871–72 [S16, S17], with substantial success, but Maxwell was apparently not too happy with the method, "...which led me into great confusion, especially in treating of the diffusion of gases" [M27]. He preferred a more rigorous mathematical approach based on his equations of transfer [M26], which led eventually to the Chapman-Enskog gas

kinetic theory [C6, C7, M26]. This approach, although rigorous and ultimately immensely fruitful, unfortunately completely abandoned porous media.

Maxwell's suspicion of simple arguments in kinetic theory was in fact well founded. Such arguments, although they can supply vivid physical descriptions of the processes involved, can be quite tricky and can lead to erroneous results, sometimes of a very subtle and well-concealed nature. The history of kinetic theory has so many examples of this type that most workers would probably agree with the remark of H. A. Kramers [K6] about "...those unimprovable speculations of which the kinetic theory of gases affords such ghastly examples."

The momentum-transfer approach was neglected for many years, and then apparently rediscovered by Frankel [F5] and by Present and deBethune [P4], among others. It was used quite extensively during World War II in developing the theory of isotope separation by the gaseous diffusion process [P3]. Incidentally, Graham devised this same method for separating gas mixtures (obviously not isotopes, which were then unknown) by diffusion through a porous barrier. He called the method "atmolysis" [G6], but this had probably been forgotten by World War II.

Following Maxwell's brief use of the dusty-gas model, it was completely forgotten for nearly a century. It was independently re-invented in 1957 by Deriagin (also spelled Derjaguin and Deryagin) and Bakanov [D8, D9], who used it to calculate the flow of a single gas through a porous medium near the free-molecule region. No application to diffusion was made, and their treatment made no provision for viscous flow, so that it was valid only for very porous solids at very low pressures. Their calculations were quite complicated because of their detailed treatment of the gas-dust collisions, but they nevertheless succeeded in giving a good theoretical rationale for a minimum which is often observed in the permeability coefficient as a function of gas pressure. The model was shortly thereafter independently re-invented once more by Evans, Watson, and Mason [E5], who avoided the complicated part of the problem, namely the explicit calculation of parameters depending on the structure of the porous medium, and used the model only to determine the proper flow equations. By formal variation of the mole fraction of the "dust" particles, the whole pressure range from the free-molecule to the continuum region could be covered in a unified way. Again, no provision was made for viscous flow, but it was possible to give a quantitative account of diffusion at uniform pressure. Some of these ideas were soon adapted for a treatment of transport in charged membranes [A11], as well as for the more elaborate kinetic

theory treatment [B12, W12] of gas flow and diffusion along the lines indicate by Deriagin and Bakanov [D8, D9]. The most recent independent reinvention of the model seems to have occurred in 1971, as a kinetic theory model for ion movement through biological membranes [M2].

The effect of pressure gradients on diffusion was handled by adding a term involving the pressure gradient to the dusty-gas transport equations [E6]. The coefficient of this term had to be treated empirically, because the dusty-gas model contained no provision for a viscous flow mechanism. Although this procedure gave good agreement with experiments on diffusion in porous graphite it was apparent that something was not quite right, because the full set of transport equations was not completely symmetric with respect to the interchange of the subscripts representing the species [E6]. The generalization to multicomponent mixtures was also not clear. However, a consistent account of thermal transpiration was obtained [M21], where the symmetry problem did not appear because only a single gas in a temperature gradient was involved. A consistent way to include viscous flow was not developed until recourse to fundamental kinetic theory was made [M22], motivated by the desire to include the effects of molecular internal degrees of freedom and the effects of higher kinetic theory approximations. This formulation, with some clarification and elaboration, is the one described in this monograph.

The development of the dusty-gas model as described here did not occur as straightforwardly as the foregoing account might suggest. The original approach to the problem by at least one of the participants was from the point of view of an analogy with the Kirkendall effect in solids, which is a net drift of inert markers placed near a diffusion interface. A similar effect exists in gases [M29, M33]. This had led to the erroneous view, already mentioned, that the diffusion flow ratio at uniform pressure should involve the first power of the mass ratio [M29]. A chance meeting between G. M. Watson and E. A. Mason at a conference in Oak Ridge in 1960 led to a spirited exchange of views, and an arrangement to resolve some of the problems which were identified. It soon became clear from the experimental data [E4, H12, H13] that the square-root law was correct, but the reason was unclear. The conventional explanation for effusion was obviously inapplicable, and Hoogschagen's momentum-transfer argument was regarded with suspicion, for reasons related to the comment of Kramers already quoted. The argument did contain an obvious approximation, in which the average of a product of two quantities was taken as the product of the averages. The idea of the dusty-gas model occurred on noticing a lot of terms involving square roots of molecular masses in the

expressions for the force on small particles suspended in a non-uniform gas. This aerosol problem was being considered by the methods of Chapman-Cowling kinetic theory, a problem suggested by Sydney Chapman [M14] after reading a paper by Ludwig Waldmann [W1]. The earlier inventions of the model by Maxwell and by Deriagin and Bakanov were unknown. The latter was pointed out during a visit to the University of Maryland in 1961 by P. C. Carman, who recalled a presentation of the Russian work at a Faraday Society Discussion [B1]. The original work of Maxwell was uncovered in 1969 independently by P. G. Wright and E. A. Mason, who were preparing to attend a Thomas Graham Memorial Symposium at the University of Strathclyde in Glasgow (the centenary of Graham's death). The connection between the Kirkendall effect in gases and the phenomenon of diffusive slip was pointed out in 1961 by J. Kistemaker [K7], after a routine exchange of reprints with E. A. Mason. The marker motion in the Kirkendall effect is, it turns out, completely analogous to the rise or fall of the water level in Graham's uniform-pressure diffusion experiments. The connection of all this activity with Graham's original work was unsuspected by everyone concerned until 1966, when a pedagogical paper [R6] on Graham came to light during a literature survey undertaken in connection with a critical review of gaseous diffusion coefficients [M8]. Although the author of this paper appears to have been just as confused as everyone else as to the meaning of Graham's results, a table of some of Graham's experimental measurements was included in the paper. One look at the accuracy of the square-root law was enough to convince one that the current explanation in terms of Loschmidt diffusion coefficients had to be wrong. There was no recourse but to go back to Graham's original papers, where everything was of course quite clear. (Scientists and engineers are curiously indifferent to the histories of their subjects, and this indifference is sometimes costly.)

Regardless of the convoluted path by which the dusty-gas model was developed, its results now seem sufficiently reliable to be worthy of the attention of engineers.

Chapter II

THEORY

Although this monograph features the dusty-gas model, the essential aspects of the model can be exhibited in a simple way without the necessity of first discussing all the mathematical complexities of the kinetic theory of gases [M15, M18]. The first section of this chapter is therefore devoted to an elementary discussion of gas transport in porous media that sets out these essential features. This elementary discussion may also serve to suggest why many of the results of the dusty-gas model hold in considerable generality, and are not model-specific. In the second section of this chapter, the same major results are obtained, but with a better theoretical pedigree, by means of the dusty-gas model, plus a number of more minor but interesting features that require some of the complexities of kinetic theory for their elucidation. The third section concerns a discussion of the influence of the geometrical structure of the medium on the gas transport; it can be treated as a separate problem in the present methodology. The fourth section summarizes the mathematical relationships that are developed in the previous sections of this chapter.

A. ELEMENTARY ARGUMENTS

This section is divided into four parts: the first is an outline of the procedure and a qualitative statement of the results; the second is a phenomenological description of the modes of gas transport, in mathematical form; then follows a discussion of the way these individual descriptions are coupled together to describe simultaneous transport by more than one mode or mechanism; finally, the generalization to multicomponent mixtures is discussed.

1. General Procedure

The most important aspect of the theory is the statement that gas transport through porous media (or tubes) can be divided into three **independent** modes or mechanisms, as follows:

(1) Free-molecule or Knudsen flow, in which the gas density is so low that collisions between molecules can be ignored compared to collisions of molecules with the walls of the porous medium or tube.

(2) Viscous flow, in which the gas acts as a continuum fluid driven by a pressure gradient, and molecule-molecule collisions dominate over molecule-wall collisions. This is sometimes called convective or bulk flow.

(3) Continuum diffusion, in which the different species of a mixture move relative to each other under the influence of concentration gradients (concentration diffusion), temperature gradients (thermal diffusion), or external forces (forced diffusion). Here molecule-molecule collisions again dominate over molecule-wall collisions.

This classification obviously neglects one mode of transport that is sometimes important in practice, namely

(4) Surface flow or diffusion, in which molecules move along a solid surface in an adsorbed layer. This motion will be assumed to be independent of the preceding three modes of motion. We shall not be primarily concerned with this mechanism, but will later indicate how it can be incorporated into the computational scheme.

Justifications for the validity of the above classification scheme, especially the independence of the modes of transport, will be discussed later. At this stage we can regard it as an empirical assumption based on a number of experimental studies going back to Thomas Graham [G3 — G6].

Transport coefficients correspond to each of the above transport mechanisms: the Knudsen diffusion coefficient D_{iK} (for species i), the viscosity coefficient η, the ordinary diffusion coefficient $\mathcal{D}_{ij}$ for continuum concentration diffusion and forced diffusion (for a binary mixture of species i and j), an analogous thermal diffusion factor α_{ij} for continuum thermal diffusion, and a surface diffusion coefficient D_{iS}. These transport modes can occur in all sorts of combinations, and the problem for theory is to discover how to combine the individual mathematical descriptions in a unified way. For example, the combination of viscous flow and free-molecule flow leads to the phenomenon of slip flow, involving the slipping of a gas over a solid surface. Another combination is that between continuum concentration diffusion and viscous flow, which gives rise to another surface slip phenomenon known as diffusive slip. Many other combinations give rise to well-known phenomena such as the diffusion baroeffect, thermal transpiration, thermal creep, and so on. In this section of the chapter, we will give simple arguments for the

method of combining the different transport mechanisms; later on we will present more elaborate kinetic-theory justifications for the method. But at this point we just state the results in the form of a simple electrical analogy.

The electrical analogy [M15] for combined modes of transport, which should be regarded as only a mnemonic device and not a basis for physical interpretation of transport coefficients, is shown in Fig. 1. Diffusive flows are combined like resistors in series, where voltage drops are additive, and the resultant total diffusive flow is then combined with the viscous flow and the surface flow like resistors in parallel, where currents are additive. This recipe applies locally around each point or small region in the system, and yields a general set of differential equations for the transport of all the species in the mixture in terms of the gradients of pressure, concentration, and temperature. In real applications it is usually necessary to integrate these differential equations, which means that boundary conditions must be specified. It is at this point that the question of the geometrical structure of the medium in which the transport is occurring first arises. It is remarkable that this question arises so late in the problem, and in fact one of the chief virtues of the present approach is that it avoids the geometrical-structural question until nearly the end, when it can be handled separately. A straightforward approach to combined convective flow and diffusion in porous media along classical lines would appear to involve the structure of the medium from the beginning, as will be discussed later, and would probably be impossibly complex.

In the present formulation, the structure of the medium is absorbed into the values of the transport coefficients or into simple constants of proportionality. Corresponding to the three main transport mechanisms are three parameters characteristic of the medium: the Knudsen flow parameter K_o, the viscous flow parameter B_o, and the porosity-tortuosity factor ε/q for continuum diffusion. These parameters are all simply related for a medium of simple geometry, such as a long circular capillary of radius r,

$$K_o = r/2, \qquad B_o = r^2/8, \qquad \varepsilon/q = 1 . \tag{1}$$

But for an actual porous medium the relationships are complicated and usually unknown, and the three parameters are most often found from experiment rather than by calculation from some assumed geometry. Similarly, the surface diffusion coefficients D_{is} are usually determined experimentally.

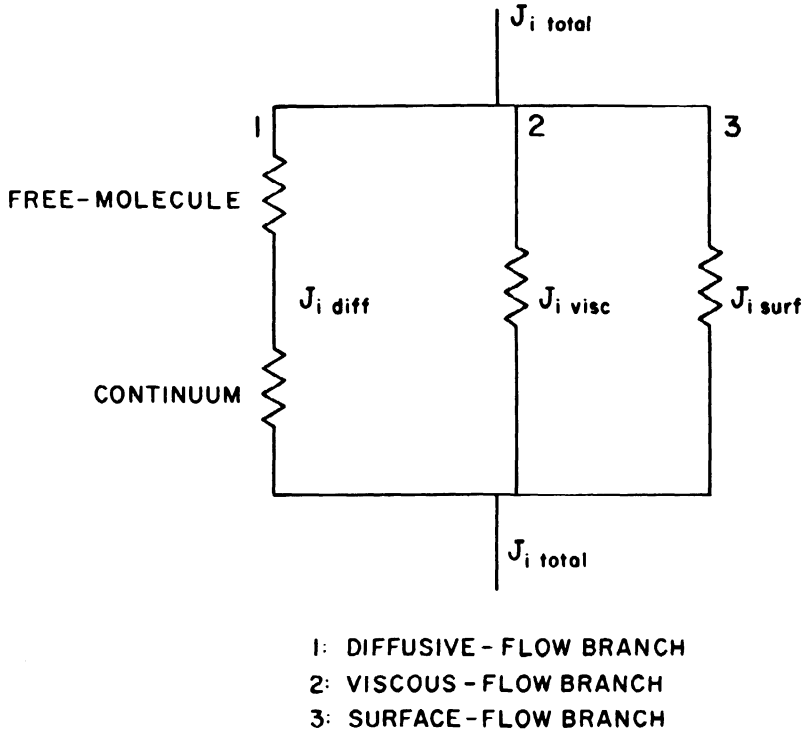

Fig. 1. Electrical analogue circuit as a mnemonic device for combining different transport mechanisms. Diffusive fluxes combine in series (analogue of voltage drops), and the total diffusive flux then combines in parallel with the viscous flux and surface flux (analogue of currents). This applies locally around each point in the system.

If the medium is homoporous, the coefficients in the differential equations describing the transport do not vary with position (except for their universal dependence on pressure, temperature, and composition). Integration of the differential equations is then a relatively straightforward problem, although sometimes a complicated one. If, however, the medium is heteroporous, the coefficients in the differential equations are different in different regions of space because the medium is, and the integration problem becomes more difficult. One straightforward approach is to divide the medium into homoporous

segments, integrate the differential equations in each segment, and then match solutions at the segment boundaries. This approach can lead to very complicated mathematical manipulations, but it is sometimes necessary (e.g., if the pore size distribution is strongly bimodal). What is surprising, however, is how successful it often is to treat a heteroporous medium as an equivalent homoporous one with average values of K_o, B_o, and ϵ/q. This simple approximation was the one adopted for most of the original work on the dusty-gas model. In Section C we will present some results on model calculations for heteroporous media that account for the success of the equivalent homoporous medium approximation. It is also possible to establish some bounds for the errors involved in this approximation.

A point we wish to emphasize here is that the dusty-gas model is not restricted to the use of the equivalent homoporous medium approximation, even though this approximation has been used for most of the illustrative examples. In the dusty-gas model, the geometrical-structural problem is an independent one, and can be made as simple or as complicated as necessary. In much of the engineering literature there has been a tendency to regard the homoporous approximation as an inherent characteristic of the dusty-gas model; this is an unnecessary restriction.

2. Modes of Gas Transport

a. Free-Molecule or Knudsen Flow. The original studies of free-molecule flow were limited to small holes in very thin plates. This assured that the molecules made no collisions with each other during their passage through the hole, which we now know is the important criterion. When this criterion is met, molecules of different species move entirely independently of each other, and there is no fundamental distinction between flow and diffusion, as there is in the continuum regime. Moreover, the flux (i.e., the rate of flow per unit area normal to the flow) of molecules of any species through any kind of hole is equal to the number of molecules of that species passing into the entrance of the hole per unit area per unit time multiplied by the probability that a molecule that enters the hole will eventually get all the way through and not bounce back out the entrance. This probability depends only on the geometry of the hole and the law of reflection for molecules hitting the inner walls of the hole. Such free-molecule flow was studied in considerable detail around 1907–08 by Knudsen [K5], and is now often called Knudsen flow.

If there is a gas with a molecular density of n molecules/cm^3 at one end of the hole and a vacuum at the other, the free-molecule or Knudsen flux J_K is

$$J_K = wn\bar{v} \ , \tag{2}$$

where J_K has units of molecules/cm^2-sec, w is a dimensionless probability factor, and $\bar{v}$ is the mean molecular speed,

$$\bar{v} = (8k_BT/\pi m)^{1/2} \ , \tag{3}$$

k_B being Boltzmann's constant, T the absolute temperature, and m the molecular mass. For an infinitesimally thin orifice, w = 1/4, and for a long straight circular tube of radius r and length L (L >> r), from whose surface the molecules rebound diffusely, the value of w is (2/3)(r/L). If there is a gas mixture instead of a single gas, each species acts independently, and the total flow is a sum of terms like Eq. (2),

$$J_K = \sum_i w_i n_i \bar{v}_i \ , \tag{4}$$

where i denotes the particular gas species.

For gas on both sides of the hole, the net flux is proportional to the difference in gas number densities at the two ends. It is customary to write this relation in differential form and thereby define a Knudsen diffusion coefficient D_{iK} having units of cm^2/sec,

$$\underset{\sim}{J}_{iK} = - D_{iK} \underset{\sim}{\nabla} n_i \ , \tag{5}$$

for species i. The minus sign is a convention adopted so that the gas moves "down" the gradient when D_{iK} is positive. Comparing Eq. (5) with Eq. (2), we see that D_{iK} is proportional to the mean molecular speed $\bar{v}$. It is customary to make this proportionality explicit by defining a **Knudsen flow parameter** or **permeability coefficient** K_o by

$$D_{iK} = (4/3) K_o \bar{v}_i \ . \tag{6}$$

The value of K_o depends only on the geometry of the hole and the gas-surface scattering law. It can be calculated for a porous medium if the geometry and scattering law are known, but this is usually a formidable mathematical task. For a long, straight, circular tube of radius r with diffuse scattering, the value of K_o is r/2. It is usually much easier to measure K_o

experimentally than to calculate it from the geometry (which in fact is seldom known with any precision). From Eq. (6) it is evident that D_{iK} is independent of pressure and increases with temperature as $T^{1/2}$. Note also that D_{iK} has units of cm^2/sec and K_o has units of cm.

The case of two different gases at the same pressure on the two sides of the hole is an interesting simple case. From Eqs. (5) and (6) we find

$$-\underset{\sim}{J}_{1K}/\underset{\sim}{J}_{2K} = D_{1K}/D_{2K} = \bar{v}_1/\bar{v}_2 = (m_2/m_1)^{1/2} \quad , \tag{7}$$

provided that K_o is the same for both gases (same surface scattering law). This is Graham's law of effusion.

For a multicomponent mixture we can combine Eq. (5) for all the components to give one equation involving the gradient of the total density.

$$\sum_i (\underset{\sim}{J}_{iK}/D_{ik}) = -\underset{\sim}{\nabla} n \quad , \tag{8}$$

$$n = \sum_i n_i \quad . \tag{9}$$

If the total presure is uniform, $\underset{\sim}{\nabla} n = 0$, and if K_o is the same for all species, Eq. (8) reduces to

$$\sum_i m_i^{1/2} \underset{\sim}{J}_i = 0 \quad , \tag{10}$$

which is the multicomponent generalization of Graham's law of effusion.

The foregoing results are exact, provided that the molecules act independently of each other.

b. Viscous Flow. By viscous flow we mean that portion of the gas flow in the continuum region that is caused by a pressure gradient. We are ignoring the inertial terms in the equation of motion for the fluid, and turbulence is obviously not included in the present treatment; strictly speaking, we treat only so-called "creeping flow." The behavior of the gas is thus described by the coefficient of viscosity, which for gases is independent of pressure. Moreover, a mixture behaves the same as a single gas, because such bulk flow has no tendency to cause a mixture to separate into its components.

The computation of the viscous flux for gases is carried out exactly as in the case of liquids to obtain Poiseuille's law, but remembering that a gas is compressible. The basic idea of the calculation is simple: if the gas is not accelerating, the net force on any element of it must be zero, so that the viscous-drag force just balances the force due to the pressure difference across the element. The result has the plausible form

$$\underset{\sim}{J}_{visc} = \text{Flow/Area} = -(nB_o/\eta)\,\underset{\sim}{\nabla} p \,, \tag{11}$$

where $\underset{\sim}{J}_{visc}$ is the viscous flux in molecules/cm^2-sec; n is the total number density; B_o, the viscous flow parameter, is a constant characteristic of the hole geometry having units of cm^2; η is the coefficient of viscosity of the gas in g/cm-sec; and p is the pressure in dyne/cm^2. The boundary condition for continuum flow is that the gas velocity is zero at the side walls. Any "slip flow" at the walls is to be regarded as a free-molecule component of the flow. The compressibility enters through the equation of state, $n = p/k_BT$, making the coefficient of ∇p in Eq. (11) dependent upon position through its dependence on p.

The value of B_o is $r^2/8$ for a long, straight, circular capillary of radius r, and Eq. (11) leads to Poiseuille's law on integration. For a porous medium or a bed of packed particles it is usually much easier to determine B_o experimentally than to calculate it from geometrical considerations, just as was the case for K_o, and to regard Eq. (11) as an empirical result like Darcy's law.

For mixtures, the viscous flux of species i is proportional to its mole fraction x_i in the mixture, since the flow is nonseparative,

$$\underset{\sim}{J}_{i\ visc} = x_i\,\underset{\sim}{J}_{visc} \,. \tag{12}$$

A simple and remarkable result of even elementary kinetic theory is that the viscosity coefficient η is independent of gas pressure at constant temperature [C9]. The physical reason is simple. According to the kinetic picture of gas behavior, viscosity is caused by the exchange of momentum between planes moving at different speeds. This momentum is carried by the molecules themselves, and so the transport is directly proportional to the number density. However, the momentum transport is impeded by collisions, and the number of molecules impeding transport by "being in the way" is also proportional to number density. The two effects exactly cancel, and η is independent of p.

This elementary argument gives essentially an exact result because only the counting of collisions is involved, and not the nature of the collisions. The sole condition is that only binary molecular collisions are important; the viscosity becomes density dependent when the density becomes large enough for ternary and higher collisions to matter. This result obviously also holds for mixtures, as long as the relative composition remains fixed.

c. Continuum, or Ordinary, Diffusion. Diffusion is the most difficult of the three main transport mechanisms to define satisfactorily. To keep the discussion simple at this point, we ignore temperature gradients and external forces; even so, a difficulty still remains. It is most convenient to define a diffusion coefficient for a mixture in which the net flux is zero, and in which there is no pressure gradient so that there is no viscous flow and no pressure diffusion. In this case the purely diffusive fluxes $\underset{\sim}{J}_{1D}$ and $\underset{\sim}{J}_{2D}$ of a binary mixture are

$$\underset{\sim}{J}_{1D} = - \mathfrak{D}_{12} \underset{\sim}{\nabla} n_1 \ , \tag{13a}$$

$$\underset{\sim}{J}_{2D} = - \mathfrak{D}_{21} \underset{\sim}{\nabla} n_2 \ , \tag{13b}$$

where the ordinary diffusion coefficients $\mathfrak{D}_{12}$ and $\mathfrak{D}_{21}$ are in cm^2/sec. It is easy to see that $\mathfrak{D}_{12} = \mathfrak{D}_{21}$, because $\underset{\sim}{J}_{1D} + \underset{\sim}{J}_{2D} = \underset{\sim}{J}_D = 0$ for no net flux, and $\underset{\sim}{\nabla}(n_1 + n_2) = \underset{\sim}{\nabla} n = 0$ for no pressure gradient. Unfortunately, such a situation is very difficult to produce experimentally, because a small pressure gradient is necessary to keep $\underset{\sim}{J}_D = 0$. This can be understood in a simple physical way as follows. Suppose we put two different gases at the same temperature and pressure into communication through a small tube (or a porous plate), as indicated in Fig. 2. The faster, light molecules tend to get through the tube more quickly than the slower, heavy ones, so that the pressure rises on the side of the heavy gas until the viscous flow induced back through the tube is just sufficient to make the net flux zero. The resulting steady-state pressure difference is very small if the tube has a large diameter, but can be appreciable for small capillaries or fine porous media. Thus, Eqs. (13) can be used only for equal countercurrent diffusion in large tubes.

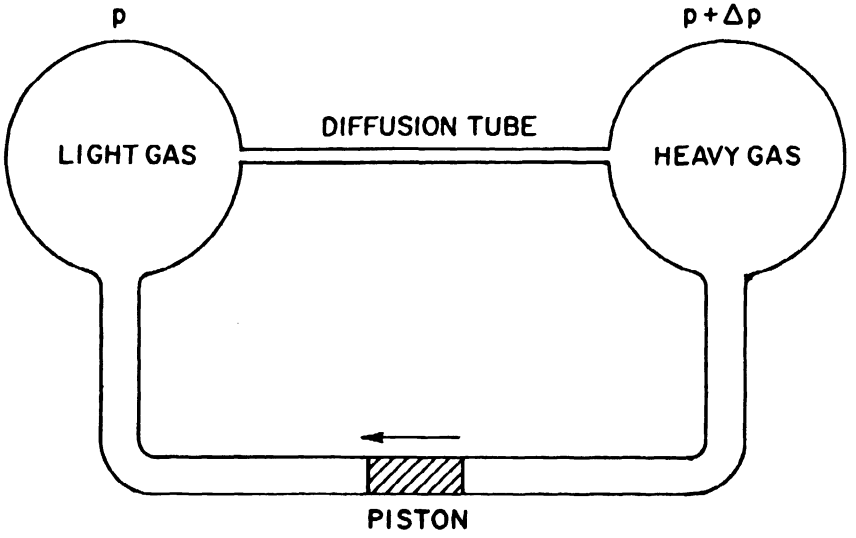

Fig. 2. Binary diffusion. If the piston is held stationary, a pressure difference develops that is just sufficient to keep the net flux zero through the diffusion tube. If the pressure is kept uniform, the piston must be moved as indicated, and there is a net flow of gas through the diffusion tube.

To keep the pressure uniform during the diffusion, an arrangement like a side tube with an impermeable, frictionless piston would be necessary, as indicated in Fig. 2. Since the piston must be moved to keep the pressure uniform, the net flux of gas is clearly not zero. We can still describe this diffusion by the same diffusion coefficients, $\mathcal{D}_{12}$ and $\mathcal{D}_{21}$, provided we allow for the net diffusive flux by including an extra term that apportions the net flux contribution to each species,

$$\underset{\sim}{J}_{1D} = -\mathcal{D}_{12}\,\underset{\sim}{\nabla} n_1 + x_1 \underset{\sim}{J}_D \,, \tag{14a}$$

$$\underset{\sim}{J}_{2D} = -\mathcal{D}_{21}\,\underset{\sim}{\nabla} n_2 + x_2 \underset{\sim}{J}_D \,, \tag{14b}$$

where $\underset{\sim}{J}_D = \underset{\sim}{J}_{1D} + \underset{\sim}{J}_{2D}$ and $x_i = n_i/n$ is the mole fraction. All the fluxes

are diffusive in this case, because there is no pressure gradient. Another way of considering Eqs. (14) is to stipulate that $\mathscr{D}_{12}$ and $\mathscr{D}_{21}$ are defined in a coordinate system moving with a velocity corresponding to the average velocity given by $\underset{\sim}{J}_D/n$. It is easy to show that $\mathscr{D}_{12} = \mathscr{D}_{21}$, by adding these two equations and noting that $\nabla n = 0$.

Equations (14) thus define pure diffusive transport in the continuum region; the key point is that the pressure is uniform, so that the viscous transport is zero. To determine the flux when the pressure is nonuniform, we must determine the viscous flux due to the pressure gradient, and then find out how to combine it with the diffusive flux. It turns out that the two fluxes are simply additive to a high degree of approximation, as was indicated in Fig. 1. Because of this simple additivity, diffusion at uniform pressure can be regarded as a more fundamental process than equal countercurrent diffusion. We must also determine how to combine free-molecule and continuum diffusion, in order to cover the whole pressure range of interest. Before considering these questions, however, it is convenient to discuss the pressure dependence of $\mathscr{D}_{12}$.

The argument concerning the pressure dependence of $\mathscr{D}_{12}$ proceeds exactly as did the argument for the pressure dependence of η, but the final results are somewhat different. The diffusive flux is a flux of number or mass, whereas the viscosity was caused by the flux of momentum, but the same arguments apply — the number of carriers and the number of interferers are both proportional to n or p, and the two effects exactly cancel as long as only binary collisions are important. However, $\mathscr{D}_{12}$ is inversely proportional to n or p, not independent like η. The reason for this apparently odd behavior lies in the definition of $\mathscr{D}_{12}$ in Eqs. (13) or (14); the gradient term in these equations is chosen to be ∇n_1, which is directly proportional to p, instead of ∇x_1, which is independent of p. The kinetic-theory argument gives $\underset{\sim}{J}_{1D}$ independent of n or p, so obviously $\mathscr{D}_{12}$ must be inversely proportional to n or p to cancel the dependence in ∇n_1. Thus, the different pressure dependence of η and $\mathscr{D}_{12}$ is the result of an arbitrary choice made for the gradient terms.

The relation between the two fluxes in Eqs. (14a) and (14b) is interesting; it was discovered experimentally [G3] that

$$-\underset{\sim}{J}_{1D}/\underset{\sim}{J}_{2D} = (m_2/m_1)^{1/2} , \qquad (15)$$

provided that the pressure is kept uniform. This is Graham's law of diffusion; it looks like the effusion law of Eq. (7), but it is quite different. Its range of validity does not depend on any special relation between the mean free path and the pore size or tube diameter, so that it holds at all pressures, whereas the effusion law holds only in the free-molecule region. A simple physical explanation for Eq. (15) can be based on a calculation of the momentum transferred to the walls by the diffusing molecules. We briefly repeat the argument here, since the same type of argument can be used to show how continuum diffusion and free-molecule diffusion combine in the transition region, and how to extend Eqs. (14) to multicomponent mixtures. We argue that the net force on the walls must be zero if there is no pressure gradient in the gas, and hence that the total momentum transferred to the walls by all the molecular collisions is zero. We can approximately calculate the average momentum transferred to the wall per unit time by species i as the product of two factors: the average momentum transferred per molecular impact, which is proportional to $m_i \bar{v}_i$, and the excess of molecular impacts in one direction over those in the opposite direction, which is proportional to $\underset{\sim}{J}_{iD}$. The sum over both species must be zero,

$$\underset{\sim}{J}_{1D} m_1 \bar{v}_1 + \underset{\sim}{J}_{2D} m_2 \bar{v}_2 = 0 \ , \tag{16}$$

or

$$- \underset{\sim}{J}_{1D} / \underset{\sim}{J}_{2D} = m_2 \bar{v}_2 / m_1 \bar{v}_1 = (m_2/m_1)^{1/2} \ , \tag{17}$$

on substitution for $\bar{v}$ from Eq. (3). The generalization to any number of components is obviously

$$\sum_i \underset{\sim}{J}_{iD} \, m_i \bar{v}_i = 0 \ , \tag{18}$$

or

$$\sum_i m_i^{1/2} \, \underset{\sim}{J}_{iD} = 0 \ , \tag{19}$$

which is the multicomponent generalization of Graham's law of diffusion.

The similarity and contrast between the effusion law of Eqs. (7) and (10) and the diffusion law of Eqs. (17) and (19) are remarkable. Both yield the same final result, but the effusion law does so because $\underset{\sim}{J}_{iK}$ is directly proportional to the speed $\bar{v}_i$, whereas the diffusion law does so because $\underset{\sim}{J}_{iD}$ is inversely proportional to the momentum $m_i\bar{v}_i$. The accuracies and ranges of validity of the two laws are also quite different. The effusion law is exact provided that the mean free path is much larger than the diameter of the aperture or tube. The diffusion law is, from the above derivation, only approximate, but its range of validity does not depend on any condition regarding the mean free path. The approximation arises from calculating the average of a product as the product of two averages; this happens to be quite accurate in this case, as is demonstrated later with the dusty-gas model.

The same line of argument, that momentum transfers are additive, suffices to give the equations for combined transport and for multicomponent diffusion.

One final detail remains. The foregoing discussion of continuum diffusion is based on the implicit assumption that the geometry of the hole or tube through which diffusion occurs is well known, which is seldom the case for porous media. It is nevertheless found experimentally that diffusion in a porous medium can be described by transport equations of the same form as Eqs. (14), provided $\mathscr{D}_{12}$ is replaced by an effective diffusion coefficient D_{12}, whose value depends on the geometry of the medium. The relation is usually written in the form

$$D_{12} = (\varepsilon/q)\mathscr{D}_{12}, \tag{20}$$

where the constant ε/q is called the porosity-tortuosity factor. This name comes from a simple model in which a porous medium is visualized as a number of tortuous holes through a solid. The free space for diffusion is then only a fraction ε of the total apparent volume of the solid, and each hole is on the average longer by some factor than a straight hole through the solid. Usually ε/q is determined by experiment rather than calculation, just as are K_o and B_o. The approximations embodied in Eq. (20) are apparently satisfactory as long as the porous medium is not too heteroporous (e.g., an extremely bimodal pore-size distribution). Effects of heteroporosity will be considered in Section C of this chapter.

d. Surface Flow or Diffusion. In general, transport of matter in an adsorbed layer can be quite as complicated as transport through the gas

phase. But because surface transport is not our main concern, we shall here indicate only the simplest treatment [F1]. We assume that each species transported along the surface behaves independently of the other species, so that its flux can be taken to be proportional only to its own surface concentration gradient. We also assume that the adsorbed layer does not interact with the gas phase, except to maintain a rapid local adsorption equilibrium for each species. The surface concentration of species i will then be proportional to its gas-phase concentration, and we can write an equation for surface flux as

$$\underset{\sim}{J}_{iS} = -D_{iS} \underset{\sim}{\nabla} n_i \ , \tag{21}$$

where $\underset{\sim}{J}_{iS}$ is the surface flux referred to apparent unit cross-sectional area of the medium, and D_{iS} is a surface diffusion coefficient having units of cm^2/sec. This equation is analogous to Eq. (5) for free-molecule diffusion, as it should be because of our assumption of independent species transport. However, $\underset{\sim}{J}_{iS}$ and $\underset{\sim}{J}_{iK}$ combine differently with the continuum diffusive flux $\underset{\sim}{J}_{iD}$, as indicated in Fig. 1 and discussed in more detail below.

All the complexities of porous medium geometry, surface structure, adsorption equilibrium, etc., are contained in the surface diffusion coefficients, D_{iS}. At best, Eq. (21) would be expected to be useful only at low surface coverages.

3. Combined Transport

Let us consider first how free-molecule and continuum diffusive flows combine, by an extension of the momentum-transfer argument presented earlier. According to Newton's second law of motion, if species i is not accelerated on the average, then the average momentum transferred to it by collisions with the walls and with other species must be balanced by some force. If no external forces like gravity or electrical fields are present, the effective force can be ascribed to the gradient of the partial pressure of the species, $\underset{\sim}{\nabla} p_i$. This force can be considered to be made up of separate contributions, each just sufficient to balance the momentum transfer by wall collisions and by collisions with each of the other species in the mixture. With this picture in mind, we rewrite Eqs. (14) and (5) for species 1 as

$$-(\underset{\sim}{\nabla} p_1)_{molecule} = (k_B T/D_{12})(\underset{\sim}{J}_{1D} - x_1 \underset{\sim}{J}_D) \ , \tag{22}$$

$$-(\nabla p_1)_{wall} = (k_B T/D_{1K})\, \underset{\sim}{J}_{1K} , \tag{23}$$

where we have used Eq. (20) for D_{12} and also $p_1 = n_1 k_B T$. Thus it is the same individual ∇p_1 terms that add; moreover, $\underset{\sim}{J}_{1D}$ and $\underset{\sim}{J}_{1K}$ are really the same, just as the current through two resistors in series is the same. Combining Eqs. (22) and (23) in this way, we obtain

$$-\nabla p_1 = (k_B T/D_{1K})\, \underset{\sim}{J}_{1D} + (k_B T/D_{12})(\underset{\sim}{J}_{1D} - x_1 \underset{\sim}{J}_D) , \tag{24}$$

with a similar equation for species 2. This equation describes the diffusion of one component of a binary mixture (not of a multicomponent mixture) at uniform total pressure throughout the entire pressure range between the free-molecule limit and the continuum limit.

If a gradient of total pressure exists, the viscous fluxes must be added to the diffusive flux. The reason for this simple additivity follows from kinetic theory in that there are no viscous terms in the diffusion equations, and no diffusion terms in the viscous-flow equations; the two are entirely independent in the sense that there are no direct coupling terms in these equations. This independence is really quite general, and holds for any isotropic system, not just for gases. It depends only on the fact that the various flows are proportional to gradients (linear laws), and that quantities of different tensorial character do not couple in the linear approximation in isotropic systems [M22]. This result is sometimes known as Curie's theorem.

Similarly, as shown in Fig. 1, the surface flux must also be added to the diffusive flux. It is harder to justify this result than the additivity of the viscous flow; it is basically more of an ad hoc physical assumption than the result of any more general principle.

Whatever the justifications, we now write

$$\underset{\sim}{J}_1 = \underset{\sim}{J}_{1D} + \underset{\sim}{J}_{1visc} + \underset{\sim}{J}_{1S} = \underset{\sim}{J}_{1D} + x_1 \underset{\sim}{J}_{visc} + \underset{\sim}{J}_{1S} , \tag{25a}$$

$$\underset{\sim}{J}_2 = \underset{\sim}{J}_{2D} + \underset{\sim}{J}_{2visc} + \underset{\sim}{J}_{2S} = \underset{\sim}{J}_{2D} + x_2 \underset{\sim}{J}_{visc} + \underset{\sim}{J}_{2S} , \tag{25b}$$

and the total flux is

$$\underset{\sim}{J} = \underset{\sim}{J}_1 + \underset{\sim}{J}_2 = \underset{\sim}{J}_D + \underset{\sim}{J}_{visc} + \underset{\sim}{J}_S . \tag{26}$$

The viscous flux $\underset{\sim}{J}_{visc}$ is given in terms of ∇p by Eq. (11). These results are to be combined with Eq. (24); the easiest way to do this is to solve for $\underset{\sim}{J}_{1D}$ from Eq. (25a) and $\underset{\sim}{J}_D$ from Eq. (26), and substitute the results into Eq. (24) to yield

$$-\frac{1}{k_B T}\underset{\sim}{\nabla} p_1 = \left(\frac{1}{D_{1K}} + \frac{1}{D_{12}}\right)\underset{\sim}{J}_1 - \frac{x_1}{D_{12}}\underset{\sim}{J} - \frac{x_1}{D_{1K}}\underset{\sim}{J}_{visc}$$

$$- \left(\frac{1}{D_{1K}} + \frac{1}{D_{12}}\right)\underset{\sim}{J}_{1S} + \frac{x_1}{D_{12}}\underset{\sim}{J}_S \,. \qquad (27)$$

Substituting for $\underset{\sim}{J}_{visc}$ from Eq. (11) and for $\underset{\sim}{J}_{1S}$ from Eq. (21) and rearranging, we can obtain the following neat form:

$$\underset{\sim}{J}_1 = -D_1\left[1 + \frac{D_{1S}}{D_1} + x_1\frac{(D_{1S} - D_{2S})}{D_{12}}\right]\underset{\sim}{\nabla} n_1 + x_1\delta_1\underset{\sim}{J}$$

$$- x_1\gamma_1\left(\frac{nB_o}{\eta}\right)\underset{\sim}{\nabla} p + \frac{x_1}{k_B T}\left(\frac{D_{2S}}{D_{12}}\right)\underset{\sim}{\nabla} p \,, \qquad (28)$$

where

$$\frac{1}{D_1} = \frac{1}{D_{1K}} + \frac{1}{D_{12}} \,, \qquad (29)$$

$$\delta_1 = \frac{D_1}{D_{12}} = \frac{D_{1K}}{D_{1K} + D_{12}} \,, \qquad (30)$$

$$\gamma_1 = \frac{D_1}{D_{1K}} = \frac{D_{12}}{D_{1K} + D_{12}} = 1 - \delta_1 \,. \qquad (31)$$

A similar equation holds for $\underset{\sim}{J}_2$,

$$\underset{\sim}{J}_2 = -D_2\left[1 + \frac{D_{2S}}{D_2} + x_2\frac{(D_{2S} - D_{1S})}{D_{12}}\right]\underset{\sim}{\nabla} n_2 + x_2\delta_2\underset{\sim}{J}$$

$$- x_2\gamma_2\left(\frac{nB_o}{\eta}\right)\underset{\sim}{\nabla} p + \frac{x_2}{k_B T}\left(\frac{D_{1S}}{D_{12}}\right)\underset{\sim}{\nabla} p \,, \qquad (32)$$

with corresponding definitions of D_2, δ_2, and γ_2.

A complete phenomenological description of isothermal diffusion and flow in a binary mixture over the whole pressure range is furnished by Eqs. (28) and (32). The nice thing about the form of these equations is that they clearly exhibit different behaviors as different transport mechanisms dominate, as well as the behavior in the transition region. For one thing, the relevance of surface diffusion is explicitly exhibited as the ratio of surface diffusion coefficients to other diffusion coefficients. Apart from surface diffusion, which we henceforth ignore, the behavior in various regions is manifested through the pressure dependence of D_1, δ_1, and γ_1. These dependences are listed in Table I and follow from the facts that

TABLE 1

High and low pressure limits of diffusion parameters[a]

Limit	D_1	δ_1	γ_1	$n\gamma_1$
$p \to 0$, $n \to 0$	D_{1K}	0	1	0
$p \to \infty$, $n \to \infty$	D_{12}	1	0	nD_{12}/D_{1K}

[a]Note that nD_{12} and D_{1K} are independent of pressure.

D_{1K} is independent of pressure, D_{12} is inversely proportional to pressure, and n is independent of pressure. Thus at very low pressures, $D_1 = D_{1K}$, $\delta_1 = 0$, and $n\gamma_1 = 0$, so that Eq. (5) for free-molecule diffusion is recovered. At high pressures, $D_1 = D_{12}$, $\delta_1 = 1$ and $\gamma_1 = 0$ (but $n\gamma_1 = nD_{12}/D_{1K}$ = constant), so that Eqs. (14) for continuum diffusion are recovered if the pressure gradient is zero. The interplay of the various terms in Eq. (28) or Eq. (32) at different pressures leads to quite interesting behavior, especially in the transition region. For example, the explicit viscous flow term, $(nB_o/n)\nabla p_j$, is important only in the transition region. It vanishes in the free-molecule region, and in the continuum region is dominated by the term involving J [E1, E2, M22].

The behavior and predictions of these flux equations will be discussed in more detail in connection with experimental tests of the theory. Other forms of the flux equations can be obtained by mathematical manipulation,

and there is often a real advantage in using one form in preference to another, depending on the experimental situation. There are also some additional subtleties in the coefficients that do not appear in this phenomenological treatment, but that are revealed by the dusty-gas model — for instance, D_{iK} exhibits a small pressure dependence at pressures just above the free-molecule regime. We postpone these matters here, and turn now to the multicomponent generalization of the present elementary treatment.

4. Multicomponent Mixtures

The key to the description of multicomponent mixtures lies with continuum diffusion — in Knudsen diffusion, the species act completely independently, and in viscous flow, they are completely coupled together. To use the previous momentum-transfer argument, we must first isolate the expression for the momentum transferred to species 1 by collisions with species 2 (or vice versa), in a form which suggests a generalization to include momentum transferred to species 1 by collisions with a number of other species. To this end we rewrite Eq. (22) by substituting $\underset{\sim}{J}_D = \underset{\sim}{J}_{1D} + \underset{\sim}{J}_{2D}$ into it, obtaining

$$-(\nabla p_1)_{\text{molecule}} = (k_B T/D_{12})(x_2 \underset{\sim}{J}_{1D} - x_1 \underset{\sim}{J}_{2D}) \ . \tag{33}$$

We now define an average diffusion velocity $\underset{\sim}{\bar{V}}_{iD}$ for species i as

$$\underset{\sim}{\bar{V}}_{iD} \equiv \underset{\sim}{J}_{iD}/n_i \ . \tag{34}$$

This is much different from the mean molecular speed $\bar{v}_i$; in a diffusing gas mixture $\underset{\sim}{\bar{V}}_{iD}$ is usually of the order of magnitude of 1 cm/sec, and decreases to zero as the mixture finally becomes uniform, whereas $\bar{v}_i$ is of the order of magnitude of 10^4 cm/sec at ordinary temperatures. Then Eq. (33) can be written as

$$-(\nabla p_1)_{\text{molecule}} = k_B T(n_1 n_2/n D_{12})(\underset{\sim}{\bar{V}}_{1D} - \underset{\sim}{\bar{V}}_{2D}) \ . \tag{35}$$

A similar equation exists for $(\nabla p_2)_{\text{molecule}}$, but it is the same as Eq. (35) with reversed signs. Equation (35) can be interpreted in the following way: the momentum transferred to species 1 by species 2 acts like a frictional dra proportional to the difference in their mean diffusion velocities, and this drag is balanced by a gradient in the partial pressure of species 1. With

this interpretation, the extension to multicomponent mixtures is plausible: for each new species there is another momentum-transfer term on the right-hand side of the equation, plus another momentum-transfer equation,

$$-(1/k_BT)(\underset{\sim}{\nabla}p_1)_{\text{molecule}} = (n_1n_2/nD_{12})(\bar{\underset{\sim}{V}}_{1D} - \bar{\underset{\sim}{V}}_{2D}) + (n_1n_3/nD_{13})(\bar{\underset{\sim}{V}}_{1D} - \bar{\underset{\sim}{V}}_{3D}) + \cdots ,$$

$$-(1/k_BT)(\underset{\sim}{\nabla}p_2)_{\text{molecule}} = (n_2n_1/nD_{21})(\bar{\underset{\sim}{V}}_{2D} - \bar{\underset{\sim}{V}}_{1D}) + (n_2n_3/D_{23})(\bar{\underset{\sim}{V}}_{2D} - \bar{\underset{\sim}{V}}_{3D}) + \cdots ,$$

etc. (36)

For a mixture of ν species, there are ν such equations, of which only $\nu - 1$ are independent (any one equation is equal to the sum of the other $\nu - 1$ equations, as should be the case if all the forces are to balance). This set of equations is valid for continuum diffusion at constant total pressure.

Adding in the free-molecule and viscous contributions as before (and ignoring the surface transport for simplicity, although it is straightforward to include), we obtain the general result,

$$-\underset{\sim}{\nabla}n_1 = \frac{1}{D_{1K}}\left[\underset{\sim}{J}_1 + x_1\left(\frac{nB_o}{\eta}\right)\underset{\sim}{\nabla}p\right] + \frac{1}{D_{12}}(x_2\underset{\sim}{J}_1 - x_1\underset{\sim}{J}_2) + \frac{1}{D_{13}}(x_3\underset{\sim}{J}_1 - x_1\underset{\sim}{J}_3) + \frac{1}{D_{14}}(x_4\underset{\sim}{J}_1 - x_1\underset{\sim}{J}_4) + \cdots ,$$

$$-\underset{\sim}{\nabla}n_2 = \frac{1}{D_{2K}}\left[\underset{\sim}{J}_2 + x_2\left(\frac{nB_o}{\eta}\right)\underset{\sim}{\nabla}p\right] + \frac{1}{D_{21}}(x_1\underset{\sim}{J}_2 - x_2\underset{\sim}{J}_1) + \frac{1}{D_{23}}(x_3\underset{\sim}{J}_2 - x_2\underset{\sim}{J}_3) + \frac{1}{D_{24}}(x_4\underset{\sim}{J}_2 - x_2\underset{\sim}{J}_4) + \cdots ,$$

etc. (37)

For binary mixtures, these equations are equivalent to Eqs. (28) and (32). The arguments leading to Eqs. (37) are based largely on plausibility rather than on detailed theory, and the results at this stage must be regarded as phenomenological [M15]. In particular, there is no assurance that the D_{ij} in Eqs. (37) are the same as the ones in the corresponding binary mixture equations. For dilute gases, in which at most only binary encounters are important, it seems reasonable that this should be so. Detailed kinetic-theory calculations show that this is the case to a very good approximation, but the result is not exact. Put another way, the identification of the D_{ij} in Eqs. (37) with those for binary mixtures tacitly assumes that the D_{ij} are independent of mixture composition. This is nearly, but not quite, true for gases, and is an important simplification in the treatment of multicomponent gaseous diffusion. The same form of equations might be expected to apply to dense gases and liquids, but the D_{ij} would then depend on all the components in the mixture, not just on i and j.

The dusty-gas model described in the next part of this chapter gives much the same results, plus more details, but involves much more mathematical complexity than the simple arguments used above. We think it is remarkable that such simple arguments lead to such significant results with very little mathematical manipulation; this will be illustrated in a more striking way in connection with comparisons with experiment in the transition region between the free-molecule and continuum regimes.

B. DUSTY-GAS MODEL

The physical ideas behind the dusty-gas model are really quite similar to those used in the preceding elementary arguments of Section A. In particular, the additivity of the diffusive and viscous fluxes is the same in both procedures, and the reasons are the same. However, the treatment of diffusion by the dusty-gas model is much more elaborate than the simple momentum-transfer arguments used in Section A.2. In place of these simple arguments for combining free-molecule and continuum diffusion, and for describing multicomponent diffusion, a full Chapman-Enskog kinetic-theory treatment is given for a gas mixture in which the porous medium is considered as one component of the mixture. Pressure variation is then formally equivalent to variation of the mole fraction of the "dust" component. Although these two procedures appear at first sight to be fundamentally different, we wish to emphasize that they are in fact quite close in both spirit and technique. Specifically, in the lowest

order of approximation, the dusty-gas model gives the same results as do the simple momentum-transfer arguments; it is only in the higher approximations that new results appear. Moreover, attempts to refine the momentum-transfer theory of diffusion lead to a mathematically elaborate result known as Maxwell-Chapman theory, whose answers are identical to those of the more familiar Chapman-Enskog theory [P3].

What then are the advantages of the dusty-gas model? The main advantage is that it provides a point of view which allows the treatment of a number of different aspects of flow and diffusion from a single standpoint having a sound theoretical basis. It enables all the elaborate results of modern kinetic theory [C7, F3, H10] to be used without having to repeat the Chapman-Enskog solutions all over again in a somewhat different context. Thus thermal diffusion, pressure diffusion, and forced diffusion are all easily included, and many useful details about the behavior of the diffusion coefficients with pressure and composition fall readily from the theory. In addition, not being bogged down in previously worked-out mathematics, one can often see relations between apparently different phenomena that would be completely obscured by a rigorous mathematical approach from first principles. Examples are the relation of the Knudsen permeability minimum to the thermal transpiration maximum, and the relation of the height of this maximum to inelastic molecular collisions in the gas phase.

Another way of viewing the situation is as follows: For many simple transport problems, the correct results are known empirically, and it is possible to concoct various sorts of theoretical or heuristic arguments to justify or "derive" them. This can lead to a dangerous situation, because there are many wrong ways of "deriving" an already known answer, and maybe only one or two correct ways. The danger comes when a new situation arises — application of one of the wrong ways may now lead to a wrong result, because the right answer is not known in advance. The history of kinetic theory contains a number of ghastly examples of this sort, such as the prediction of the composition dependence of the binary diffusion coefficient by a simple mean free path argument, and various attempts to explain the radiometer effect. The point is that it is important to have the fundamentals clear, and to have one systematic procedure that can be applied consistently to complicated as well as simple situations.

In this section we first give a more detailed critique of the assumptions underlying the dusty-gas model than has previously appeared in the literature, and then proceed to the formulation of the transport equations and the passage

to the dusty-gas limit. Development of the relationships for special cases and comparison with experimental tests are reserved for Chapter III.

1. Description of the Model and Critique of Assumptions

The physical picture behind the model is that of a dusty gas, in which the dust particles constitute the porous medium. The array of dust particles is treated as one component of the gas mixture, consisting of giant, heavy molecules that are motionless and uniformly distributed in space. If there are any pressure gradients in the gas, an external force must be exerted on the dust particles to keep them motionless. The precise origin of this external force does not matter in the mathematical treatment; in practice it would usually arise from whatever clamping device holds the porous body stationary. The particular arrangement of the dust particles in space does not matter either, since such geometric characteristics are absorbed into the transport coefficients as constants like K_o and ε/q. Thus it is unimportant how one chooses to visualize the dust — literally as a random array of large spheres somehow stuck in space, as irregular blobs on the surface of a tortuous capillary, as indicated in Fig. 3, or in some other fashion. Pictures like Fig. 3 may be helpful as mnemonic devices, but should not be taken any more literally than the electrical circuit of Fig. 1.

By treating the dust particles as giant "molecules," we can take over the results of the Chapman-Enskog kinetic theory [C7, F3, H10] virtually intact. This theory has two independent parts, at least in the approximation in which only first-order deviations from the equilibrium Maxwellian velocity distribution are considered: a diffusion part, consisting of a set of Stefan-Maxwell diffusion equations, and a viscous-flow part, consisting of an equation of motion for the gas mixture as a whole. These two parts are independent in the sense that there are no diffusion terms in the equation of motion, and no term corresponding to the viscous transfer of momentum in the diffusion equations. This independence is the justification for assuming simple additivity of diffusive and viscous fluxes. Writing down these two parts from kinetic theory and taking them as additive is the essential heart of the whole treatment — all the rest consists of manipulations of largely mathematical character. The final result is a set of differential equations describing the gas transport. In actual problems, these must of course be integrated, subject to a few macroscopic boundary conditions.

Two observations may be made at this point. The first concerns the independence of the diffusion and viscous-flow equations, in the sense that

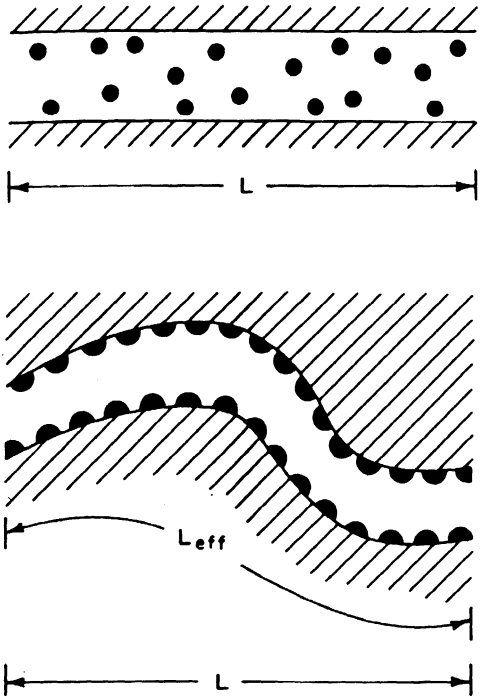

Fig. 3. Schematic ways of visualizing the dusty-gas model for gas transport.

coupling terms are absent. This does not mean that viscous flow and diffusion do not interact in a very real sense, but only that they interact through boundary conditions and the behavior of the transport coefficients, not through direct coupling terms in the equations. In most real problems the two sets of equations cannot be solved independently, but must be solved together in order to satisfy boundary conditions. For instance, we must know the viscosity in order to solve the viscous-flow equations, but the viscosity of a mixture depends on its composition, which is obtained by solution of the diffusion equation. However, the solution of the diffusion equation depends on knowledge of the flow occurring, since flow distorts the composition gradients in the mixture, and this is obtained by solution of the flow equation. Thus

we come full circle, and find that the equations are coupled in a very real way when solutions to particular problems are sought.

The second observation is that the structure of the medium is isolated as a completely independent problem. It appears only in numerical coefficients in the differential equations describing the transport, and perhaps in a few of the macroscopic boundary conditions. One of the virtues of the dusty-gas model is that it is possible to obtain the general solution of the diffusion and viscous-flow aspects of the problem without having to say anything specific about the structure of the medium. The unknown coefficients can then be found either by direct experiment, or by calculation from the structure of the medium (if it is in fact known in sufficient detail), whichever is more convenient. This isolation of the geometrical-structural part of the problem is extremely important in a practical sense. To see this, imagine trying to solve a coupled flow and diffusion problem straightforwardly from first principles. If we are safely in the continuum region, as we may assume for simplicity, then the full formulation of the problem consists of the Stefan-Maxwell diffusion equations and the equation of motion, as applied to each element of the fluid mixture within the porous medium, plus the boundary conditions throughout the medium. These boundary conditions are given by the structure of the medium. Now the differential equations must be integrated subject to these boundary conditions, to obtain the flow and diffusion fields throughout the medium. This is a hideously difficult problem for a structure of any complexity, but if it could be solved, we would have not only the overall fluxes through the medium, but also explicit results for the effective transport coefficients within the porous medium in terms of the structure. We would also have a wealth of detailed information on secondary flows, etc., in which we were not really interested. But of course it is virtually impossible to carry such a program through because the boundary-value problems involved are too difficult. Thus the structural part of the problem can prevent any progress at all toward the solution, just because of its complexity. It is thus essential that the geometrical-structural question somehow be isolated or bypassed, and all attacks on the problem of transport in porous media do so in one way or another, sometimes directly, by simply regarding the medium as a bundle of parallel capillaries, or indirectly, by assuming that the transport coefficients can be modified empirically to account for geometrical aspects.

Two fundamental questions or criticisms may now be raised regarding the dusty-gas model. (Minor questions will be dealt with as they arise in connection with the derivation given later on.) They can be formulated as follows:

(1) Chapman-Enskog theory is based on the Boltzmann equation, in which it is assumed that only binary collisions are important. This implies that the mean free path of the gas molecules must be larger than the diameter of the dust particles, to avoid multiple collisions in which several gas molecules collide with a dust particle at about the same time. This in turn suggests that the results of the dusty-gas model can only be applicable in the near-Knudsen region. How then is it justifiable to use the results in the continuum region?

(2) Is the simple additivity of diffusive and viscous fluxes really correct? Two arguments can be advanced against it. The first is that coupling terms do appear in the equations when deviations from the Maxwellian distribution are followed to the second order of small quantities. This is independent of any special considerations about interactions with solid surfaces or boundary conditions. The second argument has to do with gas-surface collisions, and can be formulated by consideration of the drag of a flowing gas on a fixed sphere. In the free-molecule region, the drag is determined by individual molecular impacts and is proportional to the pressure. As the pressure is increased, molecules may collide with the sphere, then collide with another molecule, and finally recollide with the sphere. Such correlated collisions lead to terms in the drag involving the logarithm of the pressure or Knudsen number (the ratio of the molecular mean free path to the sphere diameter) [D10, D11]. Simple additivity of diffusive and viscous fluxes cannot lead to logarithmic terms, and so cannot be correct.

Regarding the first question, a more careful examination of the Boltzmann equation shows that what is required are uncorrelated collisions, not necessarily binary collisions. Binary collisions are sufficient, but not necessary, for the applicability of the Boltzmann equation. In the present case it is the mass of the dust particles that assures uncorrelated collisions, not the size; the collision of one gas molecule with a dust particle is not influenced by the fact that another gas molecule happens to hit another part of the dust particle at about the same time, because the dust particle recoils negligibly from a molecular collision.

The second question is more serious. The first argument can be handled fairly easily, since second-order deviations from the Maxwellian distribution have been studied extensively in kinetic theory. It turns out that almost all the new terms that arise in second order can be shown to be unnecessary, either because they are small compared to the first-order terms in all cases of experimental interest, or because retaining them involves inconsistency in the

use of asymptotic series. Only one higher-order term survives this scrutiny [Z3], and it has been shown explicitly not to alter any of the results from the dusty-gas model [M22].

The second argument of the second question is less easily disposed of, and involves matters of current research activity on the kinetic theory of gases. In the drag problem in which the argument is formulated, the dusty-gas model describes the situation in terms of uncorrelated collisions (Chapman-Enskog) plus highly correlated collisions (viscous flow), and ignores the partial correlations in between. Clearly this is an approximation that cannot generate logarithmic terms in an expansion in terms of the mean free path, and it is ultimately up to experiment to decide how good or how bad the approximation is. However, attempts to find experimental evidence for the existence of such logarithmic terms have not succeeded — presumably their contribution is small and is masked by the other power-law terms. As will be seen subsequently, comparisons with experimental data indicate that this approximation of the dusty-gas model is quite accurate. There are also some recent indications of a basis for a better theoretical justification of the approximation. This arises from recent theoretical work on the drag of a flowing gas on a sphere, in which the problem is handled in a completely fundamental way by incorporating the gas-sphere interaction into the Boltzmann equation from the beginning [D11], rather than grafting it on later as a boundary condition. It appears that the dusty-gas result gives a Padé approximant expression for the transition region, and as such is likely to have good accuracy. This special problem is discussed in more detail in Chapter IV.

There have been other attempts to give better theoretical treatments of problems that the dusty-gas model handles by taking diffusive and viscous fluxes as additive, or that the model handles by absorbing the difficulties into parameters like K_o and ε/q. These valuable studies [B10 — B12, C2 — C5, L1, L2, L9 — L20, W11, W12, Z2] naturally tend to involve complicated kinetic theory formulations, and often require numerical integration in order to obtain final answers. As such they are not as directly useful for engineering purposes as a more approximate but mathematically tractable approach like the dusty-gas model, but they can serve to show the range of validity of such a model, and to deepen the understanding of its successes and failures. Since we are still far from such an understanding, for the purposes of this monograph we shall adopt the more pragmatic view that the model is to be judged by direct comparison with experimental data, as is done in Chapter III.

The foregoing considerations may serve as a reminder that we are neglecting adsorption, surface diffusion, and other surface effects. This suggests that the dusty-gas results may fail to hold when the size of the holes in the porous medium becomes comparable to the molecular diameter. No clear understanding exists at present of the nature of failure in such a regime, and the problem of transport through very fine pores remains an active research area.

One final comment on the dusty-gas model can be made. Classical gas-kinetic theory deals only with elastic collisions, so that the internal degrees of freedom of polyatomic molecules are not taken into account. When the theory is extended to include molecular internal degrees of freedom, it is found that the external forms of the transport equations are identical, in first-order approximation, with the corresponding equations for monatomic gases. The differences show up only in the expressions for the transport coefficients, which are more complex and contain inelastic collision terms [A1, M37, M39, M40]. Thus the general results obtained from the dusty-gas model will be applicable to polyatomic as well as monatomic gases, although the explicit formulas for the transport coefficients must be altered accordingly.

We now turn to the formulation of the transport equations.

2. Diffusion Equations

As might be expected from the momentum-transfer arguments of Section A of this Chapter, the diffusion equations for a multicomponent mixture appear simplest when written, not as a flux of species i being proportional to gradients of all species, but as the gradient of species i being proportional to fluxes of all species (Stefan-Maxwell form). In this form the equations for a mixture of ν species are [A1, M37, M39]

$$-\underset{\sim}{d}_i = \sum_{j=1}^{\nu} (x_j \underset{\sim}{J}_{iD} - x_i \underset{\sim}{J}_{jD})/(n \mathcal{D}_{ij}) , \tag{38}$$

where the gradient term $\underset{\sim}{d}_i$ is

$$\underset{\sim}{d}_i = \nabla x_i + x_i \left(\frac{\bar{m} - m_i}{\bar{m}}\right) \nabla \ln p - \frac{x_i}{p} \left(n\underset{\sim}{F}_i - \frac{m_i}{\bar{m}} \sum_{j=1}^{\nu} n_j \underset{\sim}{F}_j\right)$$

$$+ \sum_{j=1}^{\nu} x_i x_j \alpha_{ij} \nabla \ln T , \tag{39}$$

in which

$$\bar{m} = \sum_{j=1}^{\nu} x_j m_j \tag{40}$$

is the mean molecular mass of the mixture, and $\underset{\sim}{F}_i$ is the external force on species i. The four terms on the right-hand side of Eq. (39) represent concentration diffusion, pressure diffusion, forced diffusion, and thermal diffusion, respectively. Note that Eq. (38) is the ith of a set of ν equations, of which only $\nu-1$ are independent (any one of the set is equal to the sum of the remaining $\nu-1$ equations).

The form of the above transport equations, Eqs. (38) and (39), could have been deduced from simple momentum-transfer arguments, but the explicit expressions for the coefficients $\mathfrak{D}_{ij}$ and α_{ij} require more elaborate theoretical methods. It is at this point that the Chapman-Enskog procedure makes its special contribution. In this procedure the transport coefficients are obtained in a series of approximations, usually rapidly convergent. The first approximation for $\mathfrak{D}_{ij}$, denoted as $[\mathfrak{D}_{ij}]_1$, is

$$[\mathfrak{D}_{ij}]_1 = \frac{3}{8}\left(\frac{\pi k_B T}{2\mu_{ij}}\right)^{1/2} \frac{1}{n\pi\sigma_{ij}^2\,\Omega_{ij}^{(1,1)*}} , \tag{41}$$

where $\mu_{ij} = m_i m_j/(m_i+m_j)$ is the reduced mass of the ij pair, σ_{ij} is an arbitrary distance parameter that is usually chosen for convenience to be of the order of magnitude of the mutual collision diameter of the molecular pair, and $\Omega_{ij}^{(1,1)*}$ is a dimensionless transport collision integral (or average cross section) normalized to be unity for collisions between rigid elastic spheres of mutual diameter σ_{ij}. The detailed definition of $\Omega_{ij}^{(1,1)*}$ is rather standard in kinetic theory [H10], and need not be repeated here; it will only concern us in connection with gas-dust collisions, because for gas-gas collisions we will simply regard $\mathfrak{D}_{ij}$ as an experimental quantity. The form of Eq. (41) is unchanged when polyatomic gases are concerned, but the expression for $\Omega_{ij}^{(1,1)*}$ is more complicated than for monatomic gases [M40].

Notice that $[\mathfrak{D}_{ij}]_1$ depends only on the species i and j in the mixture, and is independent of all the other species; it is thus the same as the binary

diffusion coefficient of species i and j in this approximation. This is not true in higher approximations, which may be written as

$$\mathcal{D}_{ij} = [\mathcal{D}_{ij}]_1/(1 - \Delta_{ij}) \ . \tag{42}$$

Although Δ_{ij} is usually small compared with unity, it contains all the dependence of the binary $\mathcal{D}_{ij}$ on the composition, and all the dependence of the $\mathcal{D}_{ij}$ on the other species in a multicomponent mixture [M41]. Again, this does not concern us except for gas-dust collisions.

The quantity $\alpha_{ij} = -\alpha_{ji}$ is a generalized thermal diffusion factor that, in a sense, describes the relative separation of i and j in a temperature gradient, though it too is dependent upon all of the species in the mixture. This dependence appears in the formulas in an essential way, not just through a small correction term like Δ_{ij}. Problems involving temperature gradients thus tend to be algebraically messy, although still straightforward in principle. The multicomponent α_{ij} can be written, to the same approximation as the $\mathcal{D}_{ij}$ in Eq. (42), as the sum of the contribution from the translational motion of the species and from their internal motion [A1, M39],

$$\alpha_{ij} = (\alpha_{ij})_{tr} + (\alpha_{ij})_{int} \ . \tag{43}$$

The internal contribution $(\alpha_{ij})_{int}$ vanishes if the angular scattering pattern for ij collisions is independent of the internal energy states of i and j. Even if $(\alpha_{ij})_{int}$ does not vanish, it is almost always negligible compared to $(\alpha_{ij})_{tr}$, unless the latter happens to be almost zero because of some special combination of factors such as molecular masses and sizes (e.g., if i is ortho-H_2 and j is para-H_2, or i is HT and j is D_2) [M39]. In any event, we will henceforth neglect $(\alpha_{ij})_{int}$. The translational contribution is given by [A1, M39]

$$(\alpha_{ij})_{tr} = \frac{1}{5} \frac{(6C_{ij}^* - 5)}{n[\mathcal{D}_{ij}]_1} \left(\frac{\mu_{ij}}{k_B}\right) \left[\frac{(\lambda_j)_{tr}}{x_j m_j} - \frac{(\lambda_i)_{tr}}{x_i m_i}\right] \ , \tag{44}$$

where C_{ij}^* represents a dimensionless ratio of collision integrals whose value is near unity [H10], and $(\lambda_i)_{tr}$ is a partial contribution of the translational motion of species i in the mixture to the total translational thermal conductivity of the mixture,

$$\sum_{i=1}^{\nu} (\lambda_i)_{tr} = \lambda_{tr} \ . \tag{45}$$

Equations (44) and (45) are valid for both monatomic and polyatomic gases, but the explicit expressions for C_{ij}^*, $[\mathfrak{D}_{ij}]_1$, and the $(\lambda_i)_{tr}$ are more complicated for polyatomic gases. This need not be a cause for concern, because most of the extra complications can be absorbed into experimental quantities for the gas-gas interactions and into adjustable parameters for the gas-dust interactions, as is shown in detail in subsequent sections.

The expressions for the $(\lambda_i)_{tr}$ are rather complicated for multicomponent mixtures, even for monatomic gases. For polyatomic gases, the expressions contain many complicated extra bits which are needed to describe the inelastic collisions. Fortunately, a considerable simplification is usually possible. It has been found that the explicit inelastic-collision terms do not have much effect on the form of the dependence of λ_{tr} on composition, but mainly translate λ_{tr} to lesser values than those for corresponding monatomic gases. Thus a good approximation can be obtained by using the full polyatomic-gas formulas only for the pure-component end points, and using the monatomic-gas formulas for the mixtures as interpolation formulas for the composition dependence only [M38]. That is, the translational thermal conductivity for pure species $\underline{i}$ is calculated as

$$(\lambda_{ii})_{tr} = \frac{5}{2} \eta_{ii} \left(\frac{3}{2} \frac{k_B}{m_i} - \Delta_i^{\lambda} \right) , \tag{46}$$

where η_{ii} is the experimentally known viscosity of pure $\underline{i}$, and Δ_i^{λ} is a correction for inelastic collisions,

$$\Delta_i^{\lambda} = \frac{2(\bar{c}_i)_{int}}{\zeta_{ii}} \left[\frac{5}{2} - \frac{m_i n (\mathfrak{D}_{ii})_{int}}{\eta_i} \right] \times$$

$$\left\{ 1 + \frac{2m_i}{\pi \zeta_{ii}} \left[\frac{5}{3} \frac{(\bar{c}_i)_{int}}{k_B} + \frac{n(\mathfrak{D}_{ii})_{int}}{\eta_i} \right] \right\}^{-1} \ . \tag{47}$$

In Eq. (47), $(\bar{c}_i)_{int}$ is the internal specific heat per gram, ζ_{ii} is the number of collisions required on the average for interchange of internal and translational energy, and $(\mathfrak{D}_{ii})_{int}$ is the diffusion coefficient for internal energy, usually but not always nearly equal to the self-diffusion coefficient $\mathfrak{D}_{ii}$ of species i. The important point is that all the quantities in Eq. (47) can be measured or estimated independently. In Chapter III we will show that the converse procedure is also possible, and that values of ζ_{ii} can be found via Eq. (47) from experimental measurements of thermal transpiration. Once all the $(\lambda_{ii})_{tr}$ are known, the values of the partial $(\lambda_i)_{tr}$ in a mixture can be calculated from the monatomic-gas formulas, which are still fairly complicated determinant expressions [C7, F3, H10] ,

$$(\lambda_i)_{tr} = x_i \sum_{k=1}^{\nu} x_k \frac{|\Lambda|_{ki}}{|\Lambda|} , \qquad (48)$$

in which $|\Lambda|$ is a determinant with elements Λ_{ik}, and $|\Lambda|_{ki}$ is the cofactor of the element Λ_{ki} of the determinant. The elements are

$$\Lambda_{ii} = \frac{x_i^2}{(\lambda_{ii})_{tr}} + \frac{4}{25k_B} \sum_{\substack{k=1 \\ k\neq i}}^{\nu} \frac{x_i x_k}{(m_i+m_k)^2 \, n\mathfrak{D}_{ik}} \times$$

$$\left[\frac{15}{2} m_i^2 + \frac{5}{2}\left(\frac{5}{2} - \frac{6}{5} B_{ik}^*\right) m_k^2 + 4 m_i m_k A_{ik}^* \right] , \qquad (49)$$

$$\Lambda_{ik}(i\neq k) = -\frac{4}{25k_B} \frac{m_i m_k}{(m_i+m_k)^2} \frac{x_i x_k}{n\mathfrak{D}_{ik}} \left(\frac{55}{4} - 3B_{ik}^* - 4A_{ik}^*\right) , \qquad (50)$$

where A_{ik}^* and B_{ik}^*, like C_{ik}^*, are dimensionless ratios of collision integrals whose values are usually near unity [H10]. Equations (49) and (50) are only theoretical first approximations, but are quite accurate if experimental values are used for the $(\lambda_{ii})_{tr}$ and the $\mathfrak{D}_{ik}$.

This completes our specification of the Chapman-Enskog multicomponent diffusion equations. We turn now to the viscous-flow equations, and then consider the dusty-gas limits of both sets of equations.

3. Viscous-Flow Equations

The Chapman-Enskog treatment adds nothing essential to the more elementary computation of the viscous flux in Section A, except for an explicit formula for the viscosity of a gas or gas mixture in terms of molecular quantities. That is, the Chapman-Enskog expression for the pressure tensor still leads to the same result for creeping flow,

$$\underset{\sim}{J}_{visc} = - (nB_o/\eta)\underset{\sim}{\nabla}p \ , \tag{51}$$

where B_o is a geometric constant. Partial viscosities η_i of species i in a mixture can be calculated, but are not important in the present problem because the viscous component of the flow is nonseparative. At most we may need the formula for the viscosity of a multicomponent mixture, which is similar to that for the translational thermal conductivity [C7, F3, H10],

$$\eta = \sum_{i=1}^{\nu} x_i \sum_{k=1}^{\nu} x_k \frac{|H|_{ki}}{|H|}, \tag{52}$$

where $|H|$ is a determinant whose elements are given by

$$H_{ii} = \frac{x_i^2}{\eta_{ii}} + \sum_{\substack{k=1 \\ k\neq i}}^{\nu} \frac{x_i x_k}{(m_i+m_k)\, n\mathfrak{D}_{ik}} \left(1 + \frac{3}{5}\frac{m_i}{m_k} A_{ik}^*\right) , \tag{53}$$

$$H_{ik}(i\neq k) = - \frac{2x_i x_k}{(m_i+m_k)n\mathfrak{D}_{ik}} \left(1 - \frac{3}{5} A_{ik}^*\right) . \tag{54}$$

These expressions, like those for the thermal conductivity, are only theoretical first approximations, but are very accurate if experimental values are used for the η_{ii} and the $\mathfrak{D}_{ik}$. They hold for polyatomic as well as monatomic mixtures, the only difference being a slightly changed result for the dimensionless ratio A_{ik}^* [M40].

4. Dusty-Gas Limit

Thus far we have merely given the kinetic-theory background. To pass to the dusty-gas limit we apply six special conditions, as follows [M22]:

(1) As in the elementary discussion, we let B_o be a geometric constant of the porous medium, to be determined by experiment or separate calculation. Similarly, we define effective diffusion coefficients as $D_{ij} = (\varepsilon/q)\mathscr{D}_{ij}$, and let the porosity-tortuosity factor ε/q also be a geometric constant of the medium. Two comments should be made. First, B_o and ε/q are only locally constant parameters; they can have different values in different portions of the porous medium. Second, $\mathscr{D}_{ij}$ is replaced by D_{ij} only in Eq. (38) for the fluxes, and not in any of the equations relating $\mathscr{D}_{ij}$ to some other transport coefficient, specifically Eqs. (44), (47), (49), (50), (53), and (54).

(2) The dust particles are motionless and uniformly distributed. Therefore, $\underset{\sim}{J}_d = 0$ and $\underset{\sim}{\nabla} n_d = 0$ in Eqs. (38) and (39), where the subscript $\underline{d}$ denotes the dust component.

(3) Since the dust is stationary, it does not contribute directly to $\underline{\lambda}$ or $\underline{\eta}$ in any of the mixture formulas.

(4) The quantities n and p appearing in the various parts of the diffusion equations are not the actual gas density and pressure, but include the dust particles in the counting. To avoid confusion, we use primes on quantities when the dust particles are counted as molecules and drop the primes when only the actual gas molecules are counted; thus we write

$$n' = n + n_d \ , \quad p' = p + n_d k_B T \ , \quad \nu' = \nu + d \ . \tag{55}$$

It is a result of kinetic theory that

$$n' D'_{ij} = n D_{ij} \ , \tag{56}$$

but the analogous result for α_{ij} is more complicated and gives rise to interesting pressure dependences in thermal transpiration and thermal diffusion.

(5) The dust particles are held motionless by an external force which balances any pressure gradients in the gas.

(6) Explicit kinetic-theory expressions can be written for nD_{id} and α_{id} in terms of gas and dust properties.

Only the last two conditions require elaboration. Regarding condition (5), we can calculate the external clamping force on the dust by a simple

force-balance argument. Suppose for simplicity that no other external forces, such as gravity or electrical forces, act on either the gas molecules or the dust particles. Now consider a solid slab of material of thickness dz and cross-sectional area A, with fluid on one side at pressure p, and on the other side at pressure p + dp. The net force on the slab is Adp. Then imagine a hole of cross-sectional area a drilled in the slab, through which fluid flows. The direct force on the slab is now reduced to (A-a)dp, but there is an additional force due to the drag of the fluid on the sides of the hole as the fluid flows through the hole under the action of the pressure difference dp. If the fluid is not accelerated as it flows through the hole, then the drag force must equal the force pushing the fluid through, which is adp. The total force on the slab is therefore

$$(A-a)dp + adp = Adp \ .$$

In other words, the force on the slab is the same whether or not the slab has holes in it. This result is independent of the size and shape of the holes, and does not depend on the nature of the mechanism whereby the fluid exerts a drag on the walls of the hole. All that is required is that some such mechanism exists, and that the fluid not be accelerated. If now the slab is so riddled with holes that it appears as a collection of dust particles, the net force is still Adp, where A is the apparent area of the slab before being riddled. This must be balanced by an external clamping force on the slab to hold it motionless. If a force F_d acts on each particle, and there are n_d particles per unit volume, then the total clamping force on the riddled slab is $n_d F_d A dz$, and the force-balance equation is

$$n_d F_d A dz = Adp \ ,$$

or, more generally,

$$n_d \underset{\sim}{F}_d = \underset{\sim}{\nabla} p \ . \qquad (57)$$

Note that p here is the actual gas pressure.

If other external forces act, a similar force-balance argument leads to the expression

$$n_d \underset{\sim}{F}_d + \sum_{j=1}^{\nu} n_j \underset{\sim}{F}_j = \nabla p \ , \tag{58}$$

where the sum includes only gaseous species, and the $\underset{\sim}{F}$'s refer to all external forces, including the clamping force. The only additional assumption involved in Eq. (58) is overall electrical neutrality within the porous medium; that is, any charge on the dust particles must be balanced by the total charge on the gas molecules. This result is of little importance for gases in porous media, but it does become important in the extension to general membrane transport given in Chapter IV, since charged membranes and charged electrolyte species are commonly encountered. The viscous-flow equation must also be modified in such cases; in place of Eq. (51) we obtain

$$\underset{\sim}{J}_{visc} = -(nB_o/\eta)\left(\nabla p - \sum_{j=1}^{\nu} n_j \underset{\sim}{F}_j\right) \ , \tag{59}$$

subject to the same conditions as Eq. (58).

Before proceeding to the explicit formulas for nD_{id} and α_{id}, we can now write down the complete set of transport equations. Applying the dusty-gas conditions to Eqs. (38) and (39), we obtain, after some algebra, the result (for $i, j \neq d$),

$$\frac{n_i}{n} \sum_{j=1}^{\nu} \frac{n_j(1-\Delta'_{id})}{n[D_{ij}]_i}\left[\frac{\underset{\sim}{J}_{iD}}{n_i} - \frac{\underset{\sim}{J}_{jD}}{n_j}\right] + \frac{1-\Delta'_{id}}{n[D_{iK}]_1} \underset{\sim}{J}_{iD} =$$

$$= -\nabla\left(\frac{n_i}{n}\right) - \frac{n_i}{n} \nabla \ln p + \frac{n_i}{p} \underset{\sim}{F}_i - \frac{n_i}{n}\left[\sum_{j=1}^{\nu} \frac{n_j}{n'} (\alpha'_{ij})_{tr} + \right.$$

$$\left. + \frac{n_d}{n}(\alpha'_{id})_{tr}\right] \nabla \ln T \ , \tag{60}$$

where the summations now exclude the dust. The Knudsen diffusion coefficient $[D_{iK}]_1$ is defined as

$$[D_{ik}]_1 \equiv (n/n_d)[D_{id}]_1 \ . \tag{61}$$

Most of the complicated pressure- and forced-diffusion terms have cancelled out because of Eq. (58). Before adding in the viscous flow, we make the

following useful approximation. Since Δ_{ij} in a binary mixture is usually fairly small, it seems reasonable to take the multicomponent Δ'_{ij} in Eq. (60) as also small and approximately equal to Δ_{ij}. Thus we write

$$[D_{ij}]_1/(1-\Delta'_{ij}) \approx D_{ij} \ , \tag{62}$$

where D_{ij} is the binary diffusion coefficient. It will also be useful to make an analogous binary-mixture approximation for the Δ'_{id}, which will be seen to contain some small but interesting pressure effects. We now put the viscous flow into Eq. (60) and obtain equations for the total fluxes,

$$\sum_{j=1}^{\nu} \frac{n_j}{nD_{ij}} \left[\frac{\underset{\sim}{J}_i}{n_i} - \frac{\underset{\sim}{J}_j}{n_j} \right] + \frac{1-\Delta'_{id}}{[D_{iK}]_1} \frac{\underset{\sim}{J}_i}{n_i} - \frac{1-\Delta'_{id}}{[D_{iK}]_1} \frac{\underset{\sim}{J}_{visc}}{n} =$$

$$= - \underset{\sim}{\nabla} \ln (n_i/n) - \underset{\sim}{\nabla} \ln p + \underset{\sim}{F}_i/k_B T$$

$$- (n')^{-1} \left[\sum_{j=1}^{\nu} n_j (\underset{\sim}{\alpha}'_{ij})_{tr} + n_d (\underset{\sim}{\alpha}'_{id})_{tr} \right] \underset{\sim}{\nabla} \ln T \ , \qquad i,j \neq d \ . \tag{63}$$

The last term on the left-hand side of Eq. (63) is a correction for the net drift due to viscous flow, in which $\underset{\sim}{J}_{visc}$ is given by Eq. (59). The first three terms on the right-hand side correspond to concentration diffusion, pressure diffusion, and forced diffusion, respectively. The terms involving $(\alpha'_{ij})_{tr}$ give rise to thermal diffusion, as modified by the presence of the dust, and the term involving $(\alpha'_{id})_{tr}$ gives rise to thermal transpiration (or thermomolecular pressure difference), as modified by thermal diffusion among the true gaseous components. All ν of these equations are independent, since the equation for the dust particles has been explicitly eliminated.

We need finally to have expressions for the quantities $[D_{iK}]_1$, Δ'_{id}, $(\alpha'_{ij})_{tr}$, and $(\alpha'_{id})_{tr}$. The Knudsen diffusion coefficient is related by Eq. (61) to the gas-dust diffusion coefficient $[D_{id}]_1$, which in turn is given by Eq. (41), with one component being the dust particles. We thereby obtain the expression,

$$[D_{iK}]_1 = (n/n_d)\,[D_{id}]_1 = \frac{3}{8}\left[\frac{\pi k_B T}{2m_i}\right]^{1/2} \frac{1}{n_d S_d\, \Omega_{id}^{(1,1)*}}\,, \tag{64}$$

where S_d is a geometric constant characteristic of the dust particles, and the dimensionless collision integral $\Omega_{id}^{(1,1)*}$ depends on the nature of the scattering of the gas molecules from the dust particle. For spherical particles of radius R, S_d is equal to πR^2, the cross-sectional target area for collision. Very little is known about $\Omega_{id}^{(1,1)*}$ for real systems as opposed to simplified models, but fortunately most of the results of interest will be nearly independent of this quantity. For elastic specular scattering, the value of $\Omega_{id}^{(1,1)*}$ is unity. If a fraction f of the molecules are scattered elastically but diffusely (cosine-law distribution), and the remainder are scattered elastically and specularly, the value is

$$\Omega_{id}^{(1,1)*} = 1 + \frac{4}{9} f\,. \tag{65}$$

If the diffusely scattered fraction is accommodated to the temperature of the dust particle on collision, the scattering is inelastic and the value is

$$\Omega_{id}^{(1,1)*} = 1 + \frac{\pi}{8} f\,. \tag{66}$$

These values of $\Omega_{id}^{(1,1)*}$ assume no interaction between the dust particle and a gas molecule until the two are in contact. A weak interaction can be included by the Sutherland approximation, whereby $\Omega_{id}^{(1,1)*}$ is increased by the factor [1+(s/T)], where the Sutherland constant s depends on the strength of the long-range interaction. Fortunately, most of this does not matter, because the geometry of the porous medium is usually so poorly known that $[D_{ik}]_1$ must be determined experimentally; the important part of Eq. (64) is then just the $(T/m_i)^{1/2}$ dependence. Thus Eq. (64) can be rewritten for practical purposes as

$$[D_{iK}]_1 \approx \text{constant}\,(T/m_i)^{1/2}\,, \tag{67}$$

in agreement with the results of the elementary arguments leading to Eqs. (6)–(7).

The correction term Δ'_{id} is quite complicated for a multicomponent mixture because its value may depend on all the components of the mixture, not just on species i and d. Although Δ'_{id} can be found in principle, its expression is fairly simple only for a binary mixture (i.e, one gas plus dust). Since the term is small, a simplifying approximation seems justified, and we shall use an expression for Δ'_{id} corresponding to a pseudo-binary mixture [M21, M22],

$$\Delta'_{id} \approx \frac{1}{5}\xi_i(n_d/n')(|\alpha'_{id}|)_{tr} , \tag{68}$$

where ξ_i is a numerical constant of order unity, whose value depends on the scattering pattern. This expression is correct for a binary mixture, but is only an approximation for multicomponent mixtures. We take the reciprocal of $(|\alpha'_{id}|)_{tr}$ to be linear in the mole fraction, which is correct for a binary mixture but is only an approximation otherwise, and write [M21, M22]

$$\frac{n_d + n}{(|\alpha'_{id}|)_{tr}} = \frac{n_d}{\alpha_{iL}} + \frac{n}{\alpha_{iR}} , \tag{69}$$

where α_{iL} and α_{iR} are the limiting values of $(|\alpha'_{id}|)_{tr}$ at low ($n \ll n_d$) and high ($n \gg n_d$) pressures, respectively. The subscripts L and R represent "Lorentz" and "Rayleigh", in recognition of H. A. Lorentz and Lord Rayleigh, who first studied (in other connections, to be sure) these special models — the Lorentz gas consists of a light particle moving through a bed of fixed scatterers, whereas the Rayleigh gas consists of a heavy particle moving through a swarm of much lighter particles. It is not at all obvious that Eq. (69) follows from Eq. (44), even for a binary mixture, but is nevertheless correct. For a multicomponent mixture, α_{iR} depends in general on the gas composition, but α_{iL} does not, because in the Lorentz limit the light particles interact only with the dust particles, not with each other. All of these complications are of little consequence in practical cases, where it is usually necessary to absorb the quantities n_d, ξ_i, α_{iL}, and α_{iR} into empirical constants. In particular, it is only the small term Δ'_{id} that is at issue here, and Eqs. (68) and (69) can be combined to yield

$$\frac{1}{1-\Delta'_{id}} = \frac{1 + (\pi_i/p)}{1 + (\pi'_i/p)} , \tag{70}$$

where π_i and π'_i have the dimensions of pressure and are defined as

$$\pi_i \equiv (\alpha_{iR}/\alpha_{iL})\, n_d k_B T , \tag{71}$$

$$\pi'_i \equiv \pi_i \left(1 - \frac{1}{5}\xi_i \alpha_{iL}\right) . \tag{72}$$

Since the total variation with pressure given by the right-hand side of Eq. (70) is only of the order of 10%, and the effect of α_{iR} vanishes at both very low and very high pressures, the composition dependence of α_{iR} is not expected to matter much.

The thermal diffusion factors $(\alpha'_{ij})_{tr}$ and $(\alpha'_{id})_{tr}$ that occur directly in Eq. (63), rather than in a small term like Δ'_{id}, require more careful treatment. It is necessary to use the full complexity of Eq. (44), inserting expressions for the gas-dust interaction terms where they occur. (No dust-dust interactions occur because of assumption (3) that was made in passing to the dusty-gas limit, viz., that the dust is stationary.) This is carried out in connection with specific cases in Chapter III, and there are no simplifications to be made at this point. However, it is worthwhile to note the values of α_{iL} and α_{iR} for binary mixtures (dust plus a single gas), since they are needed in the treatment of thermal transpiration. For elastic gas-dust collisions without long-range interactions, these limiting values are [M21, M22]

$$\alpha_{iL} = 1/2 , \tag{73}$$

$$\alpha_{iR} = \frac{1}{5} \frac{(\lambda_{ii})_{tr}/k_B}{n[\mathcal{D}_{id}]_1} . \tag{74}$$

The expression for α_{iR} follows directly from Eq. (44), and is, like it, only a kinetic-theory first approximation; the error is, however, probably less than 2%. The expression for α_{iL}, on the other hand, is an exact result, and is used because Eq. (44) is least accurate in the Lorentz limit.

This completes the kinetic-theory part of the problem; it only remains to perform straightforward mathematical manipulations to obtain explicit results corresponding to particular special cases. This is done in Chapter III. In the remainder of this chapter we consider the separate problem of the geometrical structure of the porous medium.

C. STRUCTURE OF THE POROUS MEDIUM

There are three major parameters characterizing the porous medium, according to both the elementary arguments and the dusty-gas model — the Knudsen permeability coefficient K_0 [which is related to the Knudsen diffusion coefficient by Eq. (6)], the viscous-flow parameter B_0, and the porosity-tortuosity factor ε/q. There are also additional minor parameters, like π_i and π_i' in Eq. (70), which depend on details of the gas-surface collisions, and which give rise to subsidiary phenomena like the Knudsen permeability minimum. (For the present discussion we ignore surface diffusion.) Much effort has been devoted to the problem of predicting values of K_0, B_0, and ε/q, given some sort of information about the geometrical structure of the porous medium, or some idealized mathematical model of the structure. Many such models have been proposed, including bundles of parallel capillaries, beds of randomly packed spheres, and so on [C1].

From a practical point of view, it is undoubtedly best to determine these parameters directly by experiment. Such experiments are usually easier to conduct than are the measurements that are required to determine the structure of the porous medium, which are otherwise needed for any theoretical calculation. Direct measurements are certainly more reliable than are calculations based on some model chosen at least partly for reasons of mathematical tractability. Where models are perhaps most valuable is in the prediction of transport parameters when only meager experimental information is available. For instance, the parameters K_0 and B_0 can be determined by permeability measurements conducted with a single gas whose molecular weight and viscosity are known. As will be seen in Chapter III, B_0 is found from the slope and K_0 from the intercept of a plot of the permeability coefficient vs. average pressure, so that as few as two permeability measurements may be sufficient. The determination of ε/q requires at least one diffusion measurement; since this may be more troublesome than permeability measurements, it would be convenient if ε/q could be calculated from values of K_0 and B_0 rather than having to be measured directly. In the first part of this section we show how a

structural model can indeed be used to get by with fewer than the minimum number of measurements required to determine all of the parameters experimentally.

However, a tacit assumption is often made about the effect of the structure of the porous medium on gas transport, which conceals a deeper and more serious problem than that of calculating parameters from structural models. Buried in almost all of the discussion thus far is the assumption of effective homoporosity of the medium — that is, the assumption that a porous medium can be characterized by only three major parameters. Even when heteroporosity is explicitly recognized, it is usually assumed that taking suitable average values of the parameters over the pore-size distribution suffices to describe the transport; in other words, the **heteroporosity** is assumed to be equivalent to an effective homoporosity [C8]. This is true as long as the fluxes are linear in the overall concentration or pressure differences, but not otherwise. In **combined flow and diffusion**, the **species fluxes** are **nonlinear** functions of the **total flow** or **pressure difference**, and this assumption fails. There have been surprisingly few general attempts to deal with this problem. The usual approach is to assume specific structural models and investigate the effects of heteroporosity by direct computation [F1, F2]. The formulas obtained tend to be fearsomely complicated in appearance, and resort to a computer follows. What is surprising is that complicated formulas for heteroporous media may have rather simple lower and upper bounds, at least for a large class of structural models, and the homoporous formula is the lower bound. These results do not seem to be widely known, and are discussed in the second part of this section. They at least make plausible the apparently unreasonably good results often obtained with the assumption of effective homoporosity.

Finally, we should mention that one additional fundamental assumption is almost always made, and which we shall also make. This assumption is that the transport inside the porous medium can be treated as one-dimensional, at least in some locally-averaged sense. Thus, gradient terms like $\langle \nabla n_i \rangle$ or ∇p can be replaced by $\partial n_i/\partial z$ or $\partial p/\partial z$.

1. Transport Parameters from Structural Models

Suppose for simplicity that the porous medium consists of a number of non-interconnected circular capillaries of radius r, having lengths L_{eff} as indicated in the lower part of Fig. 3. Further suppose that each pore of area πr^2

is contained in superficial area A of the material. Then a block of material of superficial volume AL actually has a void volume of $\pi r^2 L_{eff}$, so the porosity ε is

$$\varepsilon = \pi r^2 L_{eff}/AL \ . \tag{75}$$

The tortuosity q will obviously be related in some way to the ratio L_{eff}/L. To find the relation, let us calculate the value of B_o, which for one capillary is equal to $r^2/8$. The flux of the viscous-flow component is given by Eq. (11) or (51); per unit area of superficial surface the relation becomes

$$J_{visc} = -\frac{\pi r^2}{A}\left(\frac{n}{\eta}\right)\left(\frac{r^2}{8}\right)\frac{\partial p}{\partial z_{eff}} \ , \tag{76}$$

where z_{eff} is measured along the path of the pore. Converting z_{eff} to z, measured straight through the medium, by multiplying by L/L_{eff}, we obtain

$$J_{visc} = -\frac{\pi r^2}{A}\left(\frac{n}{\eta}\right)\left(\frac{r^2}{8}\right)\left(\frac{L}{L_{eff}}\right)\frac{\partial p}{\partial z} \ . \tag{77}$$

Substituting for ε from Eq. (75), we find the effective value of B_o to be

$$B_o = \frac{\varepsilon}{(L_{eff}/L)^2}\left(\frac{r^2}{8}\right) = \frac{\varepsilon}{q}\left(\frac{r^2}{8}\right) \ . \tag{78}$$

Notice that $q = (L_{eff}/L)^2$, and that the square arises because L_{eff}/L appears twice, once in connection with the gradient and once in connection with the void volume.

A similar calculation for Knudsen flow yields

$$K_o = (\varepsilon/q)(r/2) \ , \tag{79}$$

and for diffusive transport yields

$$D_{12} = (\varepsilon/q)\mathcal{D}_{12} \ . \tag{80}$$

Combination of Eqs. (78) and (79) gives an expression for ε/q,

$$\varepsilon/q = K_o^2/2B_o \ , \tag{81}$$

so that ε/q can be calculated from permeability measurements alone. Relations like Eq. (81) can be very useful when maximum accuracy is not required. Although they often give reasonable results (i.e., within a factor of 2 or better), their accuracy cannot be relied upon; deviations up to a factor of 5 have been reported.

Several modifications of Eq. (81) have been made to improve accuracy, or at least to explain observed inaccuracies, as follows: modification of K_o for the Knudsen permeability minimum, correction for noncircular cross section and for bends in the pore, and correction for a distribution of pore sizes. Let us consider these modifications in order. The value of $K_o = r/2$ holds for a straight circular capillary only in the limit of perfect free-molecule flow with diffuse gas-surface scattering. Extrapolation of the permeability measured at higher pressures to the zero-pressure intercept yields a lower value, $[K_o]_1$, that corresponds to the first approximation for the Knudsen diffusion coefficient rather than the exact value. It is customary to write

$$[K_o]_1 = K_o \delta \ , \tag{82}$$

where the factor δ is related to the "slip correction" for flow in the transition region. The value of δ is $3\pi/16 = 0.59$ according to Maxwell's theory of slip, about 0.81 according to Knudsen's experimental results, and according to Eqs. (70)–(72) of the dusty-gas model is

$$\delta = \pi_1'/\pi_1 = 1 - \frac{1}{5}\,\xi_1\,\alpha_{1L} \approx 0.9 \ , \tag{83}$$

for all diffuse scattering. If only a fraction $\underline{f}$ of the gas molecules are scattered diffusely, the value of δ is multiplied by a factor $(2-f)/f$. Since it is $[K_o]_1$ rather than K_o that is usually measured, Eq. (81) should be rewritten to recognize that fact.

Deviations from circular cross section change the numerical factor of 2 in the denominator of Eq. (81); bends along the length of the pore presumably have a similar effect. Thus the factor of 2 can be replaced by a numerical constant k_o, a "shape factor," to allow for variations in geometrical shape. A value of $k_o = 2.5$ has been widely used in practice.

Finally, a distribution of pore sizes affects K_o and B_o differently. The total viscous flow through a capillary is proportional to r^4; for a distribution of capillary sizes the flow is therefore proportional to $\langle r^4 \rangle$, where the angular brackets signify an average over the pore-size distribution. The open area is proportional to $\langle r^2 \rangle$, so that the flow per unit area, and hence B_o, is proportional to $\langle r^4 \rangle / \langle r^2 \rangle$. Similarly, K_o is proportional to $\langle r^3 \rangle / \langle r^2 \rangle$, so that

$$\frac{K_o^2}{B_o} \propto \frac{\langle r^3 \rangle^2}{\langle r^2 \rangle \langle r^4 \rangle} \equiv \frac{1}{\sigma_r} < 1 \ , \tag{84}$$

where σ_r is a measure of the spread in pore size, and is necessarily greater than unity (equal to unity for the homoporous case). Notice that we have made the assumption of effective homoporosity here, which is legitimate because the permeability equation is linear (i.e., the total flux is proportional to the pressure difference even for large pressure differences).

Combining these modifications, we obtain [H15]

$$\frac{\epsilon}{q} = \frac{\sigma_r [K_o]_1^2}{k_o B_o \delta^2} \ , \tag{85}$$

a useful result, but one which should still not be trusted too far. For example, with $\sigma_r = 1$ and $f = 1$, the right-hand side of Eq. (85) is often much larger than the directly measured value of ϵ/q. Although $\sigma_r > 1$, it would still be necessary to believe that f is appreciably less than unity to obtain agreement, which conflicts with much experimental knowledge on gas-surface interactions. Presumably the model leading to Eq. (85) is deficient. In this connection, it is worth noting that ϵ/q is not necessarily much trouble to measure directly; diffusion measurements of useful accuracy can often be made for porous media by minor modification of Graham's original method [E3].

2. Effect of Heteroporosity on Flux Equations

We have already mentioned that heteroporosity causes no difficulties as long as the flux equations remain linear after integration (all the flux equations are of course linear in their differential form). The only

effect is that the parameters K_0, B_0, and ϵ/q are replaced by averages over the pore-size distribution — the form of the equations themselves does not change. In particular, free-molecule flow and viscous flow are not affected. The main difficulty arises with coupled flow and diffusion, which is not linear when the total flux is large. To illustrate the problem, consider a binary mixture at constant temperature undergoing simultaneous flow and diffusion in the continuum region, where Knudsen effects are negligible. The flux equation for species 1 becomes

$$\underset{\sim}{J}_1 = - D_{12} \underset{\sim}{\nabla} n_1 + x_1 \underset{\sim}{J} , \tag{86}$$

which, for pressure gradients that are not too large, can be written (in one dimension) as

$$J_1 = - nD_{12} \frac{\partial x_1}{\partial z} + x_1 J . \tag{87}$$

At the steady state, J_1 and J are constant along the length of the pore, nD_{12} is constant except for a weak composition dependence, and thus Eq. (87) can be integrated over the length of a single pore to yield

$$J_1 = J x_1^0 - \frac{J(x_1^L - x_1^0)}{\exp(JL/nD_{12}) - 1} , \tag{88}$$

where x_1^0 and x_1^L are the mole fractions at the entrance and exit. Clearly J_1 is not linear in J, so the addition of the fluxes through a collection of pores to find a total flux leads to an equation of apparently radically different form than Eq. (88), namely a sum of terms each with a different exponential in the denominator.

The question is thus how much error is likely to be involved in applying the assumption of effective homoporosity to such a heteroporous situation — that is, in replacing the sum of terms by a single "effective" term. To investigate this question, we will consider steady-state isothermal binary diffusion in the continuum region. Although this is not the most general case, it is probably one of the worst cases possible, since free-molecule and viscous flows are linear even for large flows. (At any rate, it seems to contain all the essential difficulties.) Somewhat surprisingly, it

turns out that the maximum relative deviations from homoporous behavior result only from rather bizarre pore-size distributions, and are only moderately large; most distributions introduce only small errors [W6].

We begin with the simple model of a parallel array of uniform pores, and then build up more complicated geometries by series-parallel combinations of pore segments of various lengths and cross-sectional areas. Finally, we allow internal cross-connections among pores, so that the model hopefully embodies sufficient geometric complexity to mimic structures of real porous media.

a. Parallel Pores. We consider a parallel array of separate pores, each with its own length, and with its own cross-sectional geometry (or ϵ/q) along its entire length. To try to keep the notation unambiguous, we use lower-case j's for fluxes in individual pores, and capital J's for overall fluxes across the whole porous medium. The flux of species 1 through a pore of any particular type $\underline{i}$, $j_1^{(i)}$, is given by Eq. (88), which we rewrite as

$$j_1^{(i)} = j^{(i)} x_1^0 - \frac{j^{(i)} \Delta x_1}{\exp\,(j^{(i)}/P_i) - 1} \quad , \tag{89}$$

where $j^{(i)}$ is the total flux through the pore, and $P_i = nD_{12}^{(i)}/L_i$ is a diffusive permeability coefficient. The measured flux of species 1 across unit area of the whole porous medium, J_1, is related to $j_1^{(i)}$ by

$$J_1 = \sum_i \nu_i a_i j_1^{(i)} \quad , \tag{90}$$

where ν_i is the number of pores of type $\underline{i}$ per unit area of the septum, and a_i is the area of a pore of type $\underline{i}$. Combining Eqs. (89) and (90) we obtain

$$J_1 = x_1^0 \sum_i \nu_i a_i j^{(i)} - \Delta x_1 \sum_i \frac{\nu_i a_i j^{(i)}}{\exp(j^{(i)}/P_i) - 1} \quad . \tag{91}$$

Since the total flux J is given by

$$J = \sum_i \nu_i a_i j^{(i)} \quad , \tag{92}$$

the first term on the right-hand side of Eq. (91) could be replaced by the measurable quantity $x_1^0 J$. But the second term cannot be simply expressed, nor can it be evaluated without knowledge of ν_i, a_i, P_i, and $j^{(i)}$. It thus appears that we cannot write a simple integrated flux equation for a heteroporous medium without considerable information about the structure. However, the summation of the second term can usually be replaced by a single term to a good approximation, and definite bounds can be placed on the resulting error [W6].

To demonstrate this result, consider first the special case of a homoporous membrane, for which Eq. (91) does reduce to the simple form of Eq. (88). The $j^{(i)}$ are then all equal, as are the P_i, which can be written in terms of an overall permeability coefficient,

$$P \equiv \sum_i \nu_i a_i P_i \ . \tag{93}$$

Then Eq. (91) reduces to

$$J_1^{(0)} = J x_1^0 - \frac{\Delta x_1 J}{\exp(J/P) - 1} \ , \tag{94}$$

where the superscript $^{(0)}$ designates the homoporous result. The question is now as follows: how good (or how bad) is $J_1^{(0)}$ as an approximation to the true J_1 of Eq. (91)? The overall coefficient P for a heteroporous membrane would of course be determined experimentally by measurement of J_1 in the pure diffusion limit, where all $j^{(i)}$ are zero, for which Eq. (91) becomes, on expanding the exponential,

$$J_1 = - \Delta x_1 \sum_i \nu_i a_i P_i = - \Delta x_1 P \ . \tag{95}$$

We shall show that $J_1 \geq J_1^{(0)}$ at any given values of x_1^0, x_1^L, and J; that is, the curve of $J_1^{(0)}$ vs. J is a lower bound for all possible curves of J_1 vs. J obtained by varying the pore-size distribution at fixed x_1^0 and x_1^L.

To prove this result, it is convenient to use dimensionless variables defined as follows:

$$\alpha_i \equiv j^{(i)}/P_i \ , \tag{96}$$

$$\beta_i^o \equiv \nu_i a_i P_i/P \ , \tag{97}$$

$$Y \equiv J_1/x_1^0 P \ . \tag{98}$$

We may consider α_i as a statistical variable and the β_i^o as weight factors, and define α as an average of α_i with these weight factors,

$$\alpha = \langle\alpha_i\rangle \equiv \sum_i \beta_i^o \alpha_i = J/P \ . \tag{99}$$

Note that $\Sigma\beta_i^o = 1$. Similarly, if we define a function $\phi(\alpha_i)$ as

$$\phi(\alpha_i) \equiv \alpha_i - \frac{\Delta x_1}{x_1^0}\left[\frac{\alpha_i}{\exp\ \alpha_i - 1}\right] \ , \tag{100}$$

then we see from Eq. (91) that Y is the average of $\phi(\alpha_i)$ with the β_i^o as weight factors,

$$Y = \sum_i \beta_i^o \alpha_i - \frac{\Delta x_1}{x_1^0} \sum_i \beta_i^o \left[\frac{\alpha_i}{\exp\ \alpha_i - 1}\right]$$

$$= \sum_i \beta_i^o \phi(\alpha_i) \equiv \langle\phi(\alpha_i)\rangle \ . \tag{101}$$

From Eq. (94) we see that $Y^{(0)}$ is

$$Y^{(0)} \equiv J_1/x_1^0 P = \alpha - \frac{\Delta x_1}{x_1^0}\left[\frac{\alpha}{\exp\ \alpha - 1}\right] , \tag{102}$$

where α is given by Eq. (99). That is, $Y^{(0)}$ is a function of $\alpha = \langle\alpha_i\rangle$ with the same functional form as ϕ ,

$$Y^{(0)} = \phi\,(\langle\alpha_i\rangle) \ . \tag{103}$$

In other words, in comparing Y with $Y^{(0)}$ we are comparing the average of a function of α_i with the function of the average of α_i. These two averages are related through a mathematical theorem known as Jensen's inequality.

In its simplest form, Jensen's inequality states that the average of a function of a set of variables α_i is always greater than or equal to the function of the average of α_i, provided only that the function of α_i is everywhere concave upward (positive second derivative). The set of α_i may be continuous or discrete, and any set of non-negative weighting factors may be chosen to define the averages. The function $\phi(\alpha_i)$ considered here is everywhere concave upward provided that $\Delta x_1 = x_1^L - x_1^0 \lesssim 0$ (which can always be arranged by proper choice of the direction of the z-axis); this can easily be proved analytically and is illustrated in Fig. 4. Thus Jensen's inequality applies, and we find

$$\langle\phi(\alpha_i)\rangle \geq \phi\,(\langle\alpha_i\rangle) \ , \tag{104}$$

or

$$Y \geq Y^{(0)} \quad , \quad J_1 \geq J_1^{(0)} \ . \tag{105}$$

That is, the homoporous result is a lower bound to the exact but impractical result given by Eq. (91). If we can also find an upper bound for Y, then we can establish the maximum error possible when $Y^{(0)}$ or $J_1^{(0)}$ is used as a flux equation for heteroporous media.

An upper bound in the region $\alpha > 0$ can be determined by consideration of the behavior of Y for $\alpha \to 0$ and for $\alpha \to \infty$, and by noting that Y is always concave upward because it is a sum of everywhere concave-upward functions $\phi(\alpha_i)$ multiplied by positive numbers β_i^o. First we consider the case where all the α_i become large. Then the summation containing the exponential in Eq. (101) becomes negligible and $Y \to \alpha$; thus the slope of the curve of Y vs. α approaches unity for large α. Next we consider the other end of the curve, where all $\alpha_i \to 0$. Here the exponential terms in Eq. (101) can be expanded to show that Y becomes linear in α,

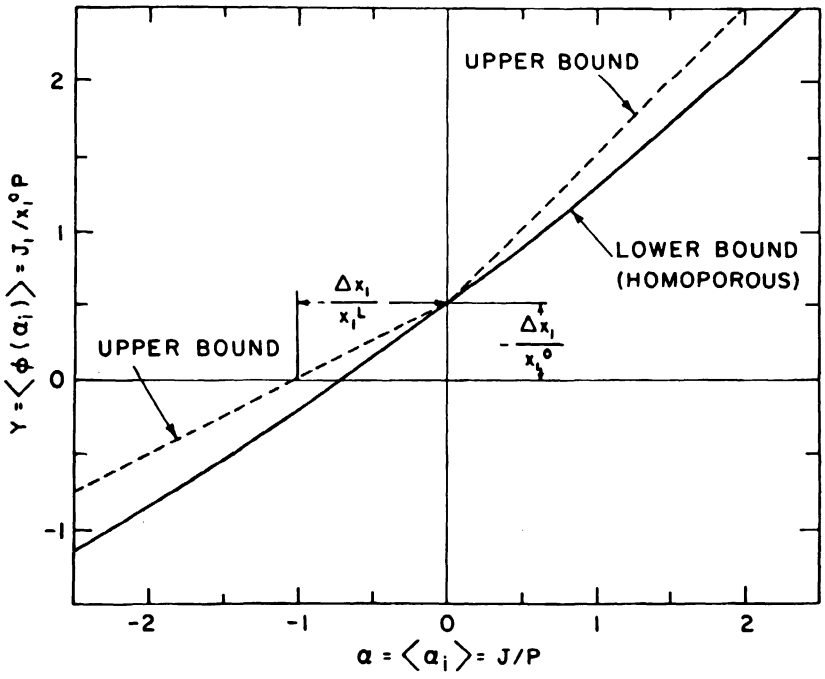

Fig. 4. Species flux versus total flux (in dimensionless form) for coupled flow and diffusion, showing bounds for heteroporosity. The curve for a heteroporous medium of any pore-size distribution must lie within the indicated regions. The concentration difference illustrated is for $\Delta x_1/x_1^0 = -0.5$.

$$Y \to \frac{1}{x_1^0}\left[\frac{1}{2}(x_1^0 + x_1^L)\,\alpha - \Delta x_1\right] \quad \text{for } \alpha \to 0 \,. \tag{106}$$

This is the equation of a straight line whose intercept is $-\Delta x_1/x_1^0$ and whose slope is $(x_1^0 + x_1^L)/2x_1^0$, which is less than unity because $x_1^0 > x_1^L$. Thus the curve of Y vs. α must start at $Y = -\Delta x_1/x_1^0$ and $\alpha = 0$ with a positive slope less than unity, and must eventually reach a constant slope of unity while always remaining concave upward, irrespective of the

values of β_1^o and hence independent of the nature of the pore-size distribution. We conclude from these statements that Y vs. α must always lie below a straight line passing through $Y = \Delta x_1/x_1^0$ at $\alpha = 0$ and having a slope of unity. That is, the upper bound on Y is the straight line,

$$Y = \alpha - \Delta x_1/x_1^0 \quad \text{for} \quad \alpha > 0 \quad . \tag{107}$$

This bound is illustrated in Fig. 4. It is now easy to find the maximum possible error involved in using $Y^{(0)}$ to approximate Y for $\alpha > 0$; it is just the maximum of the function $(Y - Y^{(0)})/Y$ with respect to α at a given $\Delta x_1/x_1^0$, where Y is given by Eq. (107) for the upper bound. This maximization is easily carried out numerically, and the corresponding maximum relative errors are given in Table 2 for several values of $\Delta x_1/x_1^0$. The largest possible relative error that can occur if the homoporous flux equation is used for a heteroporous medium is seen to be 23%, which occurs at $\alpha = 1.793$ for $-\Delta x_1/x_1^0 = 1$ (i.e., for $x_1^L = 0$). At smaller values of $-\Delta x_1/x_1^0$ the maximum relative error is less.

TABLE 2. Maximum possible relative errors from the use of the homoporous flux equation for a heteroporous medium (isothermal, continuum, binary diffusion)

$-\Delta x_1/x_1^0$	Max. $\alpha = J/P$	Max. $(J_1-J_1^{(0)})/J_1$
0	0	0
0.2	0.935	0.070
0.4	1.251	0.121
0.6	1.472	0.163
0.8	1.647	0.195
1.0	1.793	0.230

For negative values of α, i.e., when the net flow J is directed against the concentration gradient, the lower bound for Y is still $Y^{(0)}$ but now the upper bound is the straight line

$$Y = (x_1^L/x_1^0)\alpha - \Delta x_1/x_1^0 = (1 + \Delta x_1/x_1^0)\alpha - \Delta x_1/x_1^0 \quad , \text{ for } \alpha < 0 \quad , \tag{108}$$

as shown in Fig. 4. Here $x_1^L/x_1^0 = 1 + \Delta x_1/x_1^0$ is the limiting slope

obtained from Eq. (101) when all the α_i are large but negative. The difference between the upper and lower bounds is now

$$Y - Y^{(0)} = -\frac{\Delta x_1}{x_1{}^0}\left[1 - \frac{\alpha e^{\alpha}}{e^{\alpha}-1}\right], \text{ for } \alpha < 0 , \tag{109}$$

but a relative error calculation is not reasonable because both the upper bound and lower-bound curves cross the α-axis, and the relative error would become infinite. However, the maximum absolute error as given by Eq. (109) is still $-\Delta x_1/x_1{}^0$, the same as it was when α was positive.

An example of a pore-size distribution giving a flux approximately the same as the upper bound is one consisting of a few large pores and a large number of small pores. In such a case most of the open area is associated with the small pores, but most of the volume flow is through the large pores. For a numerical example, suppose 95% of the open area is associated with small pores, but that the radii of the two sets of pores are such that, at any given pressure difference, one large pore carries 1000 times as much volume flow as one small pore. Then direct numerical computation with Eq. (91) or (101) shows that the true $Y(\alpha)$ or $J_1(J)$ curve is never more than about 5% below the upper-bound straight line. That is, the flux J_1 for a medium with a few relatively large pores will quickly deviate from the homoporous approximation and approach $x_1{}^0 J$. A practical example would be a porous medium having a few large cracks or holes.

Although the above example shows that the upper bound can be approached, the pore-size distribution involved is rather special. A more interesting case is one with a very broad, but unimodal, distribution of pore sizes. As an extreme example of such a distribution, we choose a flat distribution such that each pore size represents the same total open area as any other pore size (i.e., $\nu_i a_i$ = constant). For this example we also assume that the pore area increases linearly with index number i, $a_i \propto i$ up to some maximum size at $i = i_{max}$, and that all diffusive permeability coefficients P_i are the same. We further suppose that the volume flow through any pore type follows Poiseuille's law, so that $j^{(i)} \propto a_i$, and that the distribution is smooth enough to replace summations by integrations. On applying these assumptions to Eq. (101) and carrying out some straightforward mathematical manipulations, we obtain an integral corresponding to one of the Debye functions. Direct numerical computation then shows that the result is

never more than 4% above the lower bound. Thus the homoporous approximation should be quite accurate for many types of heteroporous media.

b. Pores in Series. We consider now the integrated flux equation for a pathway consisting of ν pores in series, as shown in Fig. 5. Each pore segment $\underline{i}$ has its particular values of $j_1^{(i)}$, $j^{(i)}$, and P_i. For boundary conditions, we assume that the concentration of each species is continuous; that is, that the concentration at the end of one pore segment is the same as just inside the entrance of the next pore segment. This is probably not a very restrictive assumption for gases in porous media, but is a more serious matter for membranes, where solute rejection (sieving) at a pore entrance is a common phenomenon (see Chapter IV). To condense the notation a bit, we let c_i be a mole fraction of species 1, x_1, at the entrance to pore segment $\underline{i}$ (and at the exit of segment i-1, by assumption). Then $c_1 = x_1^0$, the mole fraction at the entrance of the first pore segment, and $c_{\nu+1} = x_1^L$, the mole fraction at the end of the last pore segment. We also let total flow rates be denoted by Q's, and reserve j's and J's for fluxes (flow rate per unit area). We shall show that the flux equation for such a series-pore model is exactly the same as for a single uniform pore [D7, W6].

At steady state, the flow rate of species 1, Q_1, and the total flow rate, Q, must be constant throughout all the pore segments,

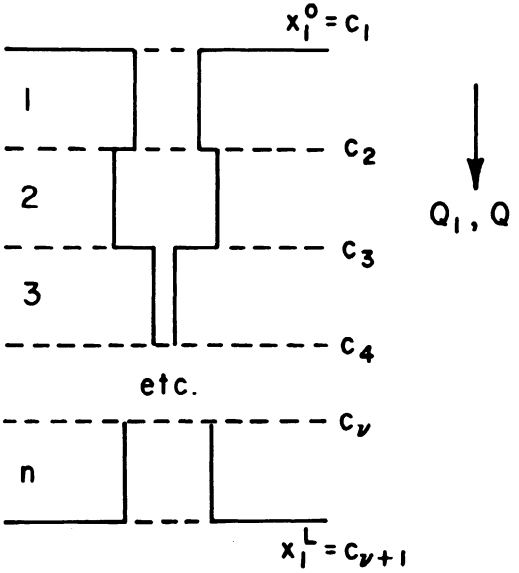

Fig. 5. Pore segments in series, with no discontinuities of concentration.

$$Q_1 = a_1 j_1^{(1)} = a_2 j_1^{(2)} = \ldots a_\nu j_1^{(\nu)} , \tag{110}$$

$$Q = a_1 j^{(1)} = a_2 j^{(2)} = \ldots a_\nu j^{(\nu)} . \tag{111}$$

The flow rate of species 1 through any pore segment $\underline{i}$ is obtained from Eq. (89) as

$$Q_1 = Qc_i - \frac{Q(c_{i+1} - c_i)}{\exp(Q/a_i P_i) - 1} , \tag{112}$$

which can be solved for c_{i+1} to yield

$$c_{i+1} = c_i e^{\alpha_i} - (e^{\alpha_i} - 1)(Q_1/Q) , \tag{113}$$

where $\alpha_i = j^{(i)}/P_i = Q/a_i P_i$, as previously defined in Eq. (96). We wish to eliminate algebraically all the intermediate concentrations c_i, leaving only the concentrations at the ends, $c_1 = x_1{}^0$ and $c_{\nu+1} = x_1{}^L$. From Eq. (113) we obtain

$$c_2 = c_1 e^{\alpha_1} - (e^{\alpha_1} - 1)(Q_1/Q) ,$$

$$c_3 = c_2 e^{\alpha_2} - (e^{\alpha_2} - 1)(Q_1/Q)$$

$$= c_1 e^{\alpha_1+\alpha_2} - (Q_1/Q)e^{\alpha_1+\alpha_2} + (Q_1/Q) ,$$

whence, by induction, it is easy to prove that

$$c_{\nu+1} = c_1 \exp(\sum_{i=1}^{\nu} \alpha_i) - (Q_1/Q) \exp(\sum_{i=1}^{\nu} \alpha_i) + (Q_1/Q) . \tag{114}$$

This can be rewritten, with $c_1 = x_1{}^0$ and $c_{\nu+1} = x_1{}^L$, as

$$Q_1 = Qx_1{}^0 - \frac{Q(x_1{}^L - x_1{}^0)}{\exp(\Sigma\alpha_i) - 1} . \tag{115}$$

This has the same mathematical form as the corresponding expression for a

single uniform pore; all that is needed to prove complete identity of the two expressions is a suitable identification of $\Sigma\alpha_i$.

Since $\Sigma\alpha_i$ contains the P_i, it represents the effect of diffusion in Eq. (115), and it is logical to identify it with measurable quantities by passing to the pure diffusion limit, $Q \to 0$, whereby Eq. (115) becomes

$$Q_1 = -Q\Delta x_1/(\Sigma\alpha_i) = -\Delta x_1/[\Sigma(1/a_iP_i)] \ . \tag{116}$$

Let the "measured" area of the pathway be A; the observed diffusive permeability P would then be defined by

$$Q_1 = -AP\Delta x_1 \ . \tag{117}$$

Comparing Eqs. (116) and (117) we find

$$1/AP = \Sigma\ (1/a_iP_i) \ , \tag{118}$$

or

$$\Sigma\alpha_i = Q\ \Sigma\ (1/a_iP_i) = Q/AP = J/P \ . \tag{119}$$

Thus the flux equation for a pathway consisting of pores in series is identical with that for a single uniform pore.

c. Interconnections of Pores. Very complicated structures can be built up by cross-connecting a series-parallel array of pore segments of various lengths and cross sections. A mathematical analysis of such structures would at first sight seem impossible, but we can show that the same bounds hold for them as hold for the simpler structures considered thus far, provided of course that no discontinuities of concentration occur and that a one-dimensional treatment can be used in each pore segment [W6].

Because pores in series obey the same equations as a single uniform pore, every nonbranching segment in the structure can be replaced by an equivalent uniform pore segment. This first step in the analysis removes from consideration all nonuniformities of cross section between internal junction points. Unequal pore segment lengths between junctions are absorbed into the individual P_i.

because of the choice of permeability coefficients. But as J is increased into the non-linear regime, J_1 tends to increase more for a heteroporous slab than for a homoporous one, with the result that the overall J_1 for the heteroporous array can only be greater than that for the homoporous array. The fact that the intermediate concentrations c_i between the slabs become different at higher J for the two arrays does not affect the sign of this inequality. Thus the homoporous array gives a lower bound for the flux through the heteroporous array, and we have the same lower bound as before. We can also show that the same upper bound holds as before, namely Eqs. (107) and (108). We note that $J_1 \to x_1^0 J$ as $J \to \infty$ for the heteroporous array, and then the argument proceeds exactly as for a single slab.

We now construct a general proof by showing that any interconnected pore structure can be reduced, in an appropriate sense, to the above special case of a series array of porous slabs. We give first an explicit demonstration of this for the simple case of two parallel pores connected by one internal shunt, as shown in Fig. 7a; the extension of the proof to more elaborate structures is then straightforward. In Fig. 7b the pore structure is redrawn to emphasize the junction points. This structure apparently differs in a fundamental way from the previous one shown in Fig. 6a, for two of the junction points are each connected to three other junction points. However, a simple construction shows that the two structures are in a sense equivalent. Suppose the concentration at the upstream

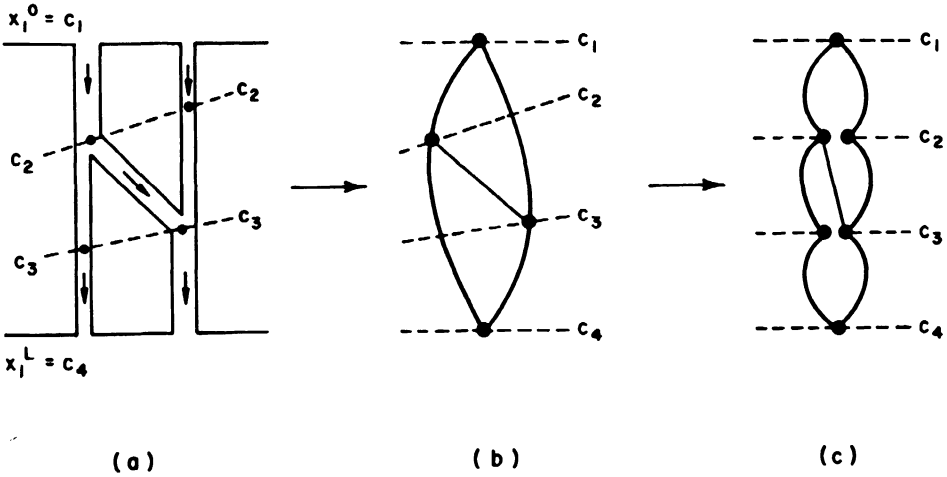

Fig. 7. Schematic diagram of a pore structure whose internal connections are more complex than those of Fig. 6. This structure is equivalent, in a sense discussed in the text, to a peculiar kind of series array of slabs.

internal junction point is c_2; there is then some point in the parallel pore that also has the concentration c_2, and we pass a hypothetical plane through these two points as shown in Figs. 7a and 7b. Similarly, we pass another hypothetical plane through the points of concentration c_3, the concentration at the downstream internal junction point. These two planes divide the structure into three slabs as shown in Fig. 7c. It should be recognized that this is not entirely the same as the special case of Fig. 6. The pressures at the points of equal concentration are not necessarily equal, and we could not connect these points physically without altering the overall flow pattern. In other words, the structures in Figs. 6 and 7 really are fundamentally different, in that their concentration and pressure distributions cannot in general both be made similar, although one or the other can be. But we are not concerned about pressure distribution here, we are concerned only with species flux and total flux, and Eq. (89) shows that pressure difference does not explicitly enter the expression for species flux in a given pore segment. Thus we are entitled to compare the upper "slab," between concentration surfaces c_1 and c_2 in Fig. 7, with a hypothetical homoporous slab having the same total flux, since the mathematical expression for species flux depends only on the variable j and not on the pressure distribution. This comparison shows that the species flux in the upper slab is equal to or greater than that in the hypothetical homoporous slab, by exactly the same reasoning used earlier to prove the lower bound for pores in parallel.

Continuing this line of reasoning for the rest of the "slabs" in Fig. 7, we conclude that the same lower bound on species flux holds for a porous medium with internal interconnections as holds for one without interconnections. A similar conclusion is reached for the upper bound, by the same method. That is, we note that the division of the interconnected porous medium into an array of slabs establishes that the curve of J_1 vs. J must be everywhere concave upward, and that $J_1 \to x_1^0 J$ as $J \to \infty$. The remainder of the argument then proceeds as before.

The extension of the simple case shown in Fig. 7 to more elaborate structures should now be apparent. A more complex structure is divided into effective slabs as follows: Proceeding downstream from the surface at $c_1 = x_1^0$, we find the internal junction point with the highest species 1 concentration; we call this concentration c_2, and pass a hypothetical surface through all the points in the structure where the concentration is c_2. This splits off the first slab. We then find the junction point downstream

that has the next highest concentration, which we call c_3, pass a hypothetical surface through all the points having concentration c_3, and thereby split off the second slab. Continuing through the membrane in this fashion, we eventually divide it into as many slabs as there are internal junction points having different species 1 concentrations, plus one more slab at the end, as shown in Fig. 7 for a structure with only two internal junction points. Once this subdivision is made, the rest of the argument proceeds exactly as for the structure of Fig. 7.

Thus the bounds on species flux as a function of total flux hold for porous media with internal connections. In this discussion we did not have to be concerned with matters such as dead-end pore segments, because we dealt only with steady-state operation. The arguments used obviously do not hold for transients, or for various other kinds of time-dependent operation. Such cases are much more complicated to analyze in detail, although a successful analysis would presumably yield structural information not available from analysis of just the steady state.

3. Remarks

The considerations in this discussion of the effects of internal structure on gas transport through a porous medium are independent of the main aim of the dusty-gas model, which is to write down the correct local (differential) equations for gas transport. The geometrical-structural part of the overall transport problem nevertheless has to be considered in any real application, and cannot be completely ignored. However, we believe that much past work on the structure of the medium has overemphasized the wrong part of the problem, namely, prediction of transport from a knowledge of the geometry, and has given scant attention to the more limited question of trying to establish bounds for reasonable cases. The foregoing discussion attempts to redress the balance somewhat, although it is clear that much remains to be done. Behavior in the transition region has not been touched upon, nor has anything more complicated than a binary mixture been considered.

We now return to the main theme of this monograph, and make use of the general transport equations for comparison with experiment. The appropriate equations are first summarized in the following section.

D. SUMMARY OF EQUATIONS

At this point, we summarize the transport equations as developed in the preceding discussions. Combining Eqs. (59) and (63), we can write the

transport equation for species i as follows:

$$\sum_{j=1}^{\nu} \frac{n_j}{nD_{ij}} \left(\frac{\underset{\sim}{J}_i}{n_i} - \frac{\underset{\sim}{J}_j}{n_j} \right) + \frac{1-\Delta'_{id}}{[D_{iK}]_1} \left[\frac{\underset{\sim}{J}_i}{n_i} + \frac{B_o}{n} (\underset{\sim}{\nabla} p - n\underset{\sim}{F}) \right] =$$

$$= - \underset{\sim}{\nabla} \ln(n_i/n) - \underset{\sim}{\nabla} \ln p + \underset{\sim}{F}_i/k_B T$$

$$- (n')^{-1} \left[\sum_{j=1}^{\nu} n_j (\alpha'_{ij})_{tr} + n_d (\alpha'_{id})_{tr} \right] \underset{\sim}{\nabla} \ln T \ , \quad i,j \neq d \ , \tag{120}$$

where

$$n\underset{\sim}{F} \equiv \sum_{j=1}^{\nu} n_j \underset{\sim}{F}_j \tag{121}$$

is the total force on the gas mixture per unit volume. Equations (37), obtained by momentum-transfer arguments, are a special case of this result, corresponding to isothermal conditions with no external forces, and with the coefficients D_{ij} and D_{iK} considered as purely phenomenological. There are ν equations like Eq. (120), one for each species (other than the "dust"), and they are all independent. This is the complete set of equations for steady-state or quasi-steady-state mass transport, and does not need to be supplemented by any additional equations of motion — the relevant equation of motion can be obtained by multiplying Eq. (120) by n_i/n and summing over all species i. If this is done, the terms involving D_{ij} sum to zero by symmetry, and the terms involving $(\alpha'_{ij})_{tr}$ vanish because $(\alpha_{ij})_{tr} = - (\alpha'_{ji})_{tr}$, as is obvious by inspection of Eq. (44). The result is, after a little rearrangement,

$$\sum_{i=1}^{\nu} \frac{\underset{\sim}{J}_i}{D_{iK}} = - \frac{1}{k_B T} (\underset{\sim}{\nabla} p - n\underset{\sim}{F}) \left(1 + \frac{pB_o}{n} \sum_{i=1}^{\nu} \frac{x_i}{D_{iK}} \right)$$

$$- (n_d/n') \left[\sum_{i=1}^{\nu} n_i (\alpha'_{id})_{tr} \right] \underset{\sim}{\nabla} \ln T \ , \tag{122}$$

where

$$D_{iK} \equiv [D_{iK}]_1/(1-\Delta'_{id}) \ . \qquad (123)$$

This is the forced-flow nonisothermal generalization of Graham's law of diffusion for multicomponent mixtures. The expressions for the coefficients appearing in the foregoing equations are given by Eqs. (64)–(74).

Equation (120) is a set of Stefan-Maxwell diffusion equations augmented by viscous-flow and thermal-diffusion terms. It is possible, by purely algebraic manipulation, to absorb the viscous-flow terms into the coefficients of the diffusion terms, giving a set of Stefan-Maxwell equations with "augmented" diffusion coefficients. In other words, the transport equations for coupled flow and diffusion can be made to appear like the transport equations for diffusion alone [M31, W15, W16]. The procedure is to solve Eq. (122) for $(\nabla p - n\underset{\sim}{F})$ and substitute back into Eq. (120); some algebraic manipulation then yields the result,

$$\sum_{j=1}^{\nu} \frac{n_j}{nE_{ij}}\left(\frac{J_i}{n_i} - \frac{J_j}{n_j}\right) + \frac{1}{E_{iK}}\frac{J_i}{n_i} = -\underset{\sim}{\nabla} \ln(n_i/n) - \underset{\sim}{\nabla} \ln p + \underset{\sim}{F}_i/k_BT$$

$$-(n')^{-1}\left[\sum_{j=1}^{\nu} n_j(\alpha'_{ij})_{tr} + n_d\theta_{id}\right] \underset{\sim}{\nabla} \ln T \ , \qquad (124)$$

where the "augmented" coefficients are defined by the equations

$$E_{iK} = D_{iK}\left(1 + \frac{pB_o}{\eta}\sum_{k=1}^{\nu}\frac{x_k}{D_{kK}}\right), \qquad (125) \Longrightarrow F$$

$$\frac{1}{E_{ij}} = \frac{1}{D_{ij}} + \frac{pB_o}{\eta E_{iK}D_{jK}} \ , \qquad (126) \Longrightarrow P$$

$$\theta_{id} = (\alpha'_{id})_{tr} - \frac{pB_o}{\eta E_{iK}}\sum_{k=1}^{\nu} x_k(\alpha'_{kd})_{tr} \ . \qquad (127)$$

Note that only the thermal diffusion factors $(\alpha'_{ij})_{tr}$ are not affected by this transformation.

Other mathematical transformations of Eq. (120) are of course possible, and sometimes yield useful forms (e.g., Nernst-Planck equations) [M31], bu we do not pursue this aspect here.

Chapter III

EXPERIMENTAL TESTS OF THE THEORY

Many experiments have been conducted on the motion of gases in various porous media, and it is not our intention to attempt a comprehensive survey of all such experimental studies. Instead, in this chapter we discuss only a small selection of measurements that actually serve to test the dusty-gas model, and do not attempt to give a complete review of even this small subset. (We apologize in advance to those workers whose results have been bypassed in our somewhat parochial selection of data.)

To test a theory whose mathematical formulation involves the use of adjustable parameters, we must have more measurements than the minimum necessary just to determine the parameters. This requires a comprehensive set of measurements on a single sample of a porous medium. Although many experimental determinations have been made, it is rare that a variety of measurements have been made on the same porous medium. Thus real tests of the theory (as opposed to mere exercises in curve-fitting) are comparatively rare. It is also difficult to keep separate two fundamentally different aspects of the theory, namely, the gas-transport part of the theory as opposed to the geometrical-structural part that refers to the porous medium. In many cases reported in the literature, it is not clear whether it is the transport equations themselves that are being tested, whether it is the approximation of effective homoporosity for the porous medium that is being tested (i.e., single values of K_o, B_o, and ε/q), or whether it is some combination of the two. In the test and illustrations given in this chapter, we have tried to keep these two aspects as separate as possible.

We begin by giving some consideration to the form of the equations used to represent experimental measurements. Although perhaps trivial from a mathematical point of view, the form is often not trivial from a practical standpoint. Direct comparisons with experiment then follow; these are divided into isothermal and nonisothermal measurements. (We use molar units consistently for flux quantities, rather than molecular or mass units.)

A. REPRESENTATION OF DATA

Since there is a set of linear equations which relate fluxes and gradients, many mathematically equivalent forms, connected by linear transformations, are possible. Such forms are often not equivalent in a practical sense, for two main reasons. The first reason is that the coefficients in one form may have a much simpler dependence on variables (such as pressure, temperature, and composition) than the coefficients in another form. For example, the diffusion coefficients D_{ij}, which appear when each gradient is written as a linear combination of all the fluxes, as in Eqs. (60) and (63), are virtually independent of mixture composition and hence are nearly the same as the corresponding coefficients in binary mixtures. However, if these equations are inverted, so that each flux is written as a linear combination of all the gradients, the resulting multicomponent diffusion coefficients have a rather strong and complicated composition dependence, and are related to the binary diffusion coefficients in a complicated way. The second reason is that some forms of the transport equations, when written in finite-difference form rather than differential form, are linear over much larger ranges than are other forms. Such near-linearity in finite-difference form is often quite helpful in the data analysis.

The second point can perhaps best be illustrated by numerical examples for a few special cases, since the complete results can be rather complicated. We select a system for which the coefficients in Eq. (120) have been measured (as discussed later in this chapter), namely, the gases helium and argon in a low-permeability graphite system of 11% open porosity and 0.447 cm thickness. The quantities needed for the present illustrations are as follows (at 25°C) [E7, E8, M22]:

$$B_o = 2.13 \times 10^{-14} \text{ cm}^2 ,$$

$$pD_{12} = 1.06 \times 10^{-4} \text{ atm-cm}^2/\text{s} ,$$

$$D_{HeK} = 3.93 \times 10^{-4} \text{ cm}^2/\text{s} ,$$

$$D_{ArK} = 1.24 \times 10^{-4} \text{ cm}^2/\text{s} ,$$

$$\eta_{He} = 198 \ \mu\text{P} ,$$

$$\eta_{Ar} = 226 \ \mu\text{P} . \qquad (128)$$

For this system, the viscosity is only weakly dependent on composition over most of its range, so that a constant mean value of $\bar{\eta} = 228$ μP can be used. This simplifies the numerical work in integrating Eqs. (120), (122), and/or (124), but makes no real difference in principle. The following results all refer to a constant arithmetic-mean pressure of $\bar{p} = 1$ atm, at several different composition differences and pressure differences across the septum, but with a fixed arithmetic-mean composition of $\bar{x}_{He} = \bar{x}_{Ar} = 0.5$. For the porous septum and flow conditions under consideration, it turns out that the transport occurs in the transition region between Knudsen and continuum diffusion, where neither mechanism dominates. Furthermore, it is assumed in the calculations that the gases are swept across the faces of the septum in such a manner that boundary layers at the surfaces can be ignored in the steady state, and that there are no discontinuities in the concentrations at the surfaces.

The point we wish to illustrate is that different ways of plotting results give curves of widely varying ranges of linearity, so that the interpretation of experimental data can be helped by an appropriate choice of plot.

We begin with the total flux, which we expect has a mathematical form consisting of a pressure-driven contribution plus a contribution due to diffusion drift. Equation (120) can be manipulated into such a form, which can then be written as the finite-difference equation

$$J = -\frac{\bar{K}_{12}}{R_o T}\frac{\Delta p}{\Delta z} - \bar{R}_{12}\frac{\Delta n_1}{\Delta z}, \tag{129}$$

where R_o is the ideal gas constant, $\bar{K}_{12}$ is a mean flow permeability coefficient, and $\bar{R}_{12}$ is a mean relative diffusive permeability coefficient. The latter two quantities are given by

$$\bar{K}_{12} = \frac{\bar{x}_1 D_1 + \bar{x}_2 D_2}{\bar{x}_1\gamma_1 + \bar{x}_2\gamma_2} + \frac{\bar{p}B_o}{\bar{\eta}}, \tag{130}$$

$$\bar{R}_{12} = \frac{D_1 - D_2}{\bar{x}_1\gamma_1 + \bar{x}_2\gamma_2}, \tag{131}$$

where, as defined by Eqs. (29) and (31),

$$\frac{1}{D_i} \equiv \frac{1}{D_{iK}} + \frac{1}{D_{12}} , \tag{132a}$$

$$\gamma_i \equiv D_i/D_{iK} . \tag{132b}$$

Results are shown in Fig. 8 for total flux as a function of pressure difference for several fixed composition differences. The relation is linear when the composition difference is zero (that is, when a uniform gas mixture is forced through the porous medium by a pressure difference), but distinct curvature is present when diffusion occurs simultaneously. Note that the diffusion term in Eq. (129) contributes to J even when the mixture has uniform composition, since $\Delta n_1 = n\,\Delta x_1 + x_1 \Delta n \neq 0$ even if $\Delta x_1 = 0$.

Another possibility is to write the flux of one component as a diffusion term plus a net drift term. It is easiest to start with Eq. (124) to obtain this result, which can then be written in finite-difference form as

$$J_i = -\bar{E}_i \frac{\Delta n_i}{\Delta z} + \bar{x}_i \epsilon_i J , \tag{133}$$

where

$$\frac{1}{\bar{E}_i} \equiv \frac{1}{\bar{E}_{iK}} + \frac{1}{E_{12}} , \tag{134}$$

$$\epsilon_i \equiv \bar{E}_i/E_{12} . \tag{135}$$

The parameter $\epsilon_i = 1$ for continuum diffusion and $\epsilon_i = 0$ for free-molecule diffusion. Results are shown in Fig. 9 for J_{He} as a function of J for several fixed composition differences. (For this example, $\epsilon_{He} = 0.860$.) The relation is linear when the composition difference is zero, as in the previous example, but otherwise the curvature is quite pronounced. Note that the diffusion term contributes to J_i even for a mixture of uniform composition, as before.

A third possibility is suggested by the treatment of membrane transport according to the principles of irreversible thermodynamics, where a relative diffusive flux is defined as

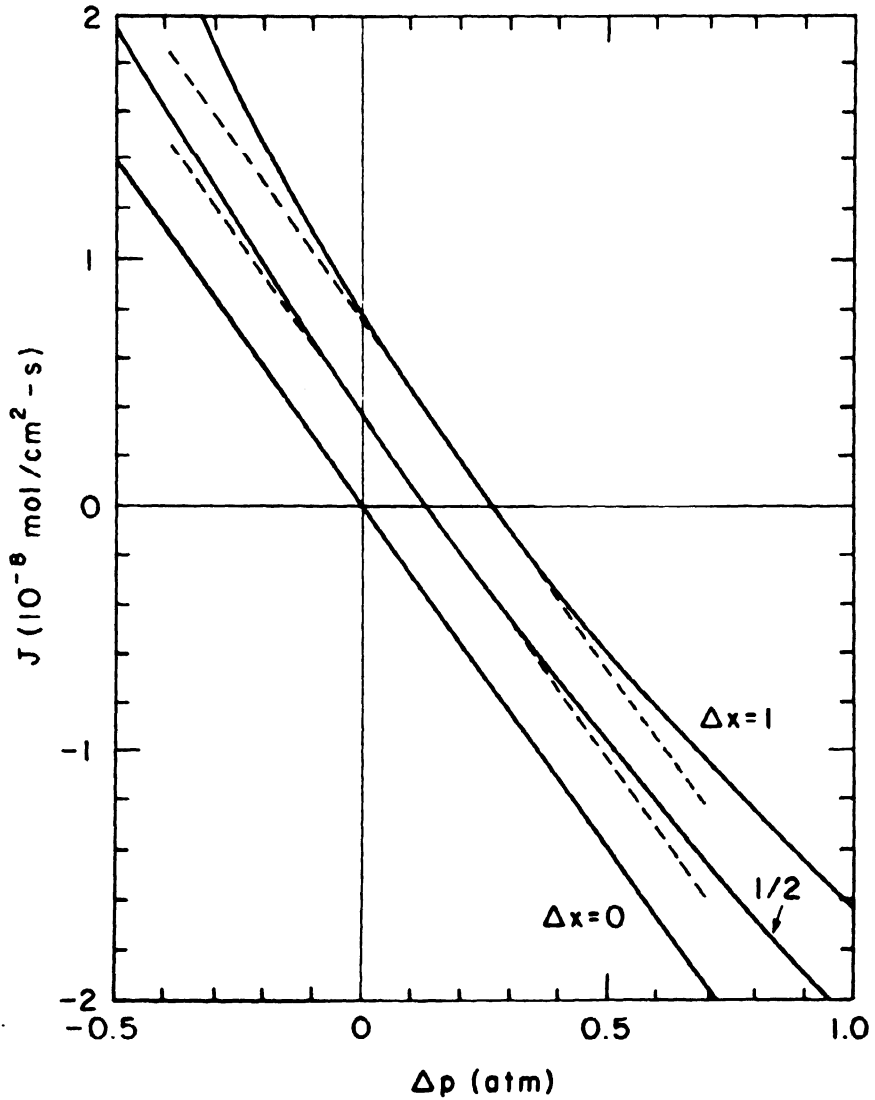

Fig. 8. Calculated total flux as a function of pressure difference for simultaneous flow and diffusion of He + Ar through a porous graphite septum. The arithmetic-mean composition is held fixed at mole fraction 0.5 for all three mole fraction differences shown. The dashed tangent straight lines are the linear approximations of Eq. (129).

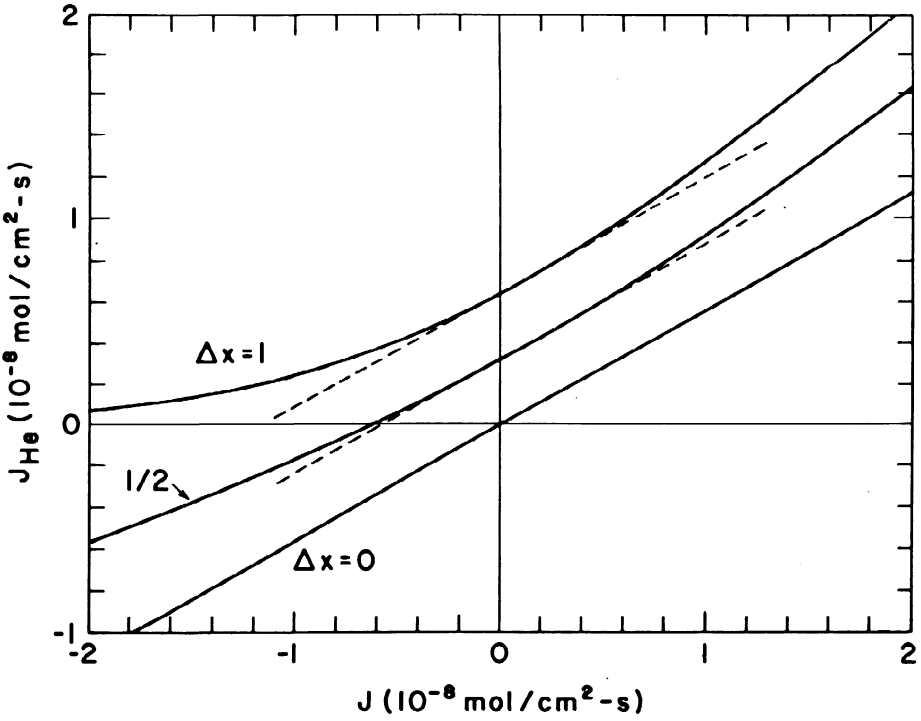

Fig. 9. Calculated component flux as a function of total flux for the same system as in Fig. 8. The dashed tangent straight lines are the linear approximations of Eq. (133).

$$J_{rel} \equiv (J_1/n_1) - (J_2/n_2) \ . \tag{136}$$

Note that this is the same sort of term that occurs in the Stefan-Maxwell equations. From Eq. (120) we obtain the finite difference linear form

$$\frac{J_1}{\bar{x}_1} - \frac{J_2}{\bar{x}_2} = - \bar{P}_{12} \frac{\Delta n_1}{\Delta z} - \frac{\bar{R}_{12}}{R_o T} \frac{\Delta p}{\Delta z} \ , \tag{137}$$

where

$$\bar{P}_{12} = \left(\frac{\gamma_1\gamma_2}{\bar{x}_1\gamma_1 + \bar{x}_2\gamma_2}\right)\left(\frac{D_1}{\bar{x}_1\gamma_1} + \frac{D_2}{\bar{x}_2\gamma_2}\right) , \qquad (138)$$

and the coefficient $\bar{R}_{12}$ is the same as the one occurring in Eq. (129) for J, by virtue of the Onsager reciprocal relations. Results are shown in Fig. 10, from which it is clear that the curvature problem is very serious [M24].

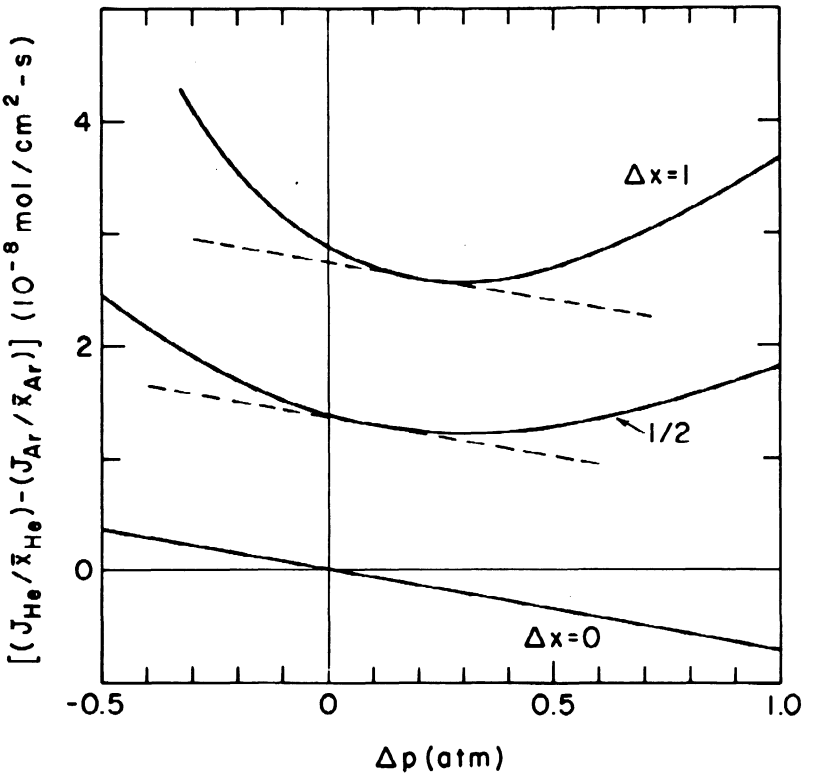

Fig. 10. Calculated relative diffusive flux, $[(J_{He}/\bar{x}_{He}) - (J_{Ar}/\bar{x}_{Ar})]$, for the same system as in Figs. 8 and 9. The dashed straight lines are the linear approximations of Eq. (137).

The final possibility we examine is similar in spirit to the first one considered, Eq. (129), but the diffusive drift term is expressed differently. It is supposed that "pure diffusion" occurs when $\nabla p = 0$, where Graham's law gives

$$J_1/J_2 = -D_{1K}/D_{2K} = -(m_2/m_1)^{1/2} , \tag{139}$$

which can be written as

$$J = \beta_1 J_1 = \beta_2 J_2 , \tag{140}$$

with

$$\beta_1 = 1 - (D_{2K}/D_{1K}) , \qquad \beta_2 = 1 - (D_{1K}/D_{2K}). \tag{141}$$

It is further supposed that the same ratios hold among the "diffusive components" of the fluxes even when $\nabla p \neq 0$. The "diffusive component" of J is therefore written as $\beta_i J_i$, and a pressure-driven contribution is added on. We can manipulate Eq. (124) into a result of this type, the finite-difference forms being [E6, M22]

$$J = \beta_1 J_1 - \frac{\bar{E}_{2K}}{R_o T} \frac{\Delta p}{\Delta z} , \tag{142a}$$

and

$$J = \beta_2 J_2 - \frac{\bar{E}_{1K}}{R_o T} \frac{\Delta p}{\Delta z} . \tag{142b}$$

This transformation finally overcomes the curvature difficulties encountered in Figs. 8–10. A plot of $(J-\beta_i J_i)$ vs. Δp is linear over a large range, and is independent of Δx_i, as shown in Fig. 11. Curves for total J are also indicated in Fig. 11, for comparison with Fig. 8.

The conclusion to be drawn from the foregoing examples is that an excellent way to analyze data on simultaneous flow and diffusion is to plot $(J-\beta_i J_i)$

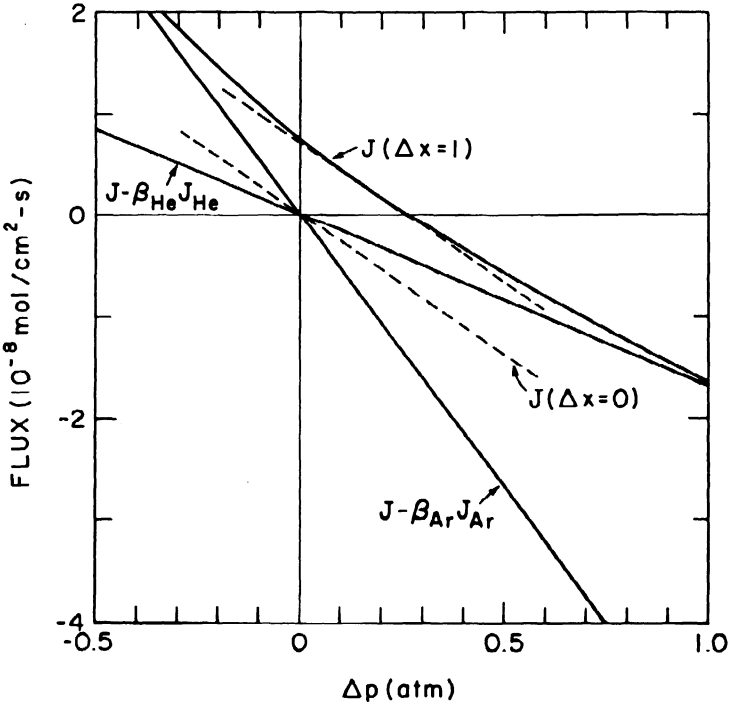

Fig. 11. Calculated fluxes as a function of pressure difference for the same system as in Figs. 8–10, showing that a plot of $(J-\beta_i J_i)$ is linear over a wide range of pressure differences and is independent of composition difference, as predicted by Eq. (142). The total flux J is also shown, the dashed straight lines representing the linear approximation of Eq. (129). Note that J depends on the composition difference, and is nonlinear in the pressure difference.

vs. Δp. The slopes of such plots determine the coefficients $\bar{E}_{iK}$. If measurements are carried out at a series of arithmetic-mean pressures, then plots of $\bar{E}_{iK}$ vs. $\bar{p}$ give straight lines whose intercepts determine D_{iK} and whose slopes determine B_o/η, as shown by Eq. (125). The augmented diffusion coefficient E_{12} can then be extracted readily from data at $J = 0$, according to Eq. (133), and D_{12} obtained from the definition of E_{12} by Eq. (126). Measurements at different values of $\bar{p}$ give an internal consistency check on E_{12} and D_{12}.

It should be noted that all of the foregoing equations — (129), (133), (137), and (142) — reduce to the same result for the degenerate case of a

single pure gas. The result is usually expressed in finite-difference form as

$$J_i = -\frac{\bar{K}_i}{R_o T}\frac{\Delta p}{\Delta z}, \tag{143}$$

where the mean flow permeability coefficient for single gas i is

$$\bar{K}_i = D_{iK} + \frac{\bar{p}B_o}{\eta_{ii}}. \tag{144}$$

It is found experimentally that plots of J_i vs. Δp give essentially straight lines whose intercepts determine D_{iK} and whose slopes determine B_o/η_{ii}.

One complication has been ignored in all of the preceding discussion. The Knudsen diffusion coefficients D_{iK} have a weak pressure dependence through the quantities Δ'_{id} as shown by Eqs. (70) and (123). This pressure dependence manifests itself only at low pressures, however, and can often be ignored for practical purposes. To give some feeling for its magnitude [M21, M22], we show in Fig. 12 a calculated curve for $\bar{K}_{He}$ vs. $\bar{p}$ at low pressures for the same septum as used in the previous examples. The parameters π_{He} and π'_{He} needed for the calculation were obtained from Eqs. (71)–(74), with the value of the parameter ξ_{He} chosen to be 2.0, a typical experimental value. The deviation of the curve in Fig. 12 from its linear high-pressure extrapolation is due entirely to the pressure dependence of D_{HeK}. We shall usually ignore this pressure dependence in subsequent discussions.

Finally, we show in Fig. 13 the pressure dependence of the principal transport coefficients, namely D_{iK}, D_{12}, E_{iK}, and E_{12}, in the form of the ratios E_{iK}/D_{iK} and E_{12}/D_{12} [M31]. It has already been pointed out that D_{12} varies inversely with pressure, and that the D_{iK} are (virtually) independent of pressure. From Fig. 13 we see that the ratio E_{iK}/D_{iK} is linear in the pressure and is the same for all species in the mixture, as is indicated explicitly in Eq. (125). We also see that E_{12}/D_{12} is almost, but not quite, independent of pressure, and approaches unity at high pressures. (We have not shown the behavior of the coefficients $\bar{K}_{12}$,

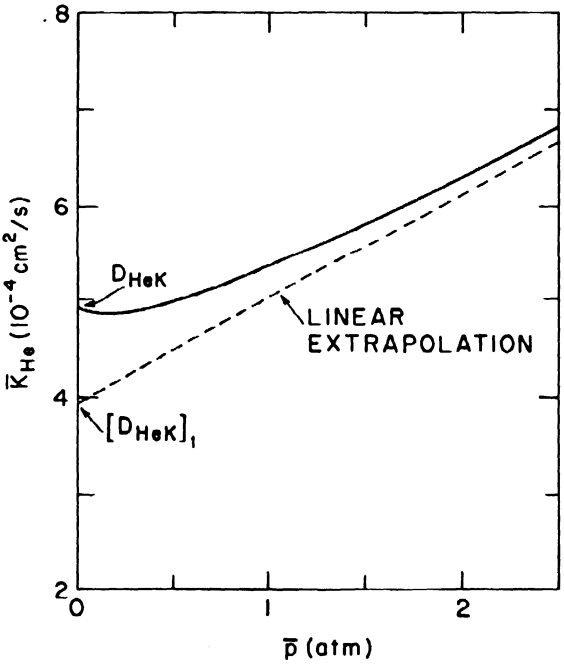

Fig. 12. Calculated He permeability coefficient as a function of mean pressure for the same graphite septum as in Figs. 8–11, showing the effect of the weak pressure dependence of D_{HeK} at low pressures.

$\bar{R}_{12}$, $\bar{P}_{12}$, $\bar{E}_i$, and ϵ_i, since Figs. 8–10 demonstrate that these coefficients do not furnish the best descriptions of simultaneous flow and diffusion in gases.)

Having found appropriate forms of the theoretical equations for representing experimental data, we now turn to a comparison of theory and experiment. We divide the experiments into isothermal and nonisothermal measurements for convenience, to isolate the more unusual phenomena that can occur in the presence of a temperature gradient.

B. ISOTHERMAL MEASUREMENTS

We proceed by way of a series of special cases, since the general results are too complicated to be easily surveyable. Most of the data come from the work of Evans, Watson, and Truitt [E7, E8] on helium and argon in a low-permeability graphite septum. The parameters of Eqs. (128) used in the preceding examples in fact were obtained from this work.

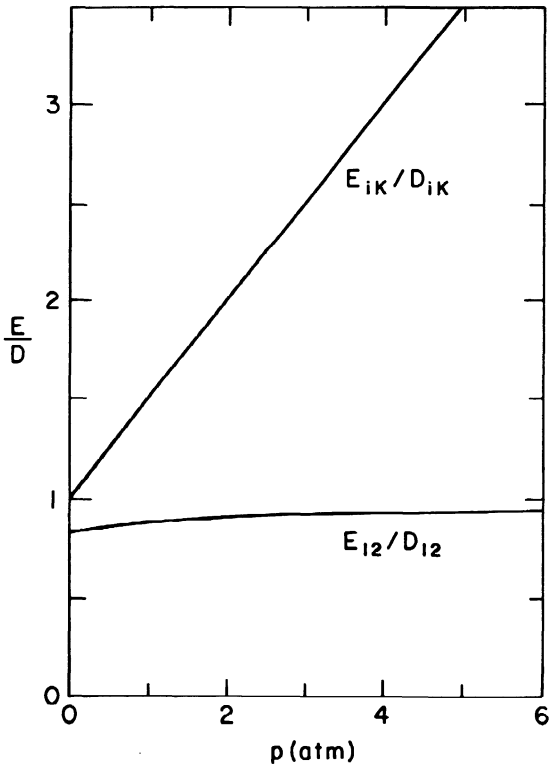

Fig. 13. Pressure dependence of the "augmented" diffusion coefficients E_{iK} and E_{12}, for the same system as in Figs. 8–10.

1. Single Gases

Here the only experiment possible is to force gas through the porous medium by a pressure difference. Two odd phenomena occur in what would at first seem to be a simple experiment — viscous slip and the Knudsen permeability minimum. Both of these are accounted for by the dusty-gas model, through Eq. (144) for the permeability coefficient $\bar{K}_i$. The classical theory of viscous flow predicts that a plot of $\bar{K}_i$ vs. $\bar{p}$ should be a straight line through the origin, whose slope is inversely proportional to the gas viscosity. Many years ago it was found that such a plot did not go through the origin; that is, the gas appeared to "slip" over the solid surface. Viscous slip was in fact demonstrated experimentally over 100 years ago by Kundt and Warburg [K8]. Equation (144) gives this result directly, the intercept, representing slip, being D_{iK} (really

$[D_{iK}]_1$, which is the apparent intercept from extrapolation of high-pressure data, as illustrated in Fig. 12). This is the basis for the determination of gas viscosity by capillary flow, or the determination of the parameters B_o and K_o for a porous medium by permeability measurements with a known gas.

In his pioneering work on low-pressure gases, Knudsen found that a plot of $\bar{K}_i$ vs. $\bar{p}$ was curved at very low pressures and might even exhibit a small minimum [K5, L5, W3]. We have already shown in Fig. 12 that Eq. (144) reproduces this feature through the weak pressure dependence of D_{iK}. To fit his experimental data, Knudsen originally proposed the empirical relation

$$\bar{K} = ap + b\left(\frac{1 + c_1 p}{1 + c_2 p}\right), \tag{145}$$

where a, b, c_1, and c_2 are constants. An excellent semiempirical equation developed by Weber [W3] has the same mathematical form. Equation (144), together with Eq. (70) for Δ'_{id}, has exactly this form, with

$$a = B_o/\eta_{ii} , \tag{146a}$$

$$b = [D_{iK}]_1(\pi_i/\pi'_i) , \tag{146b}$$

$$c_1 = 1/\pi_i , \tag{146c}$$

$$c_2 = 1/\pi'_i . \tag{146d}$$

Knudsen found that a single empirical value of 0.81 for the ratio c_1/c_2 fitted a large number of cases involving flow through capillaries. From Eq. (72), this corresponds to a value of $\xi_i\alpha_{iL} = 0.95$. For elastic gas-dust (or gas-wall) collisions, we have $\alpha_{iL} = 1/2$ from Eq. (73), and hence $\xi_i = 1.9$. This can be compared with a theoretical value for isotropic scattering (as from rigid spheres) of $\xi_i = 1.17$, which is somewhat smaller but not ridiculously so.

It is useful to pick out the location and depth of the permeability minimum (if there is one), for comparison with the location and height of

the thermal transpiration maximum to be discussed in Section C of this chapter. To shorten the notation a little, we define a pressure scale factor as

$$\pi_{\eta i} \equiv \eta_{ii}[D_{iK}]_1/B_o \ , \tag{147}$$

which has the dimensions of pressure and is a constant for a given system. The scale factor π_i of Eq. (71) can also be expressed in terms of measurable quantities through Eq. (74) for α_{iR},

$$\pi_i = (\alpha_{iR}/\alpha_{iL})n_d k_B T \approx (\varepsilon/q)T(\lambda_{ii})_{tr}/(5\alpha_{iL}[D_{iK}]_1) \ . \tag{148}$$

We can now drop the species subscript i, and designate π_i as π_g, because only a single gas is present. The expression for the permeability coefficient $\bar{K}$ of Eq. (144) then becomes

$$\frac{\bar{K}}{[D_K]_1} = \frac{p + \pi_g}{p + \pi'} + \frac{p}{\pi_\eta} \ , \tag{149}$$

which has a minimum at a pressure p_{min}, given by

$$p_{min} = [(\pi_g - \pi')\pi_\eta]^{1/2} - \pi' \ . \tag{150}$$

The value of $\bar{K}$ at the minimum is

$$\frac{\bar{K}_{min}}{[D_K]_1} = 1 + 2\left(\frac{\pi_g - \pi'}{\pi_\eta}\right)^{1/2} - \frac{\pi'}{\pi_\eta} \ . \tag{151}$$

The depth of the minimum can be taken as $\bar{K}(0) - \bar{K}_{min}$, which is

$$\frac{\bar{K}(0) - \bar{K}_{min}}{[D_K]_1} = \left[\left(\frac{\pi_g - \pi'}{\pi'}\right)^{1/2} - \left(\frac{\pi'}{\pi_\eta}\right)^{1/2}\right]^2 \ , \tag{152}$$

where, by Eq. (149), $\bar{K}(0)/[D_K]_1 = \pi_g/\pi'$. For the example shown in Fig. 12, helium in a fine-pore graphite, the value of p_{min} is 0.16 atm, and the reduced depth of the minimum as given by Eq. (152) is 0.014.

2. Binary Mixtures

Many more possibilities exist for binary mixtures than for single gases. We first show a test of the conclusions reached in Section A about an effective way to plot experimental results, and the behavior of the augmented diffusion coefficients E_{iK} for mixtures as compared to the permeability coefficients $\bar{K}_i$ for single cases. We then consider the special cases of uniform-pressure diffusion (Graham's law of diffusion), equal countercurrent diffusion (zero net molar flux), the diffusion pressure effect (diffusion baroeffect, diffusive slip), and finally we examine various fluxes as a function of pressure difference.

a. Augmented Diffusion and Permeability Coefficients. A sample of the extensive data of Evans, Watson, and Truitt [E7, E8] on the coupled flow and diffusion of helium and argon in a low-permeability graphite at 25°C is shown in Fig. 14. Here the fluxes $(J-\beta_{He}J_{He})$ and $(J-\beta_{Ar}J_{Ar})$ are shown as a function of pressure difference. As expected from the calculations shown previously in Fig. 11, the data fall nearly on straight lines, whose slopes determine the augmented Knudsen diffusion coefficients E_{HeK} and E_{ArK}. The total flux J is also shown in Fig. 14, and is seen to be also nearly linear over the range shown. The data in Fig. 14 refer to a mean pressure of $\bar{p} = 1.49$ atm, and were taken with nearly pure helium on one side of the septum ($x_{He} = 0.9917$) and nearly pure argon on the other side ($x_{Ar} = 0.9711$).

The values of the augmented diffusion coefficients E_{HeK} and E_{ArK} obtained from experiments at different mean pressures are shown as a function of $\bar{p}$ in Fig. 15, together with the permeability coefficients K_{He} and K_{Ar} obtained from separate experiments with the same graphite specimen. As might be anticipated from the previous discussion, the results are linear in $\bar{p}$ within experimental error. (The measurements are not accurate enough at very low pressures for small Knudsen minima to be noticed, if indeed they are present for these systems.) The data displayed in Fig. 15 can be summarized by eight empirical numbers — four intercepts and four slopes — but according to theory, there are only two independent parameters, B_o and K_o (or B_o and any one of the Knudsen diffusion coefficients D_{iK}). If these two are known, the other six can be predicted from a knowledge of viscosities and molecular weights. Thus a good test of the theory is to fit one straight line to the data to determine the two independent parameters, and from this fit predict the other

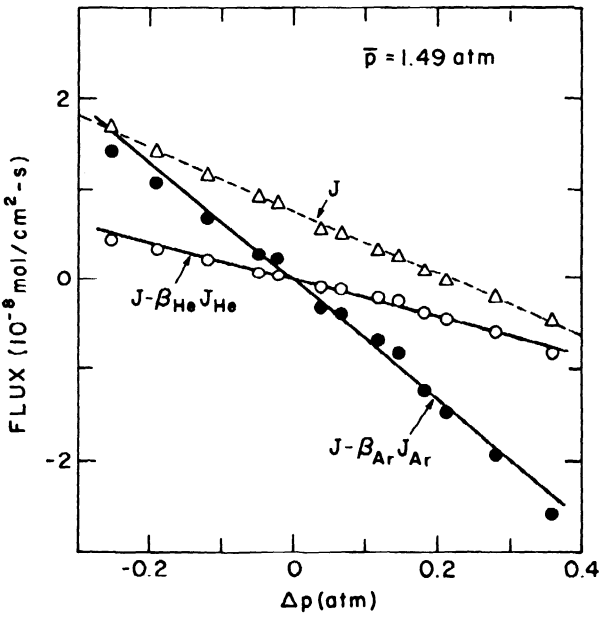

Fig. 14. Coupled flow and diffusion for a He + Ar mixture in a porous graphite septum at 25°C and 1.49 atm. The terms $\beta_{He}J_{He}$ and $\beta_{Ar}J_{Ar}$ are the contributions of diffusion to the total flux. This form of plot gives linear relations over a wide range of Δp. The slopes of the solid lines give the augmented diffusion coefficients E_{HeK} and E_{ArK} of Eqs. (125) and (142).

three lines and see how well they agree with the experimental data. Accordingly, we fitted the K_{Ar} data by least squares, obtaining the values for D_{ArK} and B_o already given in Eqs. (128). Since Eq. (67) predicts that the D_{iK} vary as $m_i^{-1/2}$, we predict the value of D_{HeK} given in Eqs. (128). This value, together with the values of B_o and η_{He}, determines the line for K_{He}. The lines for E_{ArK} and E_{HeK} are then calculated from the values of B_o, D_{ArK}, and D_{HeK} according to Eq. (125), using a mean value for the viscosity of the gas mixture. As can be seen in Fig. 15, the agreement between theory and experiment is quite good.

It should be noted that there was no restriction in the foregoing discussion regarding the relative importance of Knudsen and continuum diffusion. The method of treating the data should hold over the entire range, from the Knudsen regime to the continuum regime. As will be apparent from subsequent comparisons of theory and experiment, most of the measurements shown in Fig. 15 fall in the transition region.

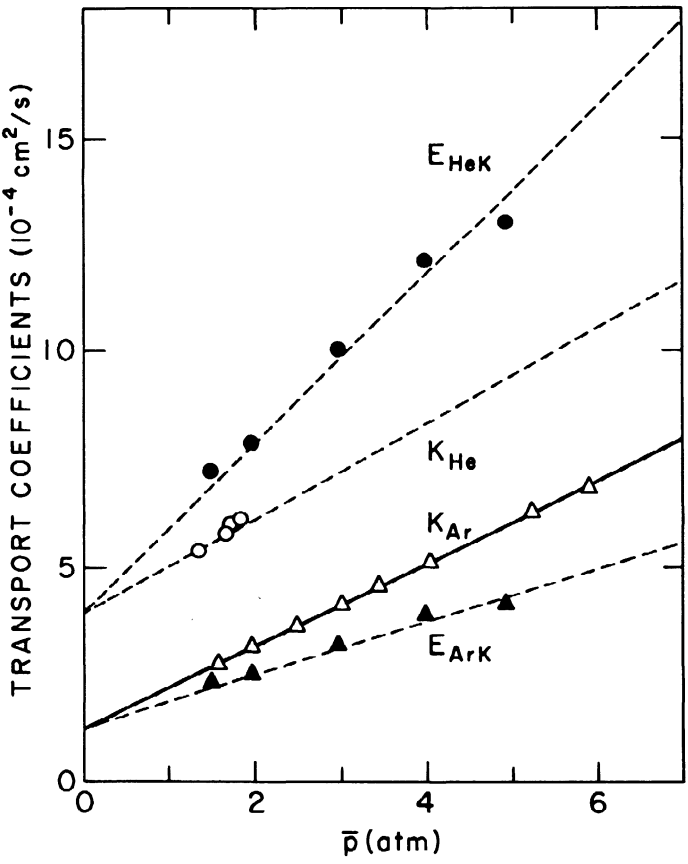

Fig. 15. Augmented diffusion and permeability coefficients as a function of mean pressure for He, Ar, and a He + Ar mixture, obtained from data such as shown in Fig. 14. Only the solid line for K_{Ar} is drawn to fit the data. The dashed lines are then determined from the K_{Ar} line according to theory.

It is also worth noting that the parameters B_o and K_o are reasonably insensitive to temperature, at least for some types of porous media [H15].

b. Uniform-Pressure Diffusion. In this type of experiment, first carried out by Thomas Graham [G3], the total pressure is kept uniform, although there are gradients of the partial pressures of the two species. We wish to comment on three tests of the theory involved in such

experiments. First, how well is Graham's law of diffusion, $J_1/J_2 = -(m_2/m_1)^{1/2}$, followed? Second, since values of D_{12} are often obtained from such experiments, how well is the relation $D_{12} = (\varepsilon/q)\mathcal{D}_{12}$ followed, where $\mathcal{D}_{12}$ is measured in free space? In other words, is ε/q a parameter characteristic of the porous medium only? Third, how do the individual fluxes J_1 and J_2 vary as the total pressure is varied in a series of experiments?

There have been a large number of tests of Graham's law of diffusion since the subject was reopened by Hoogschagen in 1953 [H12, H13]. Rather than list the various gas pairs and porous media examined experimentally, we will try to summarize the situation in a few sentences. The consensus of opinion now seems to be that Graham's law is obeyed within a few percent, except in those cases where gas-surface interactions might reasonably be expected to be prominent. Such cases include adsorbable gases, and porous media containing pores of very small radii, less than about 50 Å [01]. Indeed, deviations from Graham's law are frequently regarded as prime evidence of surface effects. However, it is only fair to mention that some theoretical solutions of the Boltzmann equation suggest deviations from Graham's law that depend on the molecular interactions [B10].

Tests of the constancy of ε/q have been less extensive than tests of Graham's law, but the constancy appears to hold within a few percent. Moreover, ε/q is nearly temperature independent [H3]. Probably the most extensive measurements have been carried out by Hawtin, Dawson, and Roberts [H4] on three types of porous graphite, using the gas mixtures $He + H_2$, $He + Ar$, and $CO_2 + CH_4$ over the range from 20 to 600°C.

Thus both Graham's law of diffusion and the constancy of ε/q appear to be satisfactorily established for porous media.

Finally, it is interesting to examine how the flux varies in uniform-pressure diffusion as the total pressure is varied. In the continuum region we expect the flux to be independent of pressure, and in the free-molecule region we expect it to be directly proportional to pressure. We can obtain a suitable expression from Eq. (120) by setting $\nabla p = 0$ and using Graham's law in the form given by Eqs. (140)—(141). In order to exhibit the pressure dependence explicitly, it is convenient to define flux and pressure scale factors,

$$\phi \equiv nD_{12}/\Delta z \ , \qquad (153a)$$

$$\pi_{Di} \equiv pD_{12}/D_{iK} , \quad i = 1,2 . \tag{153b}$$

These quantities are constants for a given system. The flux equation, in finite-difference form, can then be written as

$$\frac{J_1}{\Phi} = - \frac{(p/\pi_{D1})\ \Delta x_1}{1 + (1 - x_1\beta_1)(p/\pi_{D1})} , \tag{154}$$

with a similar expression for species 2. Thus the pressure dependence of the flux is initially linear, and reaches a constant value at high pressure. The pressure dependence is the same as that of a Langmuir adsorption isotherm.

If the finite-difference form is not accurate enough, the differential equation can be readily integrated for steady-state conditions to yield [E5, M18]

$$\frac{J_1}{\Phi} = \frac{1}{\beta_1} \ln \left[\frac{1 + (1-\beta_1 x_1^{\Delta z})\ (p/\pi_{D1})}{1 + (1-\beta_1 x_1^{0})\ (p/\pi_{D1})} \right] , \tag{155}$$

where x_1^{0} and $x_1^{\Delta z}$ are the mole fractions on the two sides of the septum.

Notice that the viscosity does not appear in any of the above equations, indicating that there is no viscous flow even though the total flux J is not zero.

A plot of Eq. (155) for He + Ar diffusion is compared with the measurements of Evans, Watson, and Truitt in Fig. 16. The fluxes of both components were measured independently; the results conform both with Graham's law of diffusion and with the predicted pressure dependence. The only adjustable parameter in the calculation is D_{12}; the value given in Eqs. (128) was in fact obtained by fitting the data shown in Fig. 16. Notice that diffusion is still in the transition region between free-molecule and continuum behavior even at pressures of several atmospheres. This is characterized by the pressure parameter π_{Di}; the diffusion is free-molecular when $p \ll \pi_{Di}$, and is continuum when $p \gg \pi_{Di}$. Numerical

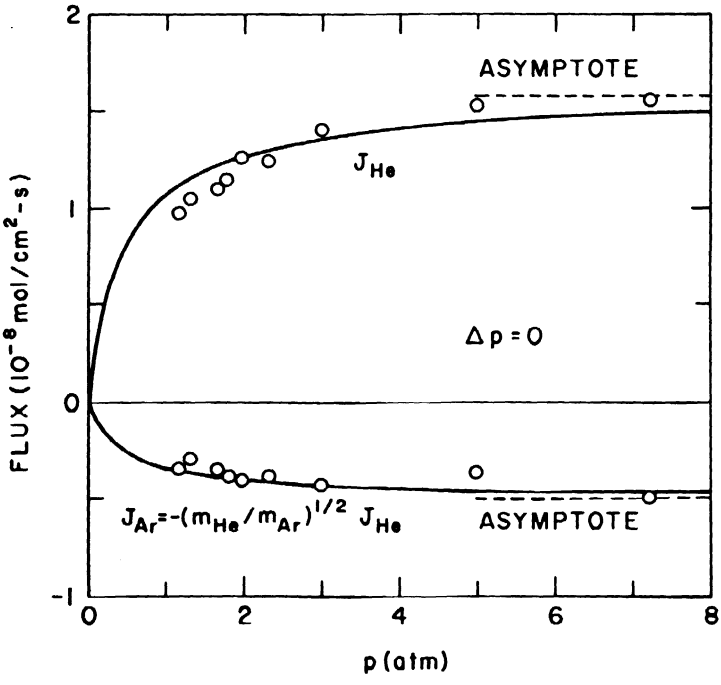

Fig. 16. Calculated and observed diffusion fluxes as a function of pressure in uniform-pressure (Graham) experiments for the same system as in Figs. 14 and 15. The curves are from Eq. (155). Note that the results conform to Graham's law of diffusion.

values for the system shown in Fig. 16 are $\pi_{DHe} = 0.27$ atm and $\pi_{DAr} = 0.85$ atm. For comparison, the same gaseous system diffusing in a capillary tube of 0.1 cm diameter would have $\pi_{DHe} = 3 \times 10^{-4}$ atm, representing a scale change of about 10^3.

A similar study of He + N_2 diffusion was carried out in capillaries by Remick and Geankoplis [R1]. They covered a pressure range of over a factor of 675 to 1 and achieved better accuracy. Agreement both with Graham's law and with the predicted pressure dependence of the fluxes was excellent. (The value of ε/q is unity for capillaries.)

c. Equal Countercurrent Diffusion. In order to keep the net molar flux zero, a small pressure difference develops automatically if diffusion occurs in a closed volume. Here we wish to examine how the species flux varies with pressure in such an experiment. Again, we expect

the flux to be constant in the continuum region and directly proportional to pressure in the free-molecule region. We can obtain a suitable expression by writing Eq. (120) for each of the two components, setting $\underset{\sim}{J}_1 = -\underset{\sim}{J}_2$ and $\underset{\sim}{\nabla} x_1 = -\underset{\sim}{\nabla} x_2$, and eliminating $\underset{\sim}{\nabla} p$ between the two equations. The resulting flux equation can be written in finite-difference form as

$$\frac{J_1}{\phi} = -\frac{(p/\pi_{D1})\,\Delta x_1}{1 - x_1\beta_1(1-\beta_1)^{-1} + (p/\pi_{D1})} , \tag{156}$$

where the scale factors ϕ and π_{D1} are as defined in Eq. (153). This equation shows the same general behavior with pressure as does Eq. (154) for the uniform-pressure case.

If the finite-difference form is inadequate, the differential equation can be integrated under steady-state conditions to yield [M18]

$$\frac{J_1}{\phi} = -\left(\frac{1-\beta_1}{\beta_1}\right)\left(\frac{p}{\pi_{D1}}\right) \ln \left\{\frac{\beta_1 x_1^{\Delta z} + (1-\beta_1)\,[1 + (p/\pi_{D1})]}{\beta_1 x_1^{0} + (1-\beta_1)\,[1 + (p/\pi_{D1})]}\right\} . \tag{157}$$

Notice that the viscosity does not appear in these equations, even though we now expect viscous back-flow to be occurring in order to keep $J_1 = -J_2$. This is a peculiarity of the $J = 0$ equal countercurrent condition. Regardless of what value the viscosity has, the pressure difference adjusts itself to keep $J = 0$. Thus the viscosity affects the steady-state pressure difference, as will be shown explicitly below, but not the flux. The viscosity appears explicitly in the flux equations, however, unless either $J = 0$ or $\nabla p = 0$.

A plot of Eq. (157) is shown in Fig. 17 for the same system as in Fig. 16 for the uniform-pressure case. The agreement with experiment is quite good. No adjustable constants are involved here, the value of D_{12} having been obtained from the independent measurements at uniform pressure shown in Fig. 16.

d. Diffusion Pressure Effect (Diffusive Slip). The pressure difference that results from diffusion in a closed system was first investigated by Kramers and Kistemaker [K7]. They recognized that this pressure difference was related to the fact that the mass-average velocity of the gas was not zero at the wall, or that there was a nonzero momentum flow, or slip, in the gas adjacent to the wall. The phenomenon was later

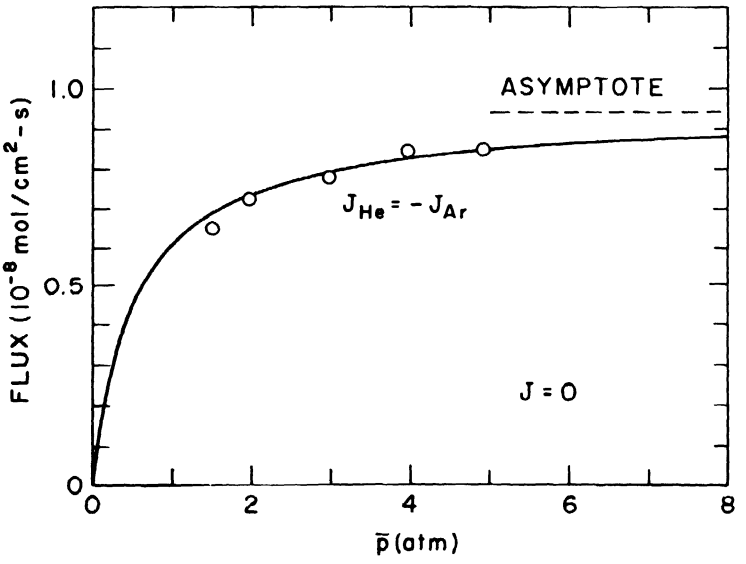

Fig. 17. Calculated and observed diffusion flux as a function of mean pressure in equal countercurrent diffusion experiments for the same system as in Figs. 14–16. The curve is from Eq. (157) and involves no adjustable parameters.

rediscovered independently and discussed as an analogue of the Kirkendall effect in solids [M29, M33]. It is also very closely related to the so-called "reflection coefficient" used in discussions of membrane transport [D1].

To find an expression for the pressure difference, we proceed as for equal countercurrent diffusion, but algebraically eliminate J_1 instead of ∇p. The result can be written in finite-difference form as follows, in a form that exhibits the pressure dependence of the effect:

$$\Delta p = \frac{p(D_{1K}-D_{2K})\,\Delta x_1}{A_0 + A_1 p + A_2 p^2} , \tag{158}$$

where the coefficients are

$$A_0 = x_1 D_{1K} + x_2 D_{2K} , \tag{159a}$$

$$A_1 = (D_{1K}\, D_{2K}/p D_{12}) + (B_o/\eta) , \tag{159b}$$

$$A_2 = [(x_1 D_{2K} + x_2 D_{1K})/pD_{12}] \, (B_o/\eta) \, , \tag{159c}$$

in which η is the viscosity of the mixture. Thus the steady-state pressure difference increases from zero linearly with p at low pressures, reaches a maximum value of

$$\Delta p_{max} = \frac{(D_{2K}-D_{1K})\Delta x_1}{A_1 + 2(A_o A_2)^{1/2}} \, , \tag{160}$$

at a pressure of

$$p_{max} = (A_o/A_2)^{1/2} \, , \tag{161}$$

and finally falls back to zero at high pressures as 1/p. Equation (158) involves the viscosity, unlike Eqs. (154) and (156). The weak pressure dependences of the D_{iK} are negligible compared to the strong dependence given explicitly in Eq. (158).

The differential equation corresponding to Eq. (158) cannot be integrated analytically because of the composition dependences of A_o, A_1, and A_2. Fortunately, the finite-difference approximation of Eq. (158) is usually adequate, as illustrated in Fig. 18 for the same system as was shown in Figs. 16 and 17, with mean values for x_1, η, and p. Only the measurement at the lowest pressure has much experimental uncertainty, as indicated in the figure, and the agreement between theory and experiment is, on the whole, rather good. No adjustable constants are involved in this comparison; the values of the necessary parameters were obtained from the analysis involved in Figs. 15 and 16.

A number of investigators in recent years have taken up the study of the diffusion pressure effect or diffusive slip, both experimentally [M18] and theoretically [B10, B11, L15]. Almost all of them have confined their attention to capillary tubes. Although the dusty-gas model usually gives an adequate overall description of the phenomenon, a number of anomalies have been observed, especially when the masses of the two diffusing species are nearly equal, so that the main effect predicted by Eq. (158) is small. For instance, a sign reversal in Δp vs. p for Ar-CO_2 diffusion has been observed [W2]. It is not always clear whether these anomalies are caused by gas-surface interactions, or by higher-order kinetic theory effects that depend on details of molecular collisions.

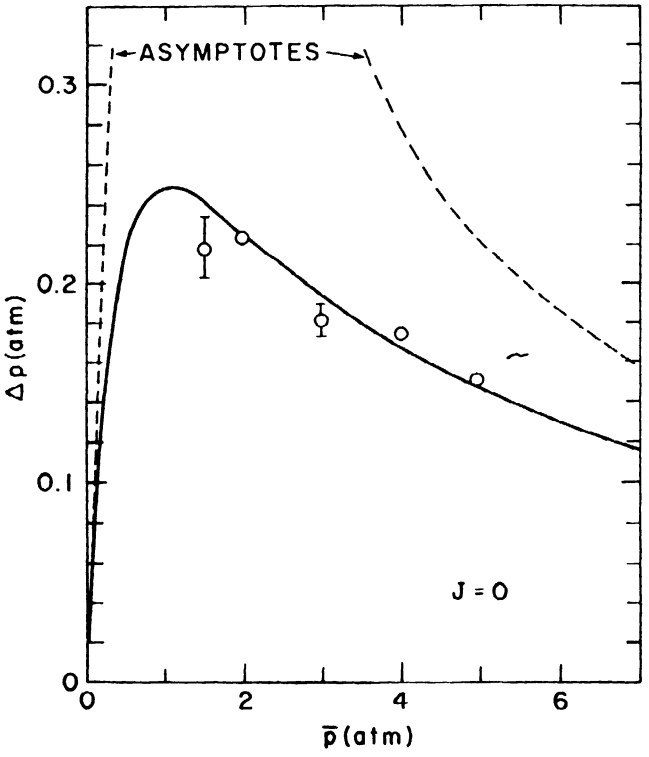

Fig. 18. Calculated and observed steady-state pressure difference at J = 0 (diffusive slip) as a function of mean pressure for the same system as in Figs. 14–17. The curve is from Eq. (158) and involves no adjustable parameters.

e. Effect of Pressure Gradients on Fluxes. Finally, we wish to examine the influence of the pressure gradient on diffusive fluxes, the mole fraction difference being held constant, and compare the calculations of the dusty-gas model with experimental results. We show J_{He}, J_{Ar}, and J as a function of Δp in Fig. 19 for $\bar{p}$ = 1.96 atm, a pressure at which the measurements of Evans, Watson, and Truitt [E7, E8] were particularly extensive. The curves shown were calculated by numerical iteration of the dusty-gas equations, since a linear finite-difference approximation is clearly inadequate because of the curvature. The numerical procedure is straightforward but somewhat complicated, and has been described elsewhere [M22].

The agreement shown in Fig. 19 is quite good, especially in view of the fact that no parameters have been adjusted to produce a good fit.

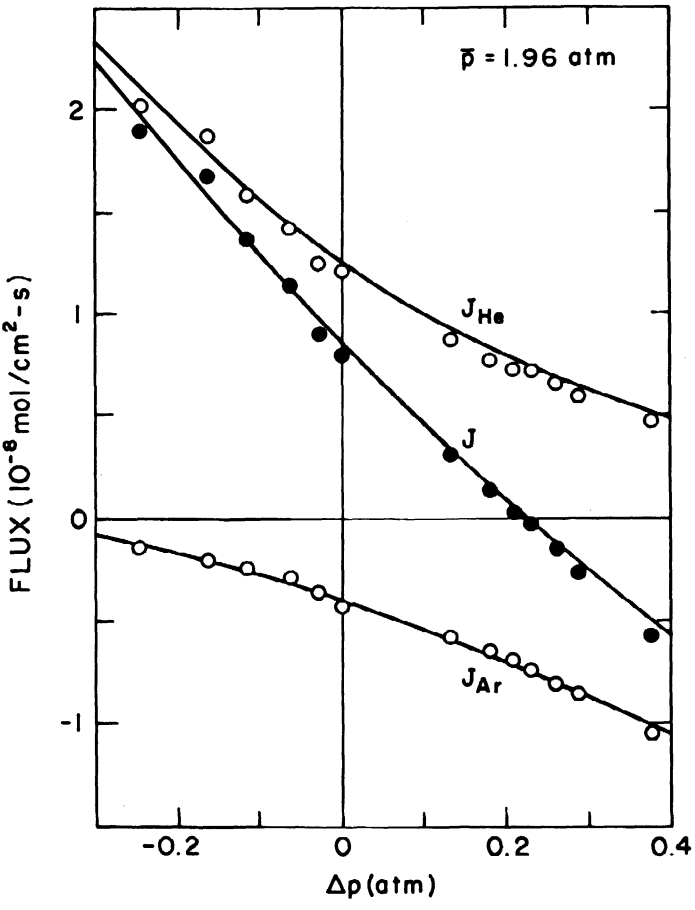

Fig. 19. Calculated and observed fluxes as a function of pressure difference at $\bar{p}$ = 1.96 atm for the same system as in Figs. 14–18. The curves are from numerical integration of the dusty-gas equations, and involve no adjustable parameters.

The parameters used were obtained from entirely independent measurements: D_{ArK} and D_{HeK} from permeability measurements with pure argon (the line labelled K_{Ar} in Fig. 15), and D_{12} from uniform-pressure diffusion measurements (Fig. 16).

3. Multicomponent Mixtures

There have been only a few experimental tests of any transport theory for multicomponent mixtures. Hesse and Köder [H6] studied the pressure

dependence of the interdiffusion of ortho- and para-H_2, in the presence of either He or Ar, through a fritted glass disk. The flux equations to be tested were those obtained by momentum-transfer arguments, but the form of the equations is the same for the dusty-gas model, as we have seen in Chapter II. Plots of measured diffusion resistances (reciprocal effective diffusion coefficients) were linear at high pressures, as predicted, but showed minima at low pressures that were similar to Knudsen permeability minima (Fig. 12). Since Knudsen diffusion coefficients appear in the expression for the diffusion resistance, the minima could well have a common source, namely, the pressure dependence of the D_{iK} through the correction term Δ'_{id}. Unfortunately, some (but not all) of the minima observed by Hesse and Köder had magnitudes that seem too large to be attributed to the Δ'_{id} as given by the dusty-gas model, so that a puzzle remains.

Some limited ternary diffusion measurements for He + Ne + Ar mixtures in capillaries were carried out by Remick and Geankoplis [R2] over a large pressure range. They verified Graham's law for ternary mixtures, $\Sigma m_i^{1/2} J_i = 0$, and compared measured and calculated fluxes as a function of pressure for uniform total pressure. The agreement obtained was good.

Rather more extensive investigations on ternary diffusion in porous media over a range of both pressure and temperature were carried out in a number of porous pellets by Feng *et al.* [F2], using the He + Ne + CH_4 mixtures, and by Patel and Butt [P2], using He + Ar + N_2 mixtures. Both investigations did not really test the flux equations alone (although Patel and Butt did check Graham's law), but instead were primarily concerned with the problem of characterizing the structure of the porous medium with a limited number of parameters. In other words, the problems of heteroporosity and/or effective homoporosity were in the forefront. Although obviously important, those problems are not our main concern in this monograph.

At first glance, there appears to be nothing special in multicomponent diffusion that was not already present in binary diffusion, except possibly a bit more mathematical complexity. No new coefficients appear in the multicomponent equations — the D_{iK} are essentially the same, the D_{ij} are virtually the same in a multicomponent mixture as in a binary mixture of species *i* and *j*, and even the formula for the mixture viscosity contains only binary-interaction terms, as shown explicitly by Eqs. (52)–(54). Somewhat surprisingly, however, the addition of only one more

component to a binary mixture can open the door to a host of new effects. Many of these are now fairly well known in the case of gases, such as the diffusion of a species against its concentration gradient, and are discussed in a monograph by Cussler [C10]. However, the fact that density inversions and convective flow can be caused by diffusion involving three or more species is less well known [M34]. Such convection will not develop unless the characteristic size of the convection cells is less than the geometrical size of the container, so there is probably little danger unless the pore size is large and the gas pressure is high. Nevertheless, it is wise to keep the possibility of diffusive convection in mind and to make at least a rough calculation to be sure it will be absent in any doubtful case. Interestingly enough, diffusion-driven convection is a well-known phenomenon in other fields, where it goes by a variety of names, such as double-diffusive convection [T4]. In oceanography, it gives rise to "salt fingers," in which one of the diffusing "species" is heat [M9].

C. NONISOTHERMAL MEASUREMENTS

Temperature gradients give rise to two phenomena. In single gases, only the phenomenon of thermal transpiration, or the thermomolecular pressure effect, exists. In mixtures there is, in addition, a relative motion of the gaseous species which gives rise to the phenomenon that is called thermal diffusion. Of course, from the standpoint of the dusty-gas model, only the phenomenon of thermal diffusion exists, and thermal transpiration is merely the manifestation of thermal diffusion between gas and dust. We expect the model to describe the pressure dependence of thermal transpiration in both single gases and mixtures, as well as the composition dependence in mixtures. We also expect it to account for the pressure dependence of the thermal diffusion factor in mixtures. In this section we discuss only single gases and binary mixtures. Multicomponent mixtures are straightforward in principle according to the dusty-gas model, but the mathematical manipulations become very complicated.

The temperature-gradient terms in the flux equations are frequently ignored in practical applications because they complicate an already difficult analysis. The few exploratory calculations that have been carried out suggest that these terms are usually of secondary importance; that is, they are not negligible, but they are not dominant, either [W13, W14].

Nevertheless, there has been a continuing interest in thermal transpiration, especially in capillary tubes. It has long been known that it can be an important source of error in pressure measurements when the manometer is not at the same temperature as the rest of the apparatus, a situation that occurs in adsorption studies and gas thermometry. More recently, thermal transpiration measurements have been used to study molecular relaxation times in gases, an unexpected connection that was first uncovered by the dusty-gas model. Our comparisons with experimental measurements are thus forced to rely mainly on data involving capillaries rather than porous media. Indeed, there were no suitable thermal transpiration measurements in porous media, other than the original 1879 work of Osborne Reynolds [R3], until the 1960's, when studies were made specifically to test the predictions of the dusty-gas model [H1, H14].

1. Single Gases

The general equation for thermal transpiration (also called thermo-osmosis) is most easily obtained from Eq. (122), the forced-flow non-isothermal generalization of Graham's law of diffusion. The summations have only one term in them, and the result for pure gas i can be written as

$$\underset{\sim}{J}_i = -\frac{E_{iK}}{k_B T}\underset{\sim}{\nabla} p - \frac{n_i n_d}{n'} D_{iK}(\alpha'_{id})_{tr}\underset{\sim}{\nabla} \ln T \,. \tag{162}$$

This equation is seldom used directly, because most experiments are carried out at steady state ($\underset{\sim}{J}_i = 0$), and a measurement is made of the pressure difference across the porous septum or capillary tube. We can obtain a differential equation for this thermomolecular pressure difference by setting $\underset{\sim}{J}_i = 0$ in Eq. (162), using Eq. (69) for $(\alpha'_{id})_{tr}$ and making a one-dimensional approximation. In order to exhibit the pressure dependence of the equation in explicit form, it is convenient to use the pressure scale factors π_i and $\pi_{\eta i}$ of Eqs. (147) and (148); the result is

$$\frac{d \ln p}{d \ln T} = \frac{\alpha_{iL}\pi_i\pi_{\eta i}}{(p+\pi_{\eta i})(p+\pi_i)} \,. \tag{163}$$

Two comments should be made about this equation. First, the scale factor $\pi_{\eta i}$ really should contain D_{iK} from Eq. (162), and not just $[D_{iK}]_1$, as defined in Eq. (147). Thus $\pi_{\eta i}$ should show a weak pressure dependence at low pressures. For most purposes this dependence is negligible in comparison with the much greater pressure dependence given explicitly in Eq. (163). Second, a factor of $(1-\Delta_p)$ should multiply the right-hand side of this equation, where Δ_p is a small pressure-dependent quantity resulting from molecular inelastic collisions in the gas phase [A10]. It arises from a small correction term that was ignored in writing Eq. (69) for $(\alpha'_{id})_{tr}$; since it is zero for monatomic gases and seemingly unimportant even for polyatomic gases, it has always been ignored in the analysis of experimental data [A5, M6, T1, T2], and we shall henceforth ignore it as well.

The problem now is to integrate Eq. (163). A straightforward finite-difference approximation to the differential terms is not entirely satisfactory because $\Delta T/T$ is often not small, although $\Delta p/p$ is. A complete integration leads to rather complicated results, because of the temperature dependence of π_i and π_η through $[D_{iK}]_1$ and η_{ii} [M6, M21, M30]. Fortunately, a semiempirical modification of the finite-difference approximation is usually satisfactory. This modification proceeds by making an exact integration for the free-molecule ($p \to 0$) limit, arranging a finite-difference form of Eq. (163) to pass to this limit, and using an empirical definition of average temperature in π_i and $\pi_{\eta i}$. To shorten the notation, we drop the species subscript i (only a single gas is involved), designate π_i as π_g, and use subscripts 1 and 2 to refer to the pressures and temperatures on the two sides of the septum or capillary. In the free-molecule region, we must have $n_1\bar{v}_1 = n_2\bar{v}_2$ according to Eq. (2), so that

$$p_1/p_2 = (T_1/T_2)^{1/2} , \tag{164a}$$

or

$$\Delta p \equiv p_2 - p_1 = [1 - (T_1/T_2)^{1/2}]p_2 , \tag{164b}$$

in which we conventionally pick $T_2 > T_1$. The same result follows from Eq. (163) on passing to the limit $p \to 0$ and choosing $\alpha_L = 1/2$. In Eq. (163) we therefore make the substitutions [M3, M21],

$$d \ln p \to \Delta p/p \ , \tag{165a}$$

$$d \ln T \to 2[1-(T_1/T_2)^{1/2}] \ , \tag{165b}$$

whereby we obtain the result,

$$\Delta p = \frac{2\alpha_L \pi_g \pi_\eta [1-(T_1/T_2)^{1/2}] \, p}{(p + \pi_\eta)(p + \pi_g)} \ . \tag{166}$$

The average temperature at which π_g and π_η are evaluated is [M3]

$$\bar{T} = \frac{1}{2} [T_2 + (T_1 T_2)^{1/2}] \ . \tag{167}$$

Notice that the expression for $\bar{T}$ is not symmetric in T_1 and T_2, and that $T_2 > T_1$. This result is essentially empirical.

Equations (166) and (167) are the working equations for thermal transpiration of a single gas. It is usual to treat α_L as an adjustable parameter. For capillaries, α_L is the only adjustable parameter, but for porous media the parameters ε/q, B_o, and K_o are also adjustable. Comparison between theory and experiment for porous media has been done only three times, with generally satisfactory agreement [H1, H14, M21]. Data for capillaries usually follow the pressure dependence predicted by Eq. (166), especially if α_L, π_g, and π_η are all treated as adjustable parameters. An example is shown in Fig. 20 for Ne, Ar, Kr, and Xe in a capillary of internal diameter 0.02 cm [M6]. (The use of p_2 instead of a mean pressure in this figure causes only trivial changes.) The agreement is excellent. The maximum in Δp occurs, according to Eq. (166), at a pressure p_{max}, given by

$$p_{max} = (\pi_g \pi_\eta)^{1/2} \ , \tag{168}$$

and the height of the maximum is

$$\Delta p_{max} = 2\alpha_L [1-(T_1/T_2)^{1/2}] \, (\pi_g^{-1/2} + \pi_\eta^{-1/2})^{-2} \ . \tag{169}$$

Besides predicting the pressure dependence of Δp accurately, Eq. (166) predicts a number of other relations that depend on the forms of the parameters π_g and π_η, and that can be tested experimentally [M10, M21]. We

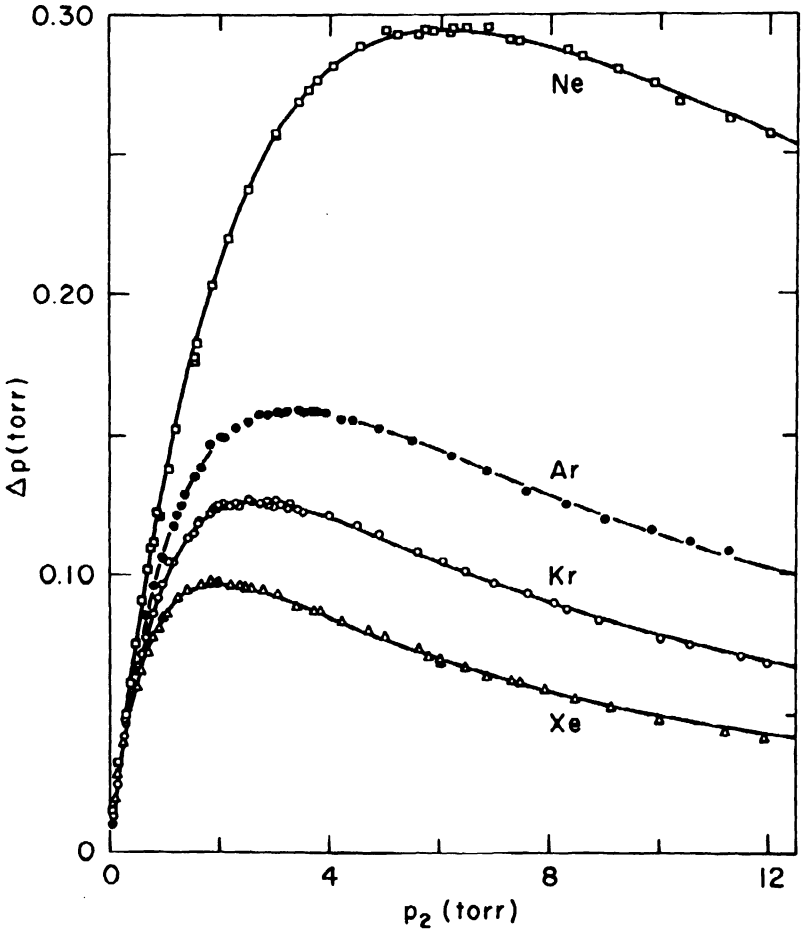

Fig. 20. Pressure dependence of the thermal transpiration effect for noble gases in 0.02 cm capillaries, with T_1 = 335.6 K, T_2 = 569.8 K. The solid curves are calculated from Eq. (166) with the parameters α_L, π_g and π_η treated as adjustable.

shall briefly discuss three of these, namely:

(1) Scaling rules for thermal transpiration.

(2) Relation of the thermal transpiration maximum to the Knudsen permeability minimum.

(3) Determination of thermal conductivities and molecular relaxation times from thermal transpiration measurements.

To demonstrate the scaling rules, we define dimensionless pressure quantities as follows:

$$p^* \equiv p/(\pi_g \pi_\eta)^{1/2} , \tag{170}$$

$$\pi^* \equiv \pi_g/\pi_\eta = \frac{27\pi}{1280}\left[\frac{(\varepsilon/q)B_o}{\alpha_L K_o^2}\right] f_{tr} , \tag{171}$$

where

$$f_{tr} \equiv \frac{2}{3}(m\lambda_{tr}/k_B\eta) , \tag{172}$$

and rewrite Eq. (166) as

$$\frac{\Delta p^*}{2\alpha_L[1-(T_1/T_2)^{1/2}]} = \frac{p^*}{[p^* + (\pi^*)^{1/2}][p^* + (\pi^*)^{-1/2}]} . \tag{173}$$

Except for f_{tr}, the so-called translational Eucken factor, the quantity π^* is essentially a constant for a given porous medium. The value of f_{tr} is nearly equal to 5/2 for all gases; according to Eq. (46), deviations from the value 5/2 are caused entirely by inelastic collisions, and in practice such deviations amount to about 10% of the monatomic gas value. Moreover, we expect that the quantity $[(\varepsilon/q)B_o/\alpha_L K_0^2]$ in π^* is only weakly dependent on the structure of the porous medium, according to the discussion in Section C.1 of this chapter (it is equal to unity for circular capillaries that reflect molecules elastically). Thus π^* is nearly a universal constant, and a plot of $\Delta p^*\{2\alpha_L[1-(T_1/T_2)^{1/2}]\}^{-1}$ vs. p^* will be nearly a universal curve according to Eq. (173). In practice it will be a close one-parameter family of curves, the single parameter π^* being characteristic primarily of the porous medium. From such a family of curves we can therefore predict how thermal transpiration (really the thermomolecular pressure difference) will vary if we change either the gas, the porous medium, or both.

The physical meaning of the scaling rules can be made clearer by consideration of the special case of capillary tubes. If we recall that the viscosity of a gas is approximately

$$\eta = \frac{1}{2} n m \bar{v} \ell , \tag{174}$$

where ℓ is the mean free path, then it is readily shown that p^* is proportional to r/ℓ, the inverse Knudsen number. Thus the scaling rules are equivalent to the statement that, for fixed values of T_1 and T_2, the quantity $\Delta p/p$ is a universal function of the Knudsen number. This result has been known since at least 1910 [K5]; it is really just a result of dimensional analysis. A modern special case is the rule [L3] that for a given gas in a series of capillaries, a plot of $r\Delta p$ vs. rp is a universal curve. The dusty-gas model can thus be viewed as a quantitative generalization of these older capillary results, and moreover a generalization that gives explicit expressions for the universal curves involved.

There have been no explicit tests of these scaling rules using modern measurements on porous media, as far as we know, but the rules are known to hold for capillaries.

Turning now to the relation between the thermal transpiration maximum and the Knudsen permeability minimum, we see from Eq. (166) that the thermal transpiration curve of Δp vs. p is characterized by the three parameters π_g, π_η, and α_L, and from Eq. (149) that the normalized permeability curve of $\bar{K}/[D_K]_1$ vs. p is characterized by the parameters π_g, π', and π_η. Since both curves involve the two parameters π_g and π_η, it is not surprising that they should be somehow related. Moreover, π' is rather close to π_g; from Eq. (72) we have

$$\pi'/\pi_g = 1 - \frac{1}{5} \xi \alpha_L . \tag{175}$$

Thus only the parameter ξ occurs in the expression for $\bar{K}/[D_K]_1$ but not in that for Δp. If a value of ξ is chosen, say by educated guesswork based on various past measurements, the permeability curve can be predicted from a measured thermal transpiration curve, or vice versa. Such a test has apparently been carried out only once, by Hanley, with fairly satisfactory results [H1].

It is worth remarking that the foregoing relation is rather obvious in terms of the dusty-gas model, because of the common occurrence of π_g and π_η, but that such a relation should exist is not nearly so obvious on a purely empirical basis, because of the different numerical magnitudes involved. To illustrate this point, we can compare the pressures at which the permeability minimum and the thermal transpiration maximum occur. From Eqs. (150) and (168) we obtain

$$p_{min}/p_{max} = (\tfrac{1}{5}\,\xi\alpha_L)^{1/2} - (\pi^*)^{1/2}(1-\tfrac{1}{5}\,\xi\alpha_L) \ . \tag{176}$$

If we take $\xi\alpha_L = 0.95$ from Knudsen's capillary data, and $\pi^* = 27\pi/512$ from Eq. (171) for capillaries, the ratio is $p_{min}/p_{max} = 0.11$. The two pressure extrema thus occur at pressures that differ by an order of magnitude, which certainly does not suggest a close connection between the two.

The third relation, involving molecular relaxation times, exploits the fact that π^* is not quite a structural parameter, but depends also on the gas involved; in other words, deviations from $f_{tr} = 5/2$ are exploited. To extract this somewhat minor deviation from experimental measurements requires some care, but it can be done. First, the most sensitive part of the thermal transpiration curve is used, which is usually regarded as Δp_{max}. Second, the apparatus (usually a bundle of capillaries in parallel to reduce equilibration times) is calibrated with a gas having an accurately known value of f_{tr}; the calibration gas is frequently argon, which has $f_{tr} = 5/2$ because it is monatomic. Third, the fact that π_η contains D_K and not $[D_K]_1$ is taken into account. From Eq. (169) we then obtain

$$\frac{\Delta p_{max}}{\Delta p_{max}(Ar)} = \frac{\lambda_{tr}}{(5/2)} \left(\frac{m}{m_{Ar}}\right)^{1/2} \left[\frac{1 + (\pi^*_{Ar})^{1/2}}{1 + (\pi^*)^{1/2}}\right]^2 \ , \tag{177}$$

from which λ_{tr} (or f_{tr}) can be calculated. Thus measurements of pressure differences give the translational part of the thermal conductivity, from which the total thermal conductivity can be obtained, or the inelastic collision number can be calculated by Eqs. (46)–(47) from the deviation of f_{tr} from the value 5/2. This is an attractive prospect, since pressure measurements are much easier to make than are direct measurements of thermal conductivity, or the measurements of sound absorption or

shock-front thicknesses that are the usual sources of knowledge about inelastic collisions. This has been the motivation for much of the recent revival of interest in thermal transpiration [A5, B15, D2, G1, H5, M3, M6, M30, T1, T2]. On the whole, the results obtained are fairly good. Thermal conductivities obtained from thermal transpiration data have an accuracy comparable to that of most direct measurements. Inelastic collision members are not obtained with high accuracy from thermal transpiration data, because they are extracted from the measurement of a deviation from $f_{tr} = 5/2$, but high accuracy is not obtainable from the more traditional techniques, either. Some typical results are shown in Table 3.

Table 3. Translational Eucken factors f_{tr} and rotational collision numbers ζ determined from thermal transpiration data at a mean temperature of 475 K. The calibration gas was argon.

Gas	f_{tr}	ζ
Ar	(2.50)	(∞)
Xe	2.48	-
O_2	2.33	5.6
N_2	2.34	6.0
CO	2.20	2.3
CO_2	2.20	2.8

Data from Annis and Malinauskas [A5].

As an aside, it is worth noting that there have been substantial efforts, especially by Loyalka, Storvick, and their coworkers [L18, S18], to achieve a better theoretical understanding of thermal transpiration, especially its relation to fundamental quantities like translational thermal conductivity and molecular relaxation time. Their procedure is to avoid the approximations inherent in the dusty-gas model by carrying out an essentially exact numerical solution of the problem for well-defined simple geometries. Unfortunately, the appropriate Boltzmann integrodifferential equation is too difficult to solve in the transition region of interest, so model equations are used in which the Boltzmann collision integral operator is replaced by a simple relaxation term. In other words, the real problem is still modelled, but the model is of a

vastly different character than that of the dusty-gas model. It is therefore gratifying that the results turn out to be mutually consistent, especially the fact that thermal transpiration is a function of f_{tr}. It is interesting that this relation, which emerges so straightforwardly from the dusty-gas model, is not at all obvious in the more rigorous theoretical treatment of Loyalka and coworkers, although it can be extracted if one knows beforehand what to look for [S18].

As a final aside, thermal transpiration was for many years discussed within the framework of the thermodynamics of irreversible processes [H2]. In fact, thermal transpiration was used as a standard example in irreversible thermodynamics for purposes of illustration, although it could be calculated from standard kinetic theory only in the Knudsen and continuum limits. The dusty-gas model gives results over the entire pressure range. The thermodynamic results are often expressed in terms of a heat of transport, Q^*, interpreted as the amount of heat that flows from the surroundings to the gas on one side of the septum (or capillary) when one mole of gas is transferred isothermally through the septum (capillary). It is related to the steady-state thermomolecular pressure difference by an expression similar to the Clapeyron equation,

$$\frac{dp}{dT} = -\frac{Q^*}{T\bar{V}}, \tag{178}$$

where $\bar{V}$ is the molar volume of the gas. Comparison of this expression with Eq. (163) gives the dusty-gas expression for Q^*, which has been discussed by Malinauskas and Mason [M4].

2. Binary Mixtures

The main complication met in dealing with mixtures is the composition dependence of the $(\alpha'_{id})_{tr}$ and the $(\alpha'_{ij})_{tr}$. The difficulties, in other words, are not those of principle, but only of complex and messy algebra.

a. Pressure and Composition Dependence of Thermal Transpiration. As for single gases, it is easiest to obtain the general equation for thermal transpiration or thermo-osmosis of a binary mixture directly from Eq. (122), the generalization of Graham's law of diffusion. If no external forces act, the result is

$$\frac{\underset{\sim}{J}_1}{D_{1K}} + \frac{\underset{\sim}{J}_2}{D_{2K}} = -\left[1 + \frac{pB_o}{\eta\langle D_K\rangle}\right]\frac{\underset{\sim}{\nabla} p}{k_B T} - \frac{n_d}{n'}\left[n_1(\alpha'_{1d})_{tr} + n_2(\alpha'_{2d})_{tr}\right]\underset{\sim}{\nabla} \ln T, \quad (179)$$

where

$$\frac{1}{\langle D_K\rangle} \equiv \frac{x_1}{D_{1K}} + \frac{x_2}{D_{2K}} \quad . \quad (180)$$

As before, we are primarily interested in the pressure difference at steady state; setting $\underset{\sim}{J}_1 = \underset{\sim}{J}_2 = 0$ and making the usual one-dimensional approximation, we obtain

$$\frac{dp}{d \ln T} = -\frac{(n_d/n')k_B T[n_1(\alpha'_{1d})_{tr} + n_2(\alpha'_{2d})_{tr}]}{1 + (p/\langle \pi_\eta\rangle)} \quad , \quad (181)$$

where

$$\langle \pi_\eta\rangle \equiv \eta\langle D_K\rangle/B_o \quad . \quad (182)$$

It should be remembered that η is the viscosity of the mixture, and that $\langle \pi_\eta\rangle$ really contains the D_{iK} and not just the $[D_{iK}]_1$. The messy part is now to extract explicit expressions for the $(\alpha'_{id})_{tr}$, starting with Eq. (44) and using Eqs. (48)–(50). Only straightforward (but tedious) algebra is required, and we find [J3, M4]

$$\frac{d \ln p}{d \ln T}\left(1 + \frac{p}{\langle \pi_\eta\rangle}\right) =$$

$$= -\frac{2x_1\alpha_{1L}\pi_1[(a_{22}-a_{12})p+2\pi_2] + 2x_2\alpha_{2L}\pi_2[(a_{11}-a_{21})p+2\pi_1]}{(a_{11}p+2\pi_1)(a_{22}p+2\pi_2) - a_{12}a_{21}p^2} \quad , \quad (183)$$

where α_{iL} and π_i are properties of the porous medium and of species i only, with π_i given by Eq. (148) for the single species i. The a_{ij} are matrix elements that occur in the expressions for the continuum values of

the thermal conductivity and thermal diffusion factor for binary mixtures of species 1 and 2. They can be expressed in terms of the Λ_{ij} of Eqs. (48)–(50) as follows:

$$a_{11} = (2/x_1)(\lambda_{11})_{tr}\,\Lambda_{11}\,, \tag{184a}$$

$$a_{22} = (2/x_2)(\lambda_{22})_{tr}\,\Lambda_{22}\,, \tag{184b}$$

$$a_{12} = (2/x_1)(\lambda_{22})_{tr}\,\Lambda_{12}\,, \tag{184c}$$

$$a_{21} = (2/x_2)(\lambda_{11})_{tr}\,\Lambda_{12}\,. \tag{184d}$$

All the a_{ij} are linear in mole fraction. For a pure species (e.g., $x_1 = 1$, $x_2 = 0$), there is cancellation between numerator and denominator of Eq. (183), which then reduces to Eq. (163) for a single gas, as it should.

It is possible to put Eq. (183) into a finite-difference form in exactly the same way as was done for a single gas in the preceding section. The result is, using T_H and T_C for the hot and cold temperatures to avoid confusion with the species subscripts,

$$\frac{\Delta p}{p[1-(T_C/T_H)^{1/2}]} =$$

$$= \frac{2x_1\alpha_{1L}\pi_1[(a_{22}-a_{12})p + 2\pi_2]+2x_2\alpha_{2L}\pi_2[(a_{11}-a_{21})p+2\pi_1]}{[(a_{11}p+2\pi_1)(a_{22}p+2\pi_2) - a_{12}a_{21}p^2][1+(p/\langle\pi_\eta\rangle)]}\,. \tag{185}$$

The composition dependence of Δp has the form of a quadratic in mole fraction divided by another quadratic in mole fraction. The pressure dependence of Δp is more interesting — it has the form of a quadratic in p divided by a cubic in p, whereas Eq. (166) for a single gas has the form of a linear term in p divided by a quadratic in p. This raises the hope that the Δp vs. p curve for a mixture has a different shape than the curves for its pure components. This would have the practical advantage that the parameters of Eq. (185) could be found by fitting the measured pressure dependence of Δp at one or more compositions, and then the free

space diffusion coefficient $\mathcal{D}_{12}$ for the two species could be extracted. The constants B_o and K_o can be found from permeability measurements with a single gas, the viscosities of the pure components can be measured independently, and the collision integral ratios A^*_{12} and B^*_{12} can be calculated with sufficient accuracy from a reasonable intermolecular potential model. The only remaining unknown quantity is then $\mathcal{D}_{12}$ occurring in the a_{ij} and the mixture η. It would be a tempting method for measuring diffusion coefficients by measuring pressures.

Unfortunately, this cannot be realized in practice, as is illustrated in Fig. 21, where experimental data on neon-argon mixtures are presented [M5]. The curves for mixtures have essentially the same shape as those for single gases, as shown by the fact that the mixture measurements can be fitted quite accurately by the formula for a single gas, namely Eq. (166). The parameters needed for such a fit unfortunately do not seem to have any physical significance, however. Thus, mixtures look like single gases as far as thermal transpiration is concerned, and $\mathcal{D}_{12}$ cannot be obtained by easy pressure measurements. Nevertheless, something useful should be salvageable from this disappointing situation: since the shape of the Δp vs. p curve is not sensitive to composition, it should be possible to predict mixture curves from the curves for the pure components. This useful possibility has not yet been examined in detail.

b. Pressure Dependence of Thermal Diffusion. In this case we are interested in the relative separation between species 1 and 2 that is produced by the temperature gradient. We define an effective thermal diffusion factor, $\alpha_{12}(\text{eff})$, by analogy with the steady-state continuum result [G7, M23],

$$\nabla \ln(x_1/x_2) = - \alpha_{12}(\text{eff}) \nabla \ln T . \qquad (186)$$

In the continuum region, $\alpha_{12}(\text{eff})$ is independent of pressure, although it depends on both composition and temperature. It is sensitive to the nature of the collisions between molecules of species 1 and 2, and has been much studied as an experimental probe of forces between unlike molecules [G7, M23]. In the free-molecule region, however, $\alpha_{12}(\text{eff})$ should be zero, since each component of the mixture behaves independently and there is no relative separation of the components even though thermal transpiration occurs. The dusty-gas model is well-suited to describe the

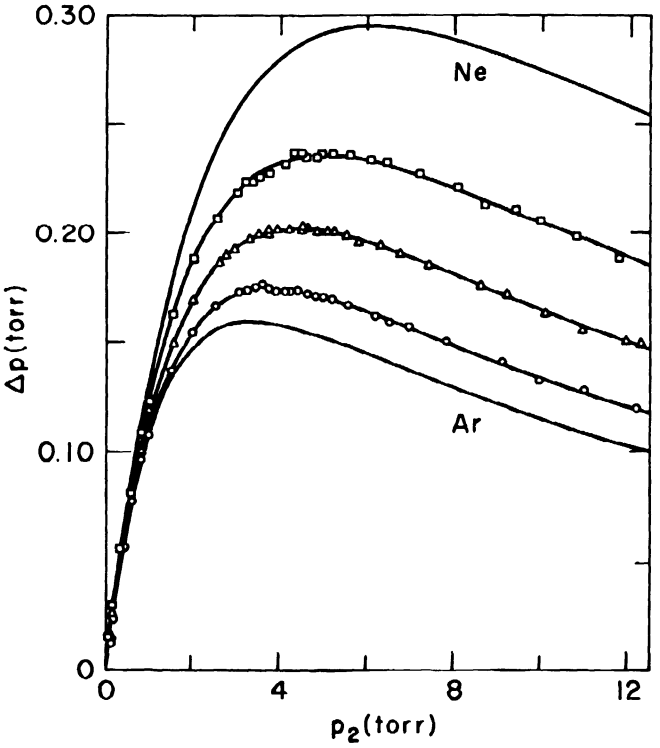

Fig. 21. Pressure dependence of the thermal transpiration effect in Ne + Ar mixtures for the same conditions as in Fig. 20. (The curves without points are the Ne and Ar curves of Fig. 20.) The mixtures are: □ x_{Ar} = 0.2900, △ x_{Ar} = 0.5350, ○ x_{Ar} = 0.7605. The solid curves were constructed using the formula for the pressure dependence of a single gas.

pressure dependence of α_{12}(eff) in the transition region, and in fact is the only theory presently available to describe this region. Simple momentum-transfer theories are notoriously bad for the description of thermal diffusion [M23, M36], and the proper solution of the Boltzmann equation, or even of its simpler relaxation models, is forbiddingly complex in this situation.

If we write Eq. (120) twice, for i = 1, and again for i = 2, and subtract the two equations [remembering that $(\alpha'_{21})_{tr} = -(\alpha'_{12})_{tr}$], we obtain

$$\frac{1}{D_{12}}\left(\frac{\underset{\sim}{J}_1}{n_1}-\frac{\underset{\sim}{J}_2}{n_2}\right)+\left(\frac{\underset{\sim}{J}_1}{n_1 D_{1K}}-\frac{\underset{\sim}{J}_2}{n_2 D_{2K}}\right)+\left(\frac{1}{D_{1K}}-\frac{1}{D_{2K}}\right)\frac{B_o}{\eta}\,(\underset{\sim}{\nabla} p - n\underset{\sim}{F}) =$$

$$= -\underset{\sim}{\nabla}\ln(n_1/n_2) + (\underset{\sim}{F}_1-\underset{\sim}{F}_2)k_B T$$

$$- (n')^{-1}\,[n(\alpha'_{12})_{tr} + n_d(\alpha'_{1d})_{tr} - n_d(\alpha'_{2d})_{tr}]\,\underset{\sim}{\nabla}\ln T\,. \qquad (187)$$

To find the relative separation at steady state, we set $\underset{\sim}{J}_1 = \underset{\sim}{J}_2 = 0$, drop the external force terms, and solve for $\underset{\sim}{\nabla}\ln(n_1/n_2)$. The resulting expression contains a term in $\underset{\sim}{\nabla}\ln T$, which represents the direct thermal separation, and another term in $\underset{\sim}{\nabla} p$, which represents the effect of the thermomolecular pressure difference on the separation. Making the one-dimensional approximation and substituting for ∇p from Eq. (181), we obtain an equation that looks like Eq. (186), with

$$\alpha_{12}(\text{eff}) = (n/n')(\alpha'_{12})_{tr} + (n_d/n')[(\alpha'_{id})_{tr}P_{\eta 2} - (\alpha'_{2d})_{tr}P_{\eta 1}]\,, \qquad (188)$$

where

$$P_{\eta i} \equiv \frac{1+(p/\pi_{\eta i})}{1+(p/\langle\pi_\eta\rangle)}\,. \qquad (189)$$

At high pressures, the continuum limit of $\alpha_{12}(\text{eff})$ is

$$\alpha_{12}(\infty) = \frac{b_1(a_{22}-a_{12}) + b_2(a_{11}-a_{21})}{a_{11}a_{22} - a_{12}a_{21}}\,, \qquad (190)$$

where the a_{ij} are given by (184), and

$$b_1 = -\frac{2}{5}(6C^*_{12}-5)\left(\frac{m_2}{m_1+m_2}\right)\frac{(\lambda_{11})_{tr}}{\mathcal{D}_{12}}\,, \qquad (191a)$$

$$b_2 = +\frac{2}{5}(6C_{12}^{*}-5)\left(\frac{m_1}{m_1+m_2}\right)\frac{(\lambda_{22})_{tr}}{\mathcal{D}_{12}} \quad . \tag{191b}$$

Substitution of the expressions for $(\alpha'_{12})_{tr}$ and $(\alpha'_{id})_{tr}$ back into Eq. (188) yields the final result [J3],

$$\alpha_{12}(\text{eff}) =$$

$$= \frac{\alpha_{12}(\infty)(a_{11}a_{22}-a_{12}a_{21})p^2 + 2(\pi_1 B_2 + \pi_2 B_1)p + 2\pi_1\pi_2(P_{\eta 1}-P_{\eta 2})}{(a_{11}p + 2\pi_1)(a_{22}p + 2\pi_2) - a_{12}a_{21}p^2} \quad , \tag{192}$$

where

$$B_1 \equiv 2b_1 + (a_{11} - a_{21})P_{\eta_1} \quad , \tag{193a}$$

$$B_2 \equiv 2b_2 - (a_{22} - a_{12})P_{\eta 2} \quad . \tag{193b}$$

For simplicity, we have set $\alpha_{iL} = 1/2$ in the above expression.

It is easy to see from Eq. (192) that $\alpha_{12}(\text{eff})$ approaches zero at very low pressures, and has the constant value $\alpha_{12}(\infty)$ at high pressures. However, the pressure dependence in the transition region can be quite complex, for the B_i and $P_{\eta i}$ are also pressure-dependent. Neglect of the thermomolecular pressure difference is equivalent to setting $P_{\eta i} = 1$ [J3, M17].

Unfortunately, there are essentially no reliable experimental data with which to compare these results. Sample calculations [J3] for He and Ar mixtures are shown in Fig. 22 for a temperature of 356 K, where the pressure dependence is fairly simple. The corresponding results with neglect of the thermomolecular pressure difference are also shown. There does not seem to be an obvious physical explanation for the enhanced separation due to the pressure difference.

D. REMARKS

In this chapter we have tried to relate the theoretical results of Chapter II and the experimental results, first by considering the best

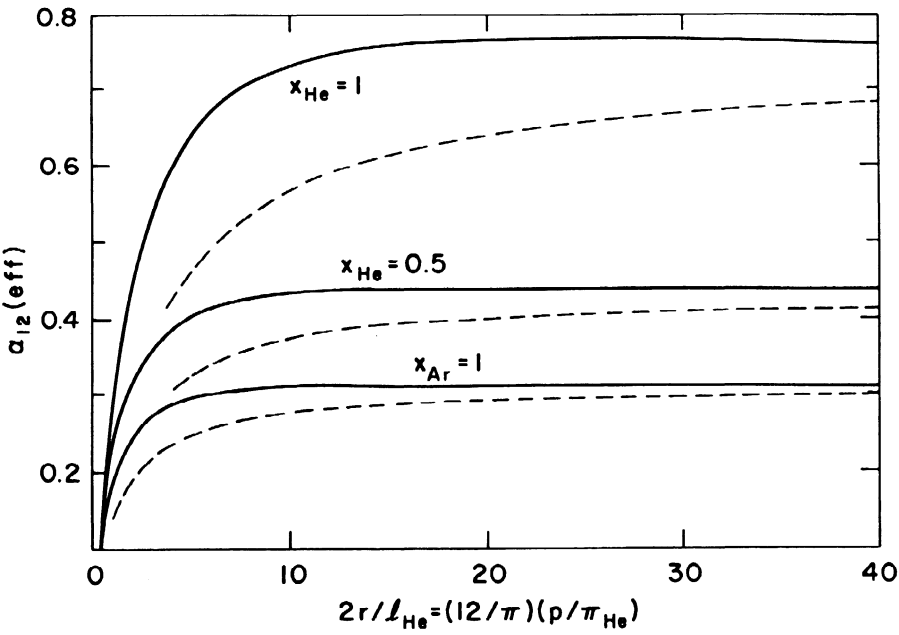

Fig. 22. Calculated thermal diffusion of He + Ar mixtures as a function of pressure and composition at 356 K. The solid curves represent Eq. (192), and the dashed curves are the calculated results with neglect of the thermomolecular pressure difference. The abscissa is given as the inverse Knudsen number for a capillary of radius r, with ℓ_{He} being the mean free path for He - He collisions only.

way to represent the experimental data, and then by a series of special examples for which data existed or might reasonably be expected to be obtained. These examples were chosen to give some feeling for the degree of confidence one might be willing to place in the dusty-gas model. As such, they correspond to "clean" laboratory cases, and not to the complicated cases usually met in engineering practice. The ideal purpose, of course, is to establish the reliability of the dusty-gas model so that it can be regarded as one of the known factors when trying to unravel the complexities of practical problems.

We believe the results in this chapter establish the reliability of the dusty-gas model for the description of gas-phase transport. Although

it is not perfect on many small details, it seems to be satisfactory for all the major phenomena so far encountered. We wish to emphasize the phrase, "gas-phase transport"; we make no claims regarding problems connected with the structure of porous media, or with adsorption and surface transport. These are important problems, but all we wish to suggest is that the dusty-gas model is a solution to only one important problem, the description of gas-phase transport.

Chapter IV

EXTENSIONS AND GENERALIZATIONS OF THE THEORY

In this chapter we discuss the application of the ideas behind the dusty-gas model to four phenomena other than gas transport in porous media. Some of these phenomena have been known for a long time and have a voluminous literature, both theoretical and experimental. We do not attempt to review this mass of material in any depth, but restrict ourselves to two modest aims only — to give examples of the wide scope of the dusty-gas model approach, and to provide an entry to the literature.

A. SLIP AND CREEP PHENOMENA IN RAREFIED GASES

At pressures somewhat less than those for which a gas behaves entirely as a continuum, the finite mean free path manifests itself as corrections to the boundary conditions at solid surfaces. These corrections take the form of various apparent discontinuities in the values of macroscopic variables (such as velocity and temperature) at the solid boundaries. In the cases we discuss here, these discontinuities (of velocity) appear as slipping or creeping motions of the gas in a thin layer adjacent to the surface. The names associated with these phenomena and the gradients that give rise to them are as follows:

(1) Viscous slip, caused by a pressure gradient parallel to the surface, which in turn gives rise to a macroscopic velocity gradient perpendicular to the surface.

(2) Thermal creep, caused by a temperature gradient parallel to the surface.

(3) Diffusive slip, caused by a composition gradient parallel to the surface.

The dusty-gas model is well-suited to treat these phenomena through the conceptual trick of regarding the solid boundary as one component of a gas mixture, such as already indicated in the lower part of Fig. 3. In fact, these phenomena are really only limiting cases at high pressures of the more general treatments given in Chapter III. The main reason for considering this

limit as a separate case is that the mathematical manipulations become particularly simple when the gas pressure is high (that is, the mean free path is much smaller than any geometric dimension of the system). Thus, it is fairly easy to include inelastic effects for polyatomic molecules, and sometimes to obtain generalizations to multicomponent mixtures, results which involve very complicated algebra in the general case of arbitrary pressures. For ease of reference, we give the connections of the slip and creep phenomena with the results of Chapter III below:

(1) Viscous slip — Section B.1 (viscous slip and the Knudsen permeability minimum).

(2) Thermal creep — Section C.2a (thermal transpiration or thermomolecular pressure difference).

(3) Diffusive slip — Section B.2d (diffusion pressure effect).

The historical background is briefly as follows. In 1879 Maxwell [M28] gave an extensive analysis of stresses arising in a moving, heated single gas consisting of structureless molecules, and discussed the phenomena of viscous slip and thermal creep. Except for some simplifications in the reasoning, no substantial changes have been made in this approach [K4, L5]. The analogous phenomenon of diffusive slip was not noticed until much later, when Kramers and Kistemaker gave an elementary theoretical discussion and demonstrated the effect experimentally in 1943 [K7]. Starting about 1957, there was a great increase in theoretical efforts to understand and calculate slip and creep phenomena, plus some experimental work. We do not attempt to survey this mass of material; the interested reader is referred to articles by Annis [A4], Cercignani [C2, C3], Loyalka and coworkers [L1, L2, L9, L11, L12, L14 — L17, L19, L20], Mason and Marrero [M18], and Zhdanov [Z1, Z2], where further references to the literature can also be found.

The application of the dusty-gas model to slip and creep phenomena seems to give the major features correctly, although some of the details may be missing or oversimplified, especially those connected with details of gas-surface scattering. Results for polyatomic gas mixtures have been derived by Annis and Mason [A6], who started with the dusty-gas results given by Eq. (120), and formed the mass-average velocity of the gas mixture,

$$\underset{\sim}{V}_o \equiv \sum_{i=1}^{\nu} m_i \underset{\sim}{J}_i \Big/ \sum_{i=1}^{\nu} n_i m_i \ . \tag{194}$$

After passing to the high-pressure limit by letting $n_d/n = 0$, it was possible, after some algebra, to identify the different slip and creep terms by inspection of $\underset{\sim}{V}_o$. That is, $\underset{\sim}{V}_o$ could be divided into several terms, and the velocity at a wall parallel to the z-direction could be written for a binary mixture as

$$V_{oz}\Big|_{y=0} = \sigma_{visc}(\partial p/\partial z) + \sigma_{ther}\ (\partial T/\partial z)$$

$$+ \sigma_{diff}[(\partial x_1/\partial z) + x_1 x_2 \alpha_{12}(\partial \ell n T/\partial z)] \ , \tag{195}$$

where the y-axis is perpendicular to the wall. We can now examine each term separately.

The simplest term is the viscous slip term. As might be expected, the continuum viscosity part of the dusty-gas equations (the part containing B_o/η) makes no contribution to slip. All the contributions to viscous slip come from the D_{iK} on the left-hand side of Eq. (120) and the $\underset{\sim}{\nabla}\ \ell n\ p$ on the right-hand side. If we neglect the small corrections Δ'_{id}, the viscous slip coefficient σ_{visc} can be written as

$$\sigma_{visc} = \frac{(4K_o/3)(8k_B T/\pi)^{1/2}}{p(x_1 m_1^{1/2} + x_2 m_2^{1/2})} \ , \tag{196}$$

where K_o is the Knudsen flow parameter defined in Eq. (6), assumed for simplicity to be the same for all species. It is more common to see the viscous slip term written in terms of the velocity gradient at the wall instead of in terms of the pressure gradient,

$$V_{oz}\Big|_{y=0} = \sigma'_{visc}\ (\partial V_{oz}/\partial y) \ . \tag{197}$$

However, in any application of the slip boundary conditions, the velocity gradient is usually eliminated in favor of a pressure gradient through the use of a momentum-balance relation. The dusty-gas model essentially does this at the outset. The slip coefficient σ'_{visc} of Eq. (197) is [Z1]

$$\sigma'_{visc} = \frac{\eta(\pi k_B T/2)^{1/2}}{p(x_1 m_1^{1/2} + x_2 m_2^{1/2})} , \qquad (198)$$

where η is the viscosity of the mixture; this result is equivalent to Eq. (196).

Except for the neglected small terms Δ'_{id}, the molecular internal degrees of freedom make no explicit contribution to the viscous slip. Similarly, the addition of further components to the mixture does not appreciably complicate the formulas. The viscosity η of Eq. (198) absorbs most of the polyatomic and multicomponent effects; the only explicit change required in Eqs. (196) and (198) is the replacement of the denominator,

$$x_1 m_1^{1/2} + x_2 m_2^{1/2} \to \sum_{i=1}^{\nu} x_i m_i^{1/2} . \qquad (199)$$

Notice that both σ_{visc} and σ'_{visc} diminish with increasing pressure as p^{-1}.

The thermal creep term arises from the gas-dust thermal diffusion terms, $(\alpha'_{id})_{tr}$, of Eq. (120). The resulting mass flow may thus be regarded as a thermal-diffusive separation between the gas and dust. Referring to Eq. (44) for the general expression for these thermal diffusion factors, we find a dependence upon the partial translational thermal conductivities, $(\lambda_i)_{tr}$. The expressions for these quantities are not altered by the presence of the dust in the high-pressure limit, and so we can combine most of these to form the total translational thermal conductivity of the mixture, according to Eq. (45). This manipulation requires that the gas-dust collisions be the same for all species, so that the factors $(6C^*_{id}-5)$ will all have the same values. (For simplicity, these may be taken to be unity [A6].) A few terms involving the $(\lambda_i)_{tr}$ are left over; since partial thermal conductivities are not experimentally observable, it is advantageous to combine these into the thermal diffusion factor for the gas pair, which is observable. Thus, the expression for the thermal creep coefficient σ_{ther} can be divided into two parts,

$$\sigma_{ther} = \sigma'_{ther} + \sigma''_{ther} , \qquad (200)$$

where

$$\sigma'_{ther} = \frac{\langle m^{3/2} \rangle \ \lambda_{tr}}{\langle m^{1/2} \rangle \langle m \rangle \ 5p} \ , \tag{201}$$

$$\sigma''_{ther} = \frac{(m_1 + m_2)(m_2^{1/2} - m_1^{1/2}) \ x_1 x_2 (\alpha_{12})_{tr} \mathcal{D}_{12}}{\langle m^{1/2} \rangle \langle m \rangle (6C^*_{12} - 5) \ T} \ , \tag{202}$$

and

$$\langle m^n \rangle \equiv x_1 m_1^{\ n} + x_2 m_2^{\ n} \ . \tag{203}$$

The advantage of this arrangement of terms is that σ'_{ther} is analogous to the corresponding result for a single gas, and can be easily generalized to a multicomponent mixture. It is only necessary to take λ_{tr} as the total translational conductivity of the mixture, and to generalize the average $\langle m^n \rangle$ as

$$\langle m^n \rangle \equiv \sum_{i=1}^{\nu} x_i m_i^{\ n} \ . \tag{204}$$

The term σ''_{ther} occurs only for mixtures, because of the factor $x_1 x_2$. The generalization of σ''_{ther} for multicomponent mixtures is somewhat more complicated, and involves a term like Eq. (202) for each gas pair in the mixture [A6].

Notice that both σ'_{ther} and σ''_{ther} diminish with increasing pressure as p^{-1}, since λ_{tr} and $(\alpha_{12})_{tr}$ are independent of p, and $\mathcal{D}_{12}$ varies as p^{-1}. Notice also that it is the free-space diffusion coefficient $\mathcal{D}_{12}$ that occurs, and not D_{12}, since the concern in this instance is with the gas space external to a solid boundary.

Only the diffusive slip term remains to be discussed. It arises from the gas-gas concentration and thermal diffusion parts of Eq. (120), namely the terms $\underset{\sim}{\nabla} \ln (n_i/n)$ and $(\alpha'_{ij})_{tr}$. However, it is neither necessary nor advantageous to have ignored the contribution of $(\alpha_{12})_{int}$ to α_{12}, as was done in deriving Eq. (120), and Eq. (195) thus

contains the total α_{12} and not just $(\alpha_{12})_{tr}$ in its last term. The expression for the diffusive slip coefficient is

$$\sigma_{diff} = \frac{(m_1 m_2)^{1/2}(m_2^{1/2} - m_1^{1/2})}{\langle m^{1/2}\rangle\langle m\rangle} \mathfrak{D}_{12} \cdot \tag{205}$$

The extension of this expression to multicomponent mixtures is complicated, and has not been carried through thus far. (However, see the results on multicomponent diffusiophoresis in Section C of this chapter.)

Notice again the appearance of $\mathfrak{D}_{12}$, not D_{12}, and the fact that σ_{diff} varies with pressure as p^{-1}. Indeed, all of the slip and creep coefficients show this pressure dependence.

In summary, polyatomic effects (inelastic collisions) on slip and creep coefficients are readily calculated by the dusty-gas model. There are no special effects for viscous and diffusive slip; the main effect occurs for thermal creep, which depends only on the translational parts of the gas thermal conductivity and thermal diffusion. The generalization to multicomponent mixtures is straightforward for viscous slip and thermal creep, but is more complicated for diffusive slip, which involves a description of multicomponent diffusion. Surface effects are purposely avoided by the dusty-gas model, but the appearance of gas-dust collision integrals suggests where some of the details of gas-surface collisions should be included. Annis and Mason [A6] have shown how some of the slip and creep formulas can be modified in this way, and the results are in general agreement with more elaborate kinetic-theory calculations [Z1, Z2].

B. RADIOMETER EFFECTS

A radiometer is usually seen in the form of a four-vaned device spinning in the display window of a novelty shop. It was originally thought to be driven by light radiation (hence the name), but its operation depends on the gas inside the glass envelope. Temperature gradients set up in the gas by unequal heating of the vanes supply the driving force on the vanes. The effect has been studied for over a century; some of the historical background can be found in the books of Kennard and Loeb [K4, L5]. Quantitative work is usually carried out by measuring the torque required to hold the vane motionless in the presence of a fixed temperature gradient that is produced by an adjacent stationary plate which is heated electrically

Radiometer forces can be calculated using the dusty-gas model by regarding the radiometer vane as an array of "giant molecules" linked together, and treating these giant molecules as one component of the gas mixture. Obviously, this viewpoint is very close to that adopted for the discussion of gas transport in porous media; the entire previous treatment of thermal transpiration or the thermomolecular pressure difference (Chapter III) can be taken over almost intact, except for two small modifications, as follows:

(1) The viscous-flow component now corresponds not to Poiseuille's law of flow, but to Stokes' law for drag. In place of Eq. (51) for $\underset{\sim}{J}_{visc}$, we therefore write

$$\underset{\sim}{V}_{visc} \equiv \underset{\sim}{J}_{visc}/n = - \underset{\sim}{F}_d/R_o'\eta \ , \tag{206}$$

where $\underset{\sim}{F}_d$ is the force on one of the giant molecules (dust particles), R_o' is a geometric constant, and η is the gas viscosity. For flow over spheres of radius r, $R_o' = 6\pi r$.

(2) Since we are now interested in the force on the vane, we should use the relation of Eq. (57), namely $n_d\underset{\sim}{F}_d = \nabla\underset{\sim}{p}$, to eliminate $\nabla\underset{\sim}{p}$ from the transport equations in favor of $\underset{\sim}{F}_d$, instead of <u>vice versa</u>, as was done for thermal transpiration.

The calculations have been performed for single gases by Mason and Block [M13], and for binary mixtures by Jenkins and Mason [J3]. By mathematically eliminating pressure and temperature gradients, we obtain the following flux equation for a binary mixture:

$$\frac{\underset{\sim}{J}_1}{D_{1K}} + \frac{\underset{\sim}{J}_2}{D_{2K}} = - \left(1 + \frac{p}{\eta\langle D_K\rangle n_d R_o'}\right) \frac{n_d \underset{\sim}{F}_d}{k_B T}$$

$$- \frac{n_d}{n'} \left[n_1(\alpha_{1d}')_{tr} + n_2(\alpha_{2d}')_{tr}\right] \underset{\sim}{\nabla} \ln T \ , \tag{207}$$

where the D_{iK} are the usual Knudsen diffusion coefficients which are defined in terms of the gas-dust diffusion coefficients by Eq. (61). The results for a single gas are obtained simply by dropping one of the components from this equation. This equation is of <u>exactly</u> the same form as Eq. (179) for thermal transpiration, with the replacements,

$$\underset{\sim}{\nabla} p \to n_d \underset{\sim}{F}_d \ , \quad B_o \to 1/n_d \ R'_o \ . \tag{208}$$

All the results for thermal transpiration therefore hold for radiometer effects, with only a small change of notation.

In particular, it is convenient to define the total force on the radiometer vane per unit temperature gradient as

$$\tau \equiv n_d \underset{\sim}{F}_d / \underset{\sim}{\nabla} \ln T \ , \tag{209}$$

which has the dimensions of torque per unit volume. Then in place of (d ln p/d ln T) for the thermomolecular pressure difference, we write τ/p and make the substitutions given by Eq. (208). The radiometer force is then given by Eq. (163) for a single gas and Eq. (183) for a binary mixture. It is not worthwhile to essentially repeat the whole discussion already given for thermal transpiration, especially since no measurements of the radiometer effect in mixtures have been reported, as far as we are aware. We therefore limit our remarks to two points about the radiometer effect in single gases: comparison with experimental data through a successful semiempirical formula, and the determination of λ_{tr} and rotational collision numbers from such data.

Very simple arguments suffice to establish the pressure dependence of τ at the two extremes of low and high pressures; namely, τ is directly proportional to p at low pressures, and inversely proportional to p at high pressures. Brüche and Littwin [B14, D14] proposed that these two limiting forms might be combined in the form

$$\tau = [(a'/p) + (p/b')]^{-1} \ , \tag{210}$$

where a' and b' are constants. (This is analogous to treating τ as composed of resistances in parallel, as in branches 1 and 2 of Fig. 1.) It was observed that this expression gave a rather good fit of experimental results, but that the experimental τ vs. p curve was a little flatter and wider than predicted by Eq. (210). If the dusty-gas model result, as given through Eq. (163), is put in this form, we find that $a' = 1/\alpha_L$ and $b' = \alpha_L \pi_g \pi_\eta$, but that an additive constant term also appears, $c' = (\pi_g + \pi_\eta)/\alpha_L \pi_g \pi_\eta$, which is the extra small feature needed to improve the fit.

The value of τ_{max} can be used to find the values of f_{tr} and hence of the rotational collision number, just as was done for thermal transpiration. Some results are given in Table 4 [M13]. The accuracy is not

Table 4. Translational Eucken factors f_{tr} and rotational collision numbers ζ determined from radiometer data.[a] The calibration gases were neon and argon.

Gas	f_{tr}	ζ
Ne	(2.50)	(∞)
Ar	(2.50)	(∞)
O_2	2.2_4	3
N_2,CO	2.3_2	4
CO_2,N_2O	2.1_3	2
CH_4	2.1_0	2

[a]Data from Brüche and Littwin [B14] via Mason and Block [M13].

great because the experimental values had to be determined from a graphical presentation of the data, but the agreement with similar values from thermal transpiration, given in Table 3, is not unreasonable.

By working at a more modest level of accuracy, and ignoring the effects of inelastic collisions, one can use radiometer measurements to determine molecular collision diameters. In terms of the present theory, one proceeds from τ_{max} to the mean free path ℓ through η by Eq. (174), and thence to the collision diameter. Miller and Bernstein [M32] used basically this procedure to study a large number of halomethanes, but had to use an older theory based on a rigid-sphere model for the gas molecules, since the present theory was not available at the time.

C. AEROSOL MOTION

The motion of small suspended particles (dust, smoke, aerosols, etc.) in a gas or gas mixture containing gradients of temperature, pressure, or composition is a subject that enters into the discussion of a great variety of phenomena of interest not only in engineering, but also in such diverse fields as environmental science, atmospheric physics, colloid chemistry, and astrophysics. The subject goes back at least to

1870, when Tyndall [T5] noticed a dust-free region in the gas space about a hot body ("Tyndall dark space"), showing that a temperature gradient has an effect on the motion of dust particles in a gas. Not surprisingly, there is a large body of literature connected with the subject, much of it reviewed in the book of Hidy and Brock [H9].

In the aerosol problem, we are concerned literally with a "dusty gas". The dusty-gas model for gas transport in porous media grew out of this problem, as was pointed out in Chapter I. In a sense, we are presenting the subject in a reverse logical order (which is the way it actually developed). As might be expected, there are many analogies between phenomena in porous media and aerosol phenomena, the latter of which are usually termed some sort of "phoresis". Table 5 lists the main analogies, as an aid to understanding the technical jargon of both fields.

The calculations for aerosol motion involve features from both the slip and creep calculations of Section A of this chapter and the radiometer calculations of Section B. To some extent we are merely repeating the radiometer calculations, inasmuch as the radiometer vane was visualized as a collection of connected aerosol particles. We thus use the same replacements for ∇p and B_o as given by Eq. (208). In addition, we assume that the aerosol dispersion is dilute enough to neglect interactions between aerosol particles, so that agglomeration is ignored. This means that we can use the limiting result $n_d/n \to 0$, as in the slip and creep calculations.

1. General Formulation

Since both the particles and the gas may be moving with respect to a laboratory or other external frame of reference, it is easiest to begin by calculating the relative velocity of gas and particles. This is just the mass-average velocity of the gas in a reference frame in which the particles are stationary, which is the case already worked out for gas transport in porous media. We use the mass-average velocity, because it is momentum that is related to force, by Newton's second law of motion. That is, we calculate

$$\mathbf{V}_{gas} - \mathbf{V}_d = \mathbf{V}_o \equiv \sum_{i=1}^{\nu} m_i \mathbf{J}_i \Big/ \sum_{i=1}^{\nu} n_i m_i \,, \tag{211}$$

Table 5. Analogies between phenomena associated with gas transport through porous media and aerosol phenomena.

Physical Conditions	Names of Phenomena	
	Porous Media	Aerosols
Flowing isothermal gas or uniform gas mixture	Permeability	Drag or mobility
	Viscous slip	Cataphoresis
	(Poiseuille-Darcy; Knudsen)	(Stokes; Millikan)
Simultaneous flow and diffusion of an isothermal gas mixture	Uniform-pressure diffusion (Graham)	Diffusiophoresis
	Diffusion pressure effect	
	Diffusive slip (Kramers-Kistemaker)	
Temperature gradient in a single gas	Thermal transpiration	Thermophoresis (Tyndall dark space)
	Thermomolecular pressure difference	
	Thermal creep	
(Irradiation)	(Radiometer effect)	(Photophoresis)
Temperature gradient in a gas mixture	Thermal transpiration	Thermodiffusiophoresis
	Pressure dependence of thermal diffusion	

where $\underset{\sim}{V}_{gas}$ is the local mass-average velocity of the gas in the laboratory frame, as determined by the boundary conditions in the gas mixture, and $\underset{\sim}{V}_d$ is the aerosol velocity in the laboratory frame. It may not be a trivial problem to calculate $\underset{\sim}{V}_{gas}$, especially for a multicomponent mixture, but this is done independently of the phoresis part of the problem and is thus not of primary concern here. The condition of $n_d/n \to 0$ makes the right-hand side of Eq. (211) comparatively easy to evaluate for multicomponent mixtures, and this generalization has been developed by Viehland and Mason [V1]. We give first the general multicomponent formulas, and then present special cases of interest.

The result of evaluating the expression in Eq. (211) can be written as

$$\underset{\sim}{V}_d = \underset{\sim}{V}_{gas} + Z\underset{\sim}{F}_d + \underset{\sim}{V}_d^0 \ , \qquad (212)$$

where $\underset{\sim}{F}_d$ is the external force on the aerosol particles, Z is the mobility of the particles in a uniform gas mixture having the same composition, pressure, and temperature as the actual nonuniform mixture at the location of the particle, and $\underset{\sim}{V}_d^0$ is the velocity that the particles would have in the absence of external forces in a gas mixture of the same local composition, pressure, and temperature whose boundary conditions were arranged so that $\underset{\sim}{V}_{gas} = 0$. It is convenient to write $\underset{\sim}{V}_d^0$ as the sum of three terms,

$$\underset{\sim}{V}_d^0 = \underset{\sim}{V}_d^0(\text{diff}) + \underset{\sim}{V}_d^0(\text{ther}) + \underset{\sim}{V}_d^0(\text{coupl}) \ . \tag{213}$$

The first term is a diffusiophoresis term, the second a thermophoresis term, and the third a coupling term in the sense that it vanishes unless both a mixture and a temperature gradient are present. In terms of the slip and creep results in Section A, $\underset{\sim}{V}_d^0(\text{diff})$ corresponds to σ_{diff}, $\underset{\sim}{V}_d^0(\text{ther})$ to σ'_{ther}, $\underset{\sim}{V}_d^0(\text{coupl})$ to σ''_{ther}, and Z to σ'_{visc}.

The expression for $\underset{\sim}{V}_d^0(\text{diff})$ is rather complicated for a multicomponent gas mixture,

$$\underset{\sim}{V}_d^0(\text{diff}) = - \sum_{i=1}^{\nu-1} [nD_{\text{eff}}^{(i)}/\rho](\underset{\sim}{\nabla} x_i + \sum_{j=1}^{\nu-1} x_i x_j \alpha_{ij} \underset{\sim}{\nabla} \ell n \ T) \ . \tag{214}$$

The α_{ij} are the usual multicomponent thermal diffusion factors of the gas species, and the $D_{\text{eff}}^{(i)}$ are effective multicomponent diffusion coefficients which have dimensions of mass as well as diffusion coefficient (e.g., g-cm^2/sec), and are given by the ratio of two $\nu x \nu$ determinants, the denominator being

$$
\begin{vmatrix}
\frac{1}{\mathfrak{D}_{1d}} & \frac{1}{\mathfrak{D}_{2d}} & \frac{1}{\mathfrak{D}_{3d}} & \cdots & \frac{1}{\mathfrak{D}_{(\nu-1)d}} & \frac{1}{\mathfrak{D}_{\nu d}} \\
-\sum_{\substack{j=1 \\ j\neq 1}}^{\nu} \frac{x_j}{\mathfrak{D}_{1j}} & \frac{x_1}{\mathfrak{D}_{12}} & \frac{x_1}{\mathfrak{D}_{13}} & \cdots & \frac{x_1}{\mathfrak{D}_{1(\nu-1)}} & \frac{x_1}{\mathfrak{D}_{1\nu}} \\
\frac{x_2}{\mathfrak{D}_{12}} & -\sum_{\substack{j=1 \\ j\neq 2}}^{\nu} \frac{x_j}{\mathfrak{D}_{2j}} & \frac{x_2}{\mathfrak{D}_{23}} & \cdots & \frac{x_2}{\mathfrak{D}_{2(\nu-1)}} & \frac{x_2}{\mathfrak{D}_{2\nu}} \\
\frac{x_{\nu-2}}{\mathfrak{D}_{1(\nu-2)}} & \frac{x_{\nu-2}}{\mathfrak{D}_{2(\nu-2)}} & \frac{x_{\nu-2}}{\mathfrak{D}_{3(\nu-2)}} & \cdots & \frac{x_{\nu-2}}{\mathfrak{D}_{(\nu-2)(\nu-1)}} & \frac{x_{\nu-2}}{\mathfrak{D}_{(\nu-2)\nu}} \\
\vdots & \vdots & \vdots & & \vdots & \vdots \\
\frac{x_{\nu-1}}{\mathfrak{D}_{1(\nu-1)}} & \frac{x_{\nu-1}}{\mathfrak{D}_{2(\nu-1)}} & \frac{x_{\nu-1}}{\mathfrak{D}_{3(\nu-1)}} & \cdots & -\sum_{\substack{j=1 \\ j\neq \nu-1}}^{\nu} \frac{x_j}{\mathfrak{D}_{(\nu-1)j}} & \frac{x_{\nu-1}}{\mathfrak{D}_{(\nu-1)\nu}}
\end{vmatrix} \tag{215}
$$

The numerator for $D_{eff}^{(i)}$ is obtained from this determinant by replacing the (i+1) row by $\{m_1, m_2, \cdots, m_{\nu-1}, m_\nu\}$. Although it may appear from Eqs. (214) and (215) that the νth species in the gas mixture is being discriminated against, the results are the same no matter which species is designated as ν. The apparent discrimination arises because the ν Stefan-Maxwell diffusion equations for the gas mixture are not independent; any one equation is equal to the sum of the other $(\nu-1)$ equations. The $\mathfrak{D}_{ij}$ are the regular gaseous diffusion coefficients, taken to be experimentally known quantities, as are the α_{ij}.

The $\mathfrak{D}_{id}$ appearing in Eq. (215) are the gas-dust diffusion coefficients, given in first approximation by Eq. (64) and in higher approximation by Eqs. (62) and (70). At this point it is convenient to introduce a change of notation to accommodate the fact that the pressure dependences of phoresis phenomena are customarily expressed through a particle Knudsen number, ℓ/r, where ℓ is the mean free path of the gas

molecules and r is the radius of the particle (assumed spherical). We first define an effective radius as

$$r \equiv R_o'/6\pi \ , \tag{216}$$

where R_o' is the modified Stokes radius of Eq. (206). In a mixture, more than one mean free path exists, and all the free paths depend on composition; we therefore define the quantities (not to be confused with the Λ_{ii} and Λ_{ik} for the thermal conductivity of gas mixtures),

$$\Lambda_i \equiv (\eta/r)(\pi k_B T/2m_i)^{1/2} \ . \tag{217}$$

These have the dimensions of pressure (analogous to the π_i used in Chapters II and III, but not identical). For a single gas, the ratio Λ/p becomes equal to ℓ/r. The $\mathfrak{D}_{id}$ can then be written as

$$n\mathfrak{D}_{id} = \frac{a_i'\Lambda_i}{6\pi r\eta(1-\Delta_{id})} \ , \tag{218}$$

$$1-\Delta_{id} = \frac{1+c_i'(\Lambda_i/p)}{1+b_i'(\Lambda_i/p)} \ , \tag{219}$$

where the dimensionless parameters a_i', b_i', and c_i' are defined as

$$a_i' \equiv 9/4\Omega_{id}^{(1,1)*} \ , \tag{220}$$

$$b_i' \equiv (n_d r/\eta)(\alpha_{iR}/\alpha_{iL})(2m_i k_B T/\pi)^{1/2} \ , \tag{221}$$

$$c_i' \equiv b_i'\left(1 - \frac{1}{5}\,\xi_i\alpha_{iL}\right) \ . \tag{222}$$

Similarly, the gas-particle thermal diffusion factors α_{id} can be written as

$$\alpha_{id} = -\frac{(6C_{id}^* - 5)}{a_i'\Lambda_i}\,\frac{6\pi r\eta}{5k_B}\,\frac{(\lambda_i)_{tr}}{x_i} \ , \tag{223}$$

where $(\lambda_i)_{tr}$ is, as before, the partial translational thermal conductivity of species i in the gas mixture.

The remaining phoresis quantities can then be written in terms of the above-defined quantities as follows:

$$Z(6\pi r\eta) = 1 + \left[\sum_{i=1}^{\nu} \frac{x_i(1-\Delta_{id})}{a_i'(\Lambda_i/p)}\right]^{-1}, \tag{224}$$

$$\underset{\sim}{v}_d^{\,0}(\text{ther}) = -\left[5p\langle m\rangle \sum_{i=1}^{\nu} \frac{x_i(1-\Delta_{id})}{a_i'(\Lambda_i/p)}\right]^{-1} \times \left[\sum_{i=1}^{\nu} \frac{x_i m_i}{a_i'(\Lambda_i/p)} \sum_{j=1}^{\nu} (6C_{jd}^{*}-5)(\lambda_j)_{tr}\right] \underset{\sim}{\nabla} T, \tag{225}$$

$$\underset{\sim}{v}_d^{\,0}(\text{coupl}) = -\left[5p\langle m\rangle \sum_{i=1}^{\nu} \frac{x_i(1-\Delta_{id})}{a_i'(\Lambda_i/p)}\right]^{-1} \times \left\{\sum_{i=1}^{\nu} x_i m_i \sum_{j=1}^{\nu} (6C_{jd}^{*}-5)(\lambda_j)_{tr}\left[\frac{1}{a_j'(\Lambda_j/p)} - \frac{1}{a_i'(\Lambda_i/p)}\right]\right\} \underset{\sim}{\nabla} T. \tag{226}$$

These equations are the complete theoretical expressions for the motion of aerosol particles in multicomponent gas mixtures with gradients of both composition and temperature. They are quite general, covering the full range from the free-molecule to the continuum regime (relative to the particle radius). Some simplifying approximations may often be possible, such as setting all the $(6C_{id}^{*}-5)$ equal to unity, as was done for slip and creep phenomena, or even ignoring the correction terms Δ_{id}.

Before illustrating the general results by giving some simple special cases, we make three remarks:

First, we have ignored some correction terms that appear in higher-order kinetic-theory calculations, just as these terms were ignored in

the discussion of gas transport in porous media. Some of the corrections have been calculated explicitly in the aerosol case by Annis [A3].

Second, we have implicitly assumed that the aerosol particles do not perturb the composition and temperature gradients in the gas. We therefore cannot consider particles with large thermal conductivities [H9], and we completely miss some thermal stress mechanisms of thermophoresis such as have been described by Sone [S10]. (We will demonstrate that the thermal conductivity effect is not as serious as might at first be expected.)

Third, we have assumed that the boundaries necessary to set up gradients in the gas are very widely spaced compared to the mean free path. When this is not the case, a new Knudsen number, corresponding to boundary spacing, must be introduced. Its effects can be taken into account by introducing additional pressure dependences of the gas transport coefficients themselves, as was shown by Annis and Mason [A7]. (An illustration, for the case of thermophoresis in a single gas, is given later in this chapter.)

2. Drag on a Particle

Perhaps the best-known formula for the drag of a gas on a spherical particle is that used by Millikan [M35] in connection with his famous oil-drop experiments for determining the charge of the electron, which can be written in terms of the mobility Z as

$$Z(6\pi r\eta) = 1 + (\ell/r)(A + Be^{-cr/\ell}) , \tag{227}$$

where A, B and c are constants. The exponential term in parentheses has no particular theoretical foundation, but furnishes an accurate interpolation over the entire range of ℓ/r from the free-molecule to the continuum region. For small ℓ/r, this formula reduces to Stokes' law, including a known first-order correction for slip,

$$Z(6\pi r\eta) = 1 + A(\ell/r) + \ldots . \tag{228}$$

When ℓ/r is large, the drag is due entirely to isolated molecular impacts and must be proportional to πr^2, the cross-sectional area presented by the sphere. In this case Eq. (227) reduces, after using Eq. (174) for η, to

$$Z = (A+B)[3n\pi\bar{v}(\pi r^2)]^{-1} , \qquad (229)$$

which again is of the correct form.

Annis, Malinauskas, and Mason [A8] have compared Eq. (224) for Z with Millikan's formula and with his measurements on oil droplets, adjusting the parameters a_i', b_i', c_i' of Eq. (224) to match Millikan's empirical values of A, B, c at small and large ℓ/r. The results are shown in Fig. 23, and cover nearly four orders of magnitude in ℓ/r. The deviation is systematic, but is small, being about the same as the experimental error of the measurements (±2%).

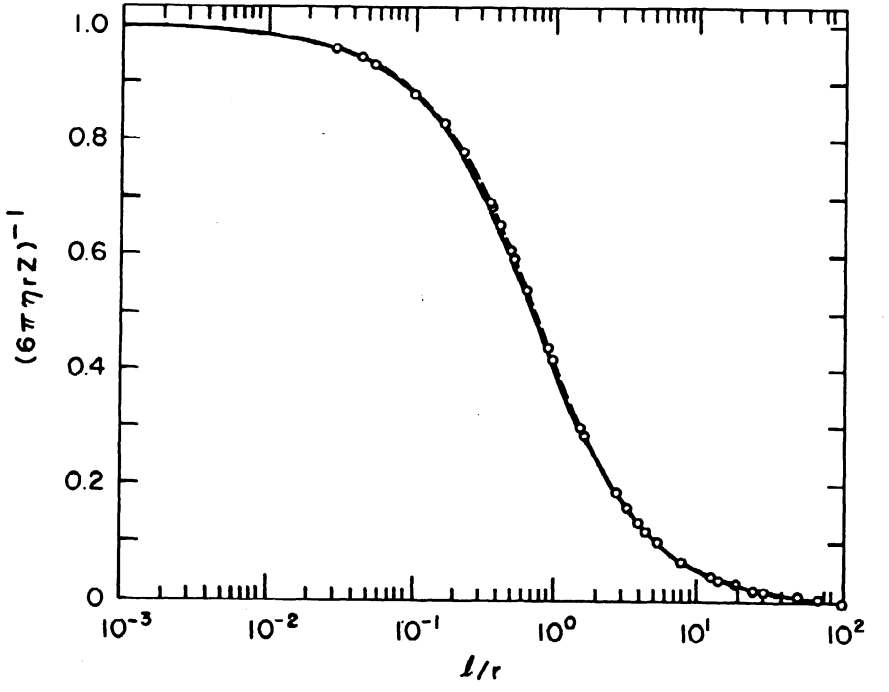

Fig. 23. Reciprocal slip factor, $(6\pi\eta rZ)^{-1}$, for oil droplets as a function of Knudsen number, ℓ/r. The circles are data for watchmaker's oil in air. The dashed curve is Millikan's formula, Eq. (227), and the solid curve is the present formula, Eq. (224), adjusted to Millikan's empirical parameters.

A more rigorous theoretical treatment of the drag problem, also spanning the entire range of ℓ/r, has been given by Cercignani and coworkers [C3 - C5], who solved the simplified Bhatnagar-Gross-Krook (BGK) model of the Boltzmann equation. The results were sufficiently complicated to require high-speed computation, and are given in Table 6 for the case of molecules which are thermally accommodated and diffusely scattered from the droplet surface. Also shown in the table are values from Millikan's formula, Eq. (227), with parameters determined from fitting oil-droplet data, and from the dusty-gas formula, Eq. (224), adjusted to Millikan's parameters (as in Fig. 23). The present results are very close to the BGK results, and both are slightly lower than the Millikan values, the maximum deviation being 2.4% over the range 0.5 to 0.9 in ℓ/r.

We can conclude that Eq. (224) reproduces the Millikan equation almost within experimental error, and is within about 1% of the accurate numerical results of the BGK model. Further comparisons for single gases can be found in the paper of Annis, Malinauskas, and Mason [A8]. Unfortunately, we know of no data suitable for testing Eq. (224) for mixtures, and the most that has been done is to see how much error might be incurred by treating air as a single gas rather than as a mixture in the analysis of Millikan's oil-drop experiments. The effect is small — the mixture value of Z is at most about 0.2% larger than the value obtained on the assumption that air is a single gas [A9].

Although data on drag in mixtures for testing Eq. (224) are lacking, it is worth pointing out what the predicted composition dependence of Z is. The composition dependence as given by Eq. (224) has a superficially simple appearance that is deceptive. It must be remembered that the viscosity η can have a fairly complicated composition dependence, and that η enters Eq. (224) not only as an explicit factor, but is also hidden in the Λ_i according to Eq. (217), and in b_i' and c_i' according to Eqs. (221) and (222). However, the composition dependence contained in η can be explicitly factored out of Eq. (224). We first notice that η cancels out of the products $b_i'\Lambda_i$ and $c_i'\Lambda_i$, so that Δ_{id} is independent of composition. Secondly, we notice that $6\pi r\eta = 1/Z_\infty$, where Z_∞ is the high-pressure limit of Z at the same composition. Then Eq. (224) can be arranged into the form

Table 6. Comparison of different results for sphere drag as a function of Knudsen number.

$\frac{\pi^{1/2}}{2}\frac{r}{\ell}$	$\frac{\ell}{r}$	Z(free-molecule)/Z		
		BGK model	Millikan	Dusty-gas
0.050	17.7	0.978	0.978	0.978
0.075	11.8	0.965	0.968	0.967
0.10	8.86	0.953	0.957	0.956
0.25	3.54	0.886	0.896	0.892
0.50	1.77	0.790	0.804	0.794
0.75	1.18	0.709	0.724	0.711
1.00	0.886	0.640	0.655	0.641
1.25	0.709	0.582	0.596	0.582
1.50	0.591	0.533	0.546	0.533
1.75	0.506	0.491	0.502	0.490
2.0	0.443	0.455	0.464	0.454
2.5	0.354	0.395	0.403	0.395
3	0.295	0.349	0.355	0.349
4	0.222	0.282	0.286	0.283
5	0.177	0.236	0.240	0.237
6	0.148	0.203	0.206	0.204
7	0.127	0.178	0.180	0.179
8	0.111	0.158	0.161	0.160
9	0.098	0.143	0.145	0.144
10	0.089	0.130	0.132	0.131

$$\frac{\eta Z_\infty}{Z-Z_\infty} = p \sum_{i=1}^{\nu} x_i C_i(p) \ , \tag{230}$$

$$C_i(p) \equiv \frac{1-\Delta_{id}(p)}{a_i'(\Lambda_i/\eta)} \ . \tag{231}$$

That is, the quantity $\eta Z_\infty/(Z-Z_\infty)$ varies linearly with mole fraction at fixed total pressure, and is nearly directly proportional to pressure at fixed composition (the pressure dependence of Δ_{id} being only of the order of 10%, and η being independent of pressure).

3. Diffusiophoresis

Because of the complexity of the formulas for multicomponent mixtures, we limit ourselves to the example of binary mixtures, and consider the calculation of both $\underset{\sim}{V}_d^0(\text{diff})$ and $\underset{\sim}{V}_{gas}$. From Eqs. (214) and (215) we obtain

$$\underset{\sim}{V}_d^0(\text{diff}) = \left(\frac{n\mathfrak{D}_{12}\,\underset{\sim}{\nabla}x_1}{\rho\quad x_1x_2}\right)\left[\frac{a_1'm_1^{1/2}}{(1-\Delta_{1d})} - \frac{a_2'\tilde{m}_2^{1/2}}{(1-\Delta_{2d})}\right]$$

$$\times\left[\frac{a_1'}{x_1m_1^{1/2}(1-\Delta_{1d})} + \frac{a_2'}{x_2m_2^{1/2}(1-\Delta_{2d})}\right]^{-1}. \qquad (2$$

Three things are worth noting. First, except for the weak composition dependence of $\mathfrak{D}_{12}$, the dependence of $\underset{\sim}{V}_d^0(\text{diff})$ on composition is rather simple — the quantity $[\rho\underset{\sim}{V}_d^0(\text{diff})]^{-1}$ varies linearly with mole fraction, and of course ρ itself also varies linearly with mole fraction. Second, the main variation of $\underset{\sim}{V}_d^0(\text{diff})$ with pressure is as p^{-1} (from the pressure dependence of $\mathfrak{D}_{12}$); the pressure variation caused by the Δ_{id} is small. Third, if the scattering patterns of both molecular species from the particle are the same, then $\underset{\sim}{V}_d^0(\text{diff})$ is proportional to $(m_1^{1/2}-m_2^{1/2})$. This dependence is responsible for the $m^{1/2}$ dependence of fluxes in uniform-pressure diffusion (Graham's law of diffusion), according to the dusty-gas model; this observation is historically responsible for the current formulation of the model.

As an example, we show in Fig. 24 a calculated plot of $\underset{\sim}{V}_d^0(\text{diff})/\mathfrak{D}_{12}\underset{\sim}{\nabla}x_1$ for a diffusing He + Ar mixture as a function of pressure (as measured by Knudsen number). The mean composition of the mixture is equimolar, and the scattering patterns are assumed to be the same for both species. It is seen that the predicted diffusiophoresis is the same in the free-molecule region as in the continuum region, but that

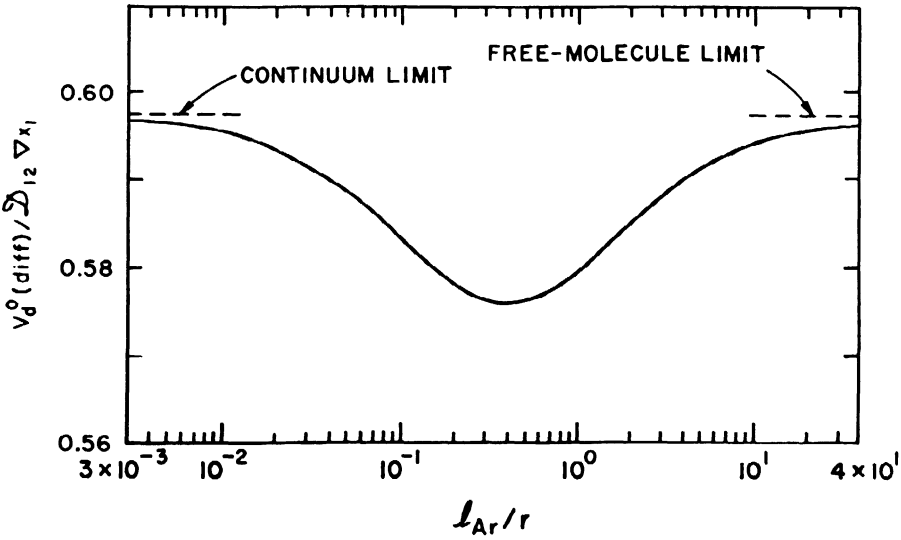

Fig. 24. Calculated diffusiophoretic velocity in a diffusing equimolar He + Ar mixture at 25°C, showing the weak minimum in the pressure dependence. The pressure is measured by the Knudsen number ℓ_{Ar}/r, where ℓ_{Ar} is the mean free path in pure Ar at that pressure.

the weak pressure dependence of the Δ_{id} produces a minimum in the transition region. The maximum effect in this case is only a few percent, and would usually be further obscured by a large value of $\underset{\sim}{V}_{gas}$, which is considered next.

In a diffusing binary gas mixture, the boundary conditions establish the relation between $\underset{\sim}{V}_{gas}$ and x_1. The diffusion fluxes are first found by solution of Fick's law,

$$\underset{\sim}{J}_1 = -n\mathcal{D}_{12}\underset{\sim}{\nabla}x_1 + x_1(\underset{\sim}{J}_1 + \underset{\sim}{J}_2) \ , \tag{233}$$

and then $\underset{\sim}{V}_{gas}$ is calculated as the mass average,

$$\underset{\sim}{V}_{gas} = (m_1\underset{\sim}{J}_1 + m_2\underset{\sim}{J}_2)/\rho \ , \tag{234}$$

where ρ is the mass density.

Although a wide variety of boundary conditions may be possible in principle, only three special cases are usually encountered, as follows:

(1) Equal countercurrent diffusion (ECD). The boundary conditions are arranged so that $\underset{\sim}{J}_1 = -\underset{\sim}{J}_2$. From Eqs. (233) and (234) we then find

$$\underset{\sim}{V}_{gas} = -(n\mathfrak{D}_{12}/\rho)(m_1-m_2)\underset{\sim}{\nabla}x_1 \ . \tag{235}$$

(2) Uniform pressure diffusion (UPD). In this case a net flux $\underset{\sim}{J} = \underset{\sim}{J}_1 + \underset{\sim}{J}_2$ must exist in order to keep the pressure uniform. The individual fluxes must be related to each other according to Graham's law of diffusion

$$-\underset{\sim}{J}_2/\underset{\sim}{J}_1 = (m_1/m_2)^{1/2} \ ,$$

from which Eqs. (233) and (234) yield

$$\underset{\sim}{V}_{gas} = -\left(\frac{n\mathfrak{D}_{12}}{\rho}\right)(m_1m_2)^{1/2}\left(\frac{m_1^{1/2} - m_2^{1/2}}{x_1m_1^{1/2} + x_2m_2^{1/2}}\right)\underset{\sim}{\nabla}x_1 \ . \tag{236}$$

(3) One component stagnant (SD). In SD the moving component of the mixture is usually an evaporating vapor, and the stagnant component is the surrounding atmosphere. If we choose $\underset{\sim}{J}_2 = 0$, then Eqs. (233) and (234) yield

$$\underset{\sim}{V}_{gas} = -\left(\frac{n\mathfrak{D}_{12}}{\rho}\right)\left(\frac{m_1}{1-x_1}\right)\underset{\sim}{\nabla}x_1 \ . \tag{237}$$

As an example, for the case considered in Fig. 24, the calculated values of $V_{gas}/\mathfrak{D}_{12}\nabla x_1$ are -1.64 for ECD, -0.60 for UPD, and -3.64 for SD, compared to the values of about +0.59 for $\underset{\sim}{V}^0(\text{diff})/\mathfrak{D}_{12}\underset{\sim}{\nabla}x_1$ shown in Fig. 24.

Further examples and comparisons of various theoretical formulas for diffusiophoresis are given by Annis, Malinauskas, and Mason [A9].

4. Thermophoresis

Here we consider only single gases. Some discussion of thermophoresis in gas mixtures has been given by Annis and Mason [A7], but virtually no experimental data exist. The numerical calculations show that the coupling term in Eq. (213), which represents the nonadditivity of diffusiophoresis and thermophoresis, is usually less than the thermophoresis term, but may be comparable to it in some cases.

We discuss two points in connection with thermophoresis in a single gas: first, the effect of the thermal conductivity of the particle itself, and second, the effect of finite boundary spacings.

Results on thermophoresis are commonly expressed in terms of the thermophoretic force, which is the force necessary to keep the particle stationary in a (non-flowing) gas having a temperature gradient. From Eq. (212), this force is seen to be given by

$$\underset{\sim}{F}_d(\text{ther}) = - \underset{\sim}{V}_d^0(\text{ther})/Z \ , \tag{238}$$

which is readily evaluated by substitution from Eqs. (224) and (225). Other formulas for $\underset{\sim}{F}_d$(ther) do not cover the complete pressure range, and Hidy and Brock [H9] recommend separate formulas for the transition regime and the near-continuum regime. These formulas include the effect of the thermal conductivity of the aerosol particle, which perturbs the temperature distribution in the gas and hence alters the thermophoretic force. Results are compared in Fig. 25 for two extreme values of particle thermal conductivity: $\lambda_{gas}/\lambda_d = 0$, corresponding to a highly conducting particle, and $\lambda_{gas}/\lambda_d = 1$, corresponding to an insulating particle. It can be seen that the effect of particle thermal conductivity is not enormous, although it is certainly non-negligible, and that the agreement with Eq. (238) is reasonable.

Equation (238) is compared with some experimental results in Fig. 26, including particles of high thermal conductivity (NaCl) as well as of low thermal conductivity (silicone oil and tricresyl phosphate). It should be emphasized that there are no adjustable parameters in the theoretical curve [A7]. The agreement is reasonable except for small ℓ/r, where the discrepancies are perhaps caused partly by neglect of the particle thermal conductivity (see Fig. 25), and partly by the casual treatment of surface accommodation effects in the dusty-gas model.

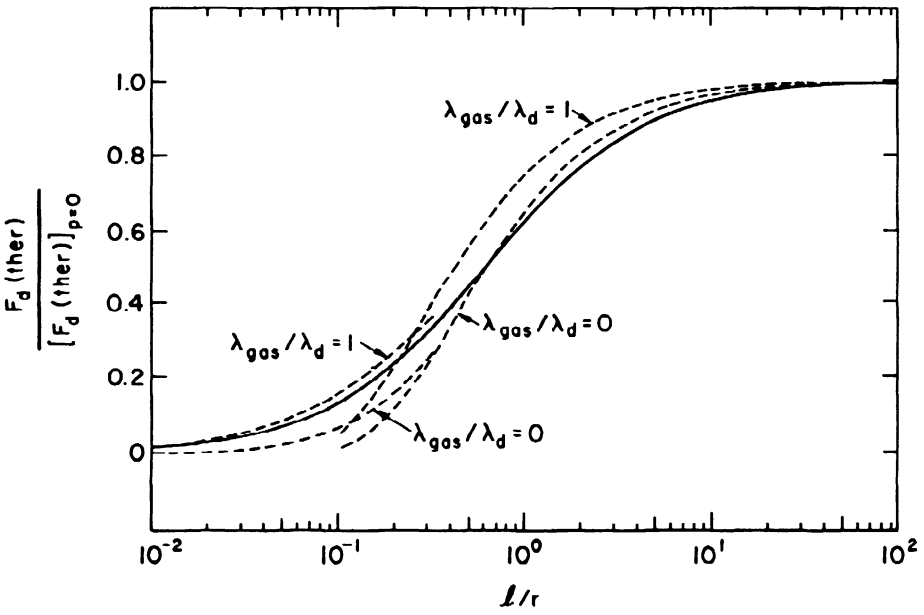

Fig. 25. Comparison of dusty-gas results (solid line) on the thermophoretic force with previous theoretical expressions for the transition region of $\ell/r > 0.2$ [B13], and for the near-continuum region of $\ell/r < 0.2$ [J2], which include the effect of particle thermal conductivity (dashed lines). A conducting particle corresponds to $\lambda_{gas}/\lambda_d = 0$. The plot is normalized by dividing by the free-molecule value of the thermophoretic force.

When the boundary spacing L is not much larger than the mean free path in a gas, three new effects occur: a pressure gradient may be set up, the mass-average velocity of the gas may be changed, and the gas transport coefficients λ_{tr}, $n\mathfrak{D}_{ij}$, and α_{ij} may become pressure dependent. The question now is how these effects might influence the motion of aerosol particles suspended in the gas.

The pressure-gradient effect need not be considered, because it has already been taken into account in the original derivation by being incorporated into $\underset{\sim}{F}_d$. The second effect would have to be considered for a gas mixture, but here we are considering only a single gas. Thus the effect of boundary spacing comes in only through its influence on λ_{tr}. For conduction between parallel plates, the pressure dependence of λ_{tr} is approximately given by [K4]

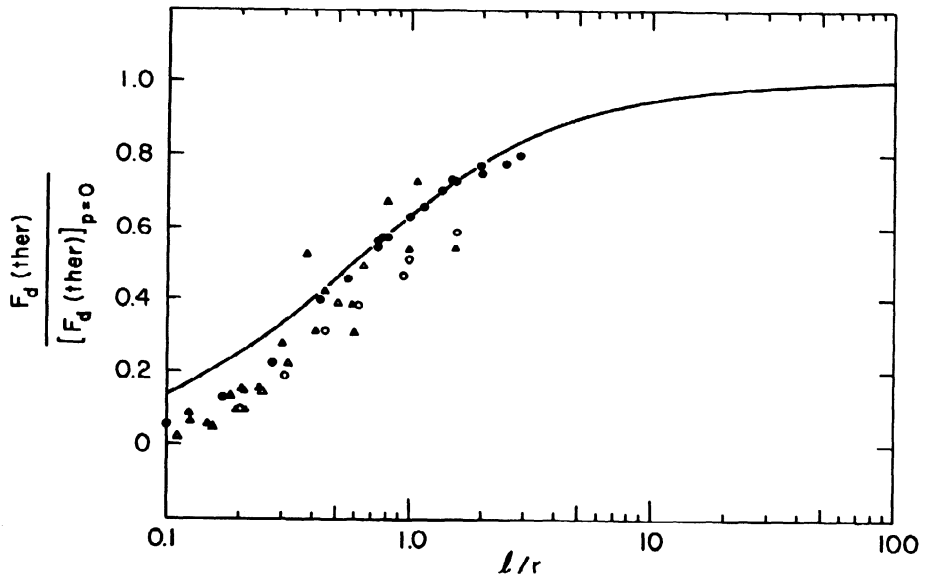

Fig. 26. Comparison of dusty-gas results on the thermophoretic force with some experimental results: ○ NaCl in air [S2], △ NaCl in Ar [J2], ● silicone oil in air [S4], ▲ tricresyl phosphate in air [R4].

$$\lambda_{tr} = \frac{\lambda_{tr}^{\infty}}{1+\beta(\ell/L)} , \tag{239}$$

where λ_{tr}^{∞} is the high-pressure limiting value of λ_{tr}, and β is a constant, approximately equal to 15/4 for perfect thermal accommodation of the gas molecules on collision with the plates.

The effect of this pressure dependence of λ_{tr} on the thermophoretic force is shown in Fig. 27, where the pressure dependence of the force is shown for the three plate spacings of $L/r = \infty$, 100 and 10. The thermophoretic force rises as pressure is decreased, and reaches a limiting plateau value for $L/r = \infty$, but for finite L/r the force reaches a maximum and eventually declines again to zero. This ultimate decline is to be expected, since for finite L only a negligible amount of gas eventually remains between the plates, and so cannot exert any force on the particles.

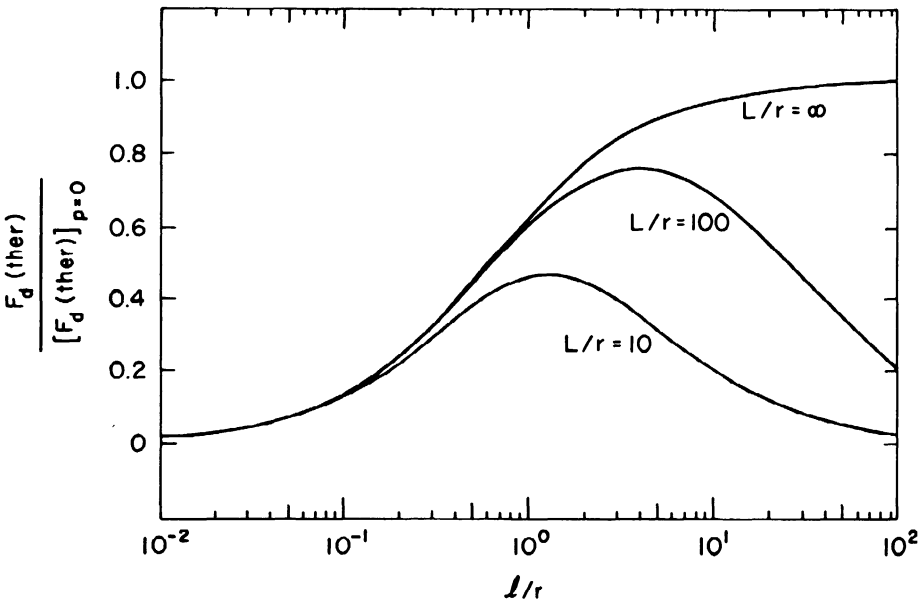

Fig. 27. Thermophoretic force as a function of the particle Knudsen number ℓ/r, for different values of the boundary spacing L.

D. MEMBRANE TRANSPORT

Membrane separation processes have come to be rather widely used in a number of engineering processes, such as desalination of water and the cleanup of waste streams. They are also important in a large number of bioengineering contexts. A minimum requirement for sensible engineering analysis and design would seem to be a knowledge of the fundamental equations that describe membrane transport — that is, the analogues of Fick's law of diffusion, Darcy's law of flow, and Ohm's law of electrical conduction (if charged particles and membranes are involved). The form that these equations should take is not at all obvious, especially when multicomponent systems are involved. Indeed, the fact that there was no general agreement on the problem for the presumably much simpler case of gases in porous media, even as recently as twenty years ago, attests to the difficulties involved. In truth, it was the work on the gas problem and the development of the dusty-gas model that finally gave enough insight to solve the more difficult membrane problem by general statistical-mechanical methods.

The many attempts to formulate transport equations for membranes can be classified into a few simple categories. Because details of membrane structure are often known only poorly, if at all, we might mention first the approaches in which the membrane is regarded as a "black box", and only very general principles are invoked. A well-known example of this approach is Kedem and Katchalsky's treatment of membrane transport according to irreversible thermodynamics [K1, K2], in which linear relations between fluxes and gradients (or finite differences) are assumed and the Onsager reciprocal relations are applied. In a second category, the membrane is represented by some simple but supposedly general model that can be characterized by only a few parameters. A familiar example is the use of generalized "frictional coefficients" by Spiegler, Kedem, and Katchalsky [K1, S12, S13] to represent membrane permeabilities. A variant on this example is the use of the Stefan-Maxwell diffusion equations for membrane transport with "effective" diffusion coefficients, the membrane being taken as a special component that is fixed in space [L4], just as in the dusty-gas model. A less familiar example in this category represents the membrane as an energy barrier, or series of barriers, that must be surmounted by a permeating substance [D3, D7, H11, M7, S3, Z4]. A third category takes quite an opposite approach with models — a very simple special problem is solved in great detail. The hope is to gain enough insight to ferret out essential difficulties or to be able to generalize the results by analogy or heuristic arguments. An example of this approach is the use of hydrodynamic models, in which the membrane is represented as a plate with parallel cylindrical pores, and the solution is a dilute suspension of rigid spheres in a continuum Newtonian fluid [A2, B4, B9]. Another example is the use of gas models in which the membrane is visualized as a collection of dust or aerosol particles held fixed in space [D1, D6, M24, M31]. This, of course, is just the dusty-gas model translated into membrane terminology, and is the approach we wish to emphasize here. Finally, there is the category in which an attempt is made to derive transport equations from some underlying fundamental principles, usually those of statistical mechanics [B5, B6, D5, D6, S9].

It was not always clear what the relationships among these various formulations were, nor even whether they were mutually consistent.

We first indicate how the dusty-gas transport equations can be generalized to apply to arbitrary solutions and membranes. The heuristic arguments for this generalization, while plausible, are basically empirical. We next describe how the results can be derived more rigorously from basic principles of statistical mechanics, using the physical insight obtained from the gas calculations. We then show how the different phenomenological theories are related, and how the dusty-gas theory has been used as a diagnostic probe to find hidden assumptions and omitted terms in these theories. Finally, we indicate briefly how the results can be extended to semipermeable membranes.

1. Generalization of the Dusty-Gas Theory

Generalizations of ideal-solution diffusion equations are usually performed by replacing gradients of concentrations or mole fractions by gradients of chemical potentials, so that the equations will reduce to the correct equilibrium limits in the case of nonideal solutions. Some additional care with concentration and pressure variables is necessary when starting from gas equations, because the absolute concentrations of the components in a gas mixture can be changed by application of pressure, without changing their relative concentrations. This variation is usually unimportant for liquid solutions, which are virtually incompressible. We start with Eq. (120) for the dusty-gas model, and identify the latent chemical potential term by noting that, at constant temperature,

$$d\mu_i = R_o T \, d \ln p_i = R_o T \, d \ln x_i + R_o T \, d \ln p \ , \qquad (240)$$

where μ_i is the chemical potential of species i, p_i is its partial pressure, and x_i its mole fraction. Altogether, we make four types of changes in Eq. (120), as follows [D1, M31]:

(1) The two terms $\nabla \ln (n_i/n)$ and $\nabla \ln p$ are replaced by $\nabla_T \mu_i$, which is the chemical potential gradient of species i in an isothermal system with the same local state variables and concentration and pressure gradients as the real system.

(2) Molecular units are changed to molar units.

(3) The diffusion coefficients are interpreted as phenomenological coefficients within the membrane. In particular, D_{ij} is no longer

assumed to be simply proportional to the free-space diffusion coefficient, as in the relation $D_{ij} = (\varepsilon/q)\mathcal{D}_{ij}$. In addition, the Knudsen diffusion coefficients D_{iK} are replaced by membrane coefficients D_{iM} to avoid the connotation of long mean free paths. The thermal diffusion factors α_{ij} are also rewritten in terms of multicomponent thermal diffusion coefficients D^T_{ij}; this step is just conventional, and has no particular physical significance.

(4) Finally, it is convenient, but not strictly necessary, to drop the fluid-membrane thermal diffusion coefficients D^T_{iM} (which correspond to the gas-dust thermal diffusion factors α'_{id}). These terms give rise to thermal transpiration effects, which are usually already negligible for gases at ordinary densities, and are almost surely negligible for liquids.

Applying the above changes to Eq. (120), we obtain the generalized equations for membrane transport,

$$\sum_{j=1}^{\nu} \frac{c_j}{cD_{ij}} \left(\frac{\underset{\sim}{J}_i}{c_i} - \frac{\underset{\sim}{J}_j}{c_j} \right) + \frac{\underset{\sim}{J}_i}{c_i D_{iM}} + \frac{B_o}{\eta D_{iM}} (\underset{\sim}{\nabla} p - c\underset{\sim}{F}) =$$

$$= -\frac{1}{R_o T} (\underset{\sim}{\nabla}_T \mu_i - \underset{\sim}{F}_i) - \sum_{j=1}^{\nu} \frac{c_j}{cD_{ij}} D^T_{ij} \underset{\sim}{\nabla} \ln T \,, \qquad (241)$$

where c_j is the molar concentration of component j, $c = \Sigma c_j$ is the total molar concentration, and the other symbols have the meanings previously given. For nonideal solutions, the chemical potential gradient would be written as

$$\underset{\sim}{\nabla}_T \mu_i = R_o T \underset{\sim}{\nabla}_T \ln a_i + \bar{V}_i \underset{\sim}{\nabla} p \,, \qquad (242)$$

where a_i is the activity of species i, $\bar{V}_i$ is its partial molar volume (not to be confused with a mean diffusion velocity), and $\underset{\sim}{\nabla} p$ refers to the total hydrostatic pressure. The reference state for the activity should be mole fraction rather than some other composition measure, in order to preserve the symmetry of Eq. (241) with respect to components.

2. Statistical-Mechanical Derivation

The set of relations given by Eqs. (241) affords a complete description of transport across a membrane that does not completely prohibit the passage of any of the species. The more empirical parts of the derivation can be eliminated by starting with the statistical-mechanical Liouville equation for a general system rather than with the Boltzmann equation for a dilute gas. The derivation can be divided into two parts: first, the passage from the Liouville equation to the equations of fluid dynamics for a flowing, diffusing, multicomponent system; second, the passage from the equations of fluid dynamics to the equations of membrane transport. The first part was accomplished by Bearman and Kirkwood [B5, B6] and by Snell, Aranow, and Spangler [S9]. Three essential assumptions are involved:

(1) The fluid can be described in terms of a local state.

(2) The local state deviates only slightly from a local equilibrium state, so that a first-order expansion of the distribution function about this local equilibrium state is valid. The first-order expansion leads to linear transport equations. The choice of the reference equilibrium state is not unique, but it turns out not to be important in the application to membranes.

(3) A quasicontinuum averaging is carried out over macroscopically small, but microscopically large, volume elements of the fluid.

The second part of the derivation was carried out by Mason and Viehland [M19], and generalized somewhat by del Castillo and Mason [D5]. It involves four additional assumptions pertaining specifically to membranes, which are quite similar to the assumptions of the dusty-gas model, as follows:

(4) The membrane is taken as one component of the multicomponent mixture, constrained to be stationary in space, and making no contribution to the mixture viscosity.

(5) A local averaging or coarse-graining is carried out over the open volume of the membrane (e.g., over the cross-sectional area in the case of a cylindrical pore).

(6) In the coarse-grained equations, the terms representing inertial effects are dropped, and those representing viscous effects are assumed to be nonseparative.

(7) The diffusion and thermal diffusion coefficients in the coarse-grained equations are taken to represent diffusion and thermal diffusion within the membrane.

It is interesting to note that extensions of transport equations to dense fluid media, similar in spirit to what has been described above, have been independently carried out for the drying of microporous materials [M1] and for the transport of water through unsaturated soil [S14, S15]. At any rate, application of the above-outlined statistical-mechanical approach leads directly to Eq. (241).

3. Comparison with Phenomenological Equations

A number of phenomenological transport equations for membranes have been proposed at various times; sometimes these have had rather different appearances. Here we briefly compare some of these equations with the results as given by Eq. (241).

a. Onsager (Kedem-Katchalsky) Linear Laws. A set of very general transport equations can be obtained by assuming a linear relation among fluxes $\underset{\sim}{J}_i$ and "forces" $\underset{\sim}{X}_j$,

$$\underset{\sim}{J}_i = \sum_j L_{ij} \underset{\sim}{X}_j \ , \tag{243}$$

where the L_{ij} are Onsager phenomenological coefficients. Onsager showed that, if the $\underset{\sim}{J}_i$ and $\underset{\sim}{X}_j$ are chosen properly, then

$$L_{ij} = L_{ji} \ , \tag{244}$$

now known as the Onsager reciprocal relations [D4]. We wish to show that Eq. (241) has this symmetry property. The demonstration is simple, and depends only on the fact that $D_{ij} = D_{ji}$. We define

$$\underset{\sim}{X}_i \equiv - (\underset{\sim}{\nabla}_T \mu_i - \underset{\sim}{F}_i) - (B_o R_o T/\eta D_{iM}) (\underset{\sim}{\nabla} p - c\underset{\sim}{F}) \ . \tag{245}$$

There should be another "force" corresponding to the $\underset{\sim}{\nabla}$ ln T term in Eq. (241), and another flux corresponding to heat flow, but we ignore these here because we are interested only in mass transfer across membranes, not heat transfer. Inclusion of these additional quantities would lead to the result, through the Onsager reciprocal relations, that the coefficients describing thermal diffusion in the mass-transfer equations were the same as the coefficients describing the diffusion thermoeffect in the

heat-transfer equation. Dropping the $\nabla \ln T$ term then, we can rearrange Eq. (241) into the form

$$\underset{\sim}{X}_i = \sum_j R_{ij} \underset{\sim}{J}_j \ , \tag{246}$$

where

$$R_{ij} = R_o T / c D_{ij} = R_{ji} \ , \qquad i \neq j \ , \tag{247a}$$

$$R_{ii} = (R_o T / c_i)(D_{iM}^{-1} + \sum_{j \neq i} c_j D_{ij}^{-1}) \ . \tag{247b}$$

Clearly R_{ij} is symmetric because D_{ij} is. If we invert Eq. (246) we obtain Eq. (243), and the resulting matrix of coefficients L_{ij} is symmetric because it is the inverse of the symmetric matrix R_{ij}. Thus Eq. (241) obeys the Onsager reciprocal relations, and no symmetry-destroying blunders have been made in the derivation of Eq. (241).

Of more specific interest is the comparison of Eq. (241) with the treatment of membrane transport by the methods of irreversible thermodynamics, as developed by Kedem and Katchalsky [K1, K2]. Their treatment is limited to two-component systems at constant temperature, and a one-dimensional finite-difference approximation is used. The entropy production per unit volume in the membrane, σ, is taken to be

$$T\sigma = -J_1(\Delta\mu_1/\Delta z) - J_2(\Delta\mu_2/\Delta z) \ . \tag{248}$$

If the solution is considered to be dilute and ideal, Eq. (248) can be transformed to the more convenient variables of pressure and concentration,

$$T\sigma = - J_V(\Delta p/\Delta z) - J_D R_o T \ (\Delta c_s/\Delta z) \ , \tag{249}$$

where the new fluxes are defined to be

$$J_V \equiv J_s \bar{V}_s + J_w \bar{V}_w \ , \tag{250}$$

$$J_D \equiv (J_s/\bar{c}_s) - (J_w/c_w) \ . \tag{251}$$

The subscript s stands for the dilute component ("solute"), and the subscript w for the solvent ("water"). The $\bar{V}_s$ and $\bar{V}_w$ are partial molar volumes. Notice that an average concentration $\bar{c}_s$ appears in the definition of J_D, but no average is needed for the c_w because the solvent is present in large excess. The particular kind of average to be used for $\bar{c}_s$ is determined by integrating the differential form of the entropy-production equation across the membrane thickness, and requiring that the overall entropy production be given by Eq. (249); thus

$$T\int_0^{\Delta z} \sigma dz = -\int_{p'}^{p''} J_V dp - R_o T \int_{c_s'}^{c_s''} [(J_s/c_s) - (J_w/c_w)]dc_s \ . \tag{252}$$

This leads to the result

$$\bar{c}_s = (c_s''-c_s')/\ell n(c_s''/c_s') \ , \tag{253}$$

where c_s' and c_s'' are the concentrations on the two sides of the membrane.

The pair of transport equations corresponding to the transformed Eq. (249) is

$$J_V = -\bar{L}_p(\Delta p/\Delta z) - \bar{L}_{pD}R_o T(\Delta c_s/\Delta z) \ , \tag{254}$$

$$J_D = -\bar{L}_{Dp}(\Delta p/\Delta z) - \bar{L}_D R_o T(\Delta c_s/\Delta z) \ , \tag{255}$$

and the corresponding Onsager reciprocal relation is

$$\bar{L}_{pD} = \bar{L}_{Dp} \ . \tag{256}$$

Three questions now present themselves:

(1) How do Eqs. (254) and (255) compare with the statistical-mechanical (or generalized dusty-gas) Eq. (241)?

(2) Is the expression for $\bar{c}_s$ given by Eq. (253) the correct one to use in the transport equation? (It is obviously the correct average for the entropy-production equation.)

(3) What is the range of validity of the reciprocal relation, Eq. (256), when Δc_s and Δp are not vanishingly small?

Regarding the first question, we can see an immediate difficulty — Eq. (241) includes viscous terms, but no viscous dissipation term was included in Eq. (248) for the entropy production. A term like $-J_V(\Delta p/\Delta z)$ should have been included in Eq. (248). However, this was fortuitously compensated by transforming the gradients of chemical potentials to gradients of p and c_s, whereby the empirical coefficient $\bar{L}_p$ then became available to absorb the viscous flow contribution. This can be seen in detail by transforming Eq. (241) to look like Eqs. (254)-(255) and identifying cofficients; the result is, for very small Δp and Δc_s [M19, M24],

$$L_p = (B_o/\eta) + (D_{wM}/cR_oT) \ , \tag{257}$$

$$L_D = (D_{sw}^{-1} + D_{sM}^{-1})^{-1}/c_sR_oT \ , \tag{258}$$

$$L_{Dp} = L_{pD} = \frac{D_{sw}}{R_oT}\left(\frac{\bar{V}_sD_{sM} - \bar{V}_wD_{wM}}{D_{sw} + D_{sM}}\right) \ , \tag{259}$$

where $c_s \ll c_w = c$. As expected, L_p contains two separate contributions, one corresponding to viscous flow (the B_o/η term), and the other to diffusive flow caused by a pressure gradient, giving rise to a gradient of chemical potential. For liquid solutions, where total pressure is not an important variable, the neglect of viscous flow in the irreversible thermodynamics formulation causes no obvious troubles. But for gases, the two terms in L_p have different pressure dependences (c is proportional to p, and the other factors are independent of p), with the result that the neglect of viscous flow leads to grossly erroneous predictions. This has been documented both experimentally and theoretically [D1], although in the equivalent language of the frictional model, which will be discussed later.

The second question, regarding $\bar{c}_s$, is more subtle. If the aim is to give an accurate approximate integration of the transport equations, then another average is suggested by the following argument. When $J_V = 0$, the

concentration profile across the membrane is linear, so that $\bar{c}_s$ in the transport equation should be approximated by

$$\bar{c}_s = \frac{1}{2}(c_s' + c_s'') \quad . \tag{260}$$

This linear average agrees with the logarithmic average of Eq. (253) only in the limit $c_s''/c_s' \to 1$. Comparison with results for the dusty-gas model shows that the linear average is much better than the logarithmic average [M24]. The nature of the difference can best be understood by reference to Fig. 9, where component flux is plotted as a function of total flux for the He + Ar system through a graphite system. For the greatest composition difference ($\Delta x = 1$), the linear average gives the dashed straight line tangent to the correct curve, as shown. The logarithmic average, however, gives a horizontal straight line (not shown) rather than a tangent line [M24]. Another difficulty with the logarithmic average is that it also sacrifices additivity of concentrations, for the sake of keeping the overall entropy production correct, in the case that the solution is not infinitely dilute. That is, $\bar{c}_1 + \bar{c}_2 \neq c$ when Eq. (253) is used for both $\bar{c}_i$, unless $c_i''/c_i' \to 1$ for both components.

In retrospect, it is possible to see what is wrong with the argument leading to the logarithmic average for the concentration. Recall first that irreversible thermodynamics claims to be correct only in the differential formulation (i.e., locally), and the use of a finite-difference expression is an approximation to a correct integration of the differential equations across the membrane thickness. Next, recall that the second law of thermodynamics makes its appearance in the (differential) expression for the entropy production; this expression is used as an aid in writing the transport equations in such a form that the Onsager reciprocal relations will hold true. That is, once the transport equations are written down in differential form, the second law has made its full contribution to the physics of the problem. The question of integrating the transport equations is now a purely mathematical boundary-value problem. The choice of $\bar{c}_s$ is concerned only with this mathematical problem, and the second law has nothing to contribute to this. Thus, choosing $\bar{c}_s$ to give the correct overall entropy production is equivalent to invoking the second law of thermodynamics to carry out

the purely mathematical task of integrating a differential equation, which is obviously inappropriate.

The third question, regarding the range of validity of Eq. (256), i.e., the overall Onsager reciprocal relation, must be referred to experiment or to a detailed kinetic theory like the dusty-gas model. Both experimental and theoretical tests have been carried out [M24], and the results can be most readily understood by reference to Figs. 8 and 10, which represent essentially Eqs. (254) and (255), namely, plots of J_V and J_D vs. Δp at fixed Δc_s. According to the Onsager relation of Eq. (256), the intercept of the J_V vs. Δp curve (Fig. 8) should be proportional to the slope of the J_D vs. Δp curve (Fig. 10). This is indeed the case for the dashed tangent lines shown in the figures, but the nonlinearity of the curves, especially the J_D vs. Δp curve, is so severe that the Onsager relation breaks down over most of the range shown. For instance, for $\Delta p > 0.5$ atm, the apparent value of $\bar{L}_{Dp}$ from the slope of the highest curve in Fig. 10 does not even agree in sign with the corresponding value of $\bar{L}_{pD}$ from Fig. 8. Thus the overall Onsager reciprocal relation has only a very restricted domain of validity in this test case.

b. Frictional Model. The frictional model is based on the idea that, at steady state, the "forces" $\underset{\sim}{X}_i$ driving the transport are balanced by frictional interactions between the various species in the system, including the membrane as one species. The frictional interaction between any two species is taken to be proportional to the difference in their average velocities. With neglect of temperature gradients as before, and with the choice of forces suggested by the Kedem-Katchalsky expression for the entropy production as given by Eq. (248), the resulting transport equations are [K1, K3, S12, S13]

$$\underset{\sim}{X}_i = -(\nabla_T \mu_i - \underset{\sim}{F}_i) = f_{iM} \frac{\underset{\sim}{J}_i}{c_i} + \sum_{j=1}^{\nu} f_{ij} \left(\frac{\underset{\sim}{J}_i}{c_i} - \frac{\underset{\sim}{J}_j}{c_j} \right), \qquad (261)$$

where the average velocities are given by $\underset{\sim}{J}_i/c_i$. The f_{ij} are the so-called frictional coefficients, and f_{iM} is the frictional coefficient between species i and the membrane. The membrane velocity has been set equal to zero in Eq. (261). Comparison with the Onsager Eq. (243) shows that the reciprocal relations require that the f_{ij} be related according to

$$c_i f_{ij} = c_j f_{ji} \ . \tag{262}$$

Comparison with the statistical-mechanical (generalized dusty-gas) Eq. (241) indicates that the viscous terms are entirely missing from the frictional-model equations, so that the frictional coefficients are identified as

$$f_{ij} = c_j R_o T / c D_{ij} \ , \tag{263a}$$

$$f_{iM} = R_o T / D_{iM} \ . \tag{263b}$$

This lack of the viscous terms leads to erroneous predictions, as has been shown by detailed comparisons with the results for gases [D1].

There are a number of reasonable ways to repair the frictional-model equations for their omission of the viscous terms [D1]. The simplest is probably to include them with the original driving forces; that is, to use the expression of Eq. (245) for the $\underset{\sim}{X}_i$ instead of just $-(\underset{\sim}{\nabla}_T \mu_i - \underset{\sim}{F}_i)$, as was done in Eq. (261). Another way, which is less obvious, is to absorb the viscous terms into the frictional coefficients themselves, just as we converted diffusion coefficients into "augmented" coefficients in Chapter II, Section D. We demonstrate this in more detail below, since much the same problem arises with the so-called diffusion model of membrane transport.

c. Diffusion Model. The equations for the diffusion model are formally the same as those for the frictional model, but the interpretation is somewhat different. The basic idea is to take the generalized Stefan-Maxwell equations for multicomponent diffusion in free space, and convert them for membrane diffusion by taking the membrane as a special component that is fixed in space. The result, of course, is just like Eq. (241) with the viscous terms missing, or is like Eq. (261) for the frictional model with frictional coefficients replaced by reciprocal diffusion coefficients [L4]. The difference arises in the interpretation of these diffusion coefficients. It is conceded that viscous effects can play a role in membrane transport, but it is proposed to allow for these by interpreting the diffusion coefficients as "effective" coefficients containing contributions from viscosity. At first sight this appears to be an inconsistent procedure, since it seems difficult to account for

momentum transfer by adjusting the coefficients of mass-transfer equations. Surprisingly, the procedure turns out to be exact, and follows the same sort of arguments as used in Chapter II, Section D, as is briefly indicated below [M19].

We multiply Eq. (241) by c_i/c and sum over all species i. The terms involving D_{ij} sum to zero by symmetry, and the thermal diffusion terms sum to zero because $D^T_{ij} = - D^T_{ji}$. After using the Gibbs-Duhem relation,

$$\sum_{i=1}^{\nu} c_i \underset{\sim}{\nabla}_T \mu_i = \underset{\sim}{\nabla} p \ , \tag{264}$$

we can arrange the results into the form

$$\sum_{i=1}^{\nu} \frac{\underset{\sim}{J}_i}{E_{iM}} = - \frac{1}{R_o T} (\underset{\sim}{\nabla} p - c\underset{\sim}{F}) \ , \tag{265}$$

where

$$E_{iM} = D_{iM} \left(1 + \frac{B_o R_o T}{\eta} \sum_{k=1}^{\nu} \frac{c_k}{D_{kM}} \right) . \tag{266}$$

Equation (265) is the analogue for membranes of the forced-flow generalization of Graham's law of diffusion for gases, Eq. (122). Substituting for $(\underset{\sim}{\nabla} p - c\underset{\sim}{F})$ back into Eq. (241), we obtain, after some algebra, the expression

$$\sum_{j=1}^{\nu} \frac{c_j}{c E_{ij}} \left(\frac{\underset{\sim}{J}_i}{c_i} - \frac{\underset{\sim}{J}_j}{c_j} \right) + \frac{\underset{\sim}{J}_i}{c_i E_{iM}} =$$

$$= - \frac{1}{R_o T} (\underset{\sim}{\nabla}_T \mu_i - \underset{\sim}{F}_i) - \sum_{j=1}^{\nu} \frac{c_j}{c D_{ij}} D^T_{ij} \underset{\sim}{\nabla} \ln T \ , \tag{267}$$

where

$$\frac{1}{E_{ij}} = \frac{1}{D_{ij}} + \frac{cB_oR_oT}{\eta E_{iM}D_{jM}} \quad . \tag{268}$$

This result looks like Eq. (241) without the viscous terms, but with the "augmented" diffusion coefficients E_{ij} and E_{iM}. Thus Eq. (267) has the same form as the Stefan-Maxwell diffusion equations, but some of the coefficients are altered. It also has the same form as the frictional-model Eq. (261), except for the addition of the thermal diffusion terms. The frictional model can therefore be interpreted as giving correct results, provided that the frictional coefficients are re-identified as

$$f_{ij} = c_jR_oT/cE_{ij} = (c_j/c_i)f_{ji} \quad , \tag{269a}$$

$$f_{iM} = R_oT/E_{iM} \quad . \tag{269b}$$

Further comparisons, including the transport equations for hydrodynamic models and the Nernst-Planck equations, are discussed by Mason and Viehland [M19].

4. Semipermeable Membranes

Semipermeable membranes prevent the passage of at least one species in the mixture, and are associated with the phenomenon of osmotic pressure. Although equilibrium osmotic pressure has been understood for many years, the transport aspects of the corresponding nonequilibrium case had never been treated quantitatively, except for the nearly trivial case of very dilute solutions, until sufficient insight was obtained from the dusty-gas model to point to a solution to the problem [D6]. Two fundamental conceptual difficulties arise with transport through semipermeable membranes; both are connected with the notion of osmotic pressure. The first difficulty occurs already with binary solutions, and has to do with the role of the pressure gradient in moving solvent across the membrane. Briefly put, there are two mechanisms for solvent transport, namely diffusion and viscous flow, and the problem is to decide how the presence of an impermeant solute affects each one.

The second difficulty is more subtle, and arises only when there are three or more components in the solution, of which at least two can pass through the membrane. The difficulty now occurs in the meaning of osmotic pressure. The osmotic pressure Π is usually thought of as the

pressure that must be applied to a solution to raise the chemical potential of the solvent to equal that of pure solvent on the other side of a semipermeable membrane. This idea is fine for binary solutions, but can be deceiving if the solvent is a mixture of two or more components. Then the application of pressure will change the chemical potentials of the solvent components by different amounts, unless they fortuitously have the same partial molar volumes. No osmotic equilibrium can be attained in general by the simple application of pressure — some redistribution of the solvent components must also occur.

In order to clarify the physical difficulties involved, we turn to the dusty-gas model and consider the simple case of a mixture of perfect gases, some of which cannot penetrate a membrane represented by a porous barrier. This gas model clarifies the first difficulty mentioned above, but is less clear on the second difficulty because all perfect gases have equal partial molar volumes. However, enough insight is obtained to guide a general statistical-mechanical derivation, along the lines indicated in Section D.2 of this chapter for an open membrane.

We begin by referring to the relevant transport equations for an open membrane — Eq. (120) for gases, or its generalization for membranes, Eq. (241). The important thing to notice is the nature of the driving terms for the transport, which are, for Eq. (241), the terms proportional to $(\nabla p - c\underset{\sim}{F})$, $(\nabla_T \mu_i - \underset{\sim}{F}_i)$, and ∇ ln T. Only the term proportional to $(\nabla p - c\underset{\sim}{F})$, which drives the viscous flow, refers to the mixture as a whole. The other terms drive specific components. Suppose we now add to the gas mixture some gas k that cannot pass the membrane, keeping the total volume constant. Clearly this added component has no effect on the driving terms $(\nabla_T \mu_i - \underset{\sim}{F}_i)$ and ∇ ln T, nor on the total force term $c\underset{\sim}{F}$, which is given by the sum $\Sigma c_i \underset{\sim}{F}_i$. The added component does add to the total pressure term, ∇p, however. A pressure gauge placed across the membrane gives a reading that is influenced by the added gas k. But it is not this pressure-gauge reading that gives the value of ∇p which is driving the viscous flow, it is the sum of the partial pressures of the permeant gases, $\Sigma \nabla p_i$, since the added gas k does not interact with the other gases. An easy way to appreciate this conclusion is to imagine the system at equilibrium. Then the partial pressures of all the permeant gases will be equal on both sides of the membrane, but the external pressure gauge still gives a reading, equal to ∇p_k. This equilibrium

pressure difference corresponds to the osmotic pressure difference in the case of solutions.

In other words, the term ∇p in Eq. (120) for gases and Eq. (241) for general solutions must be modified if an impermeant component is added. For gases, it should be reduced by ∇p_k, and for solutions by $\nabla \Pi$, which can be expressed in terms of chemical potential by the Gibbs-Duhem equation, which yields, for a single impermeant species $\underline{k}$,

$$\nabla p_k + \nabla \Pi = c_k \nabla_T \mu_k \ . \tag{270}$$

That is, only the viscous flow term is affected by the presence of an impermeable solute, and the only change needed is

$$\nabla p - c\underset{\sim}{F} + \nabla p - \nabla \Pi - c\underset{\sim}{F} \ . \tag{271}$$

Although this generalization seems plausible, it is essentially an empirical guess. It is nevertheless sufficient to guide a more rigorous statistical-mechanical derivation.

The statistical-mechanical derivation [D6] proceeds along the lines of Section D.2 of this chapter, and models impermeability by applying external forces to the impermeant species to hold them stationary. Although some care is necessary in formulating a suitable definition of osmotic pressure, the results are quite simple. If we add τ impermeant components to the ν permeable components already present, then Eq. (241) is replaced by

$$\sum_{j=1}^{\nu} \frac{c_j}{cD_{ij}} \left(\frac{\underset{\sim}{J}_i}{c_i} - \frac{\underset{\sim}{J}_j}{c_j} \right) + \frac{\underset{\sim}{J}_i}{c_i D_{iM}} + \frac{B_o}{\eta D_{iM}} (\nabla p - \nabla p_{eq} - c\underset{\sim}{F}) =$$

$$= - \frac{1}{R_o T} (\nabla_T \mu_i - \underset{\sim}{F}_i) - \sum_{j=1}^{\nu} \frac{c_j}{cD_{ij}} D_{ij}^T \nabla \ln T \ , \tag{272}$$

where

$$\nabla p_{eq} \equiv \sum_{k=\nu+1}^{\nu+\tau} c_k \nabla_T \mu_k \ . \tag{273}$$

The term ∇p_{eq} is equal to the conventional osmotic pressure term $\nabla\Pi$ only for a binary mixture. For multicomponent mixtures, the relation is more complex [D6].

The viscous-flow term can also be absorbed into the diffusion coefficients, as was shown for open membranes in Section D.3 of this chapter. In place of Eq. (272) we then obtain

$$\sum_{j=1}^{\nu} \frac{c_j}{cE_{ij}} \left(\frac{\mathbf{J}_i}{c_i} - \frac{\mathbf{J}_j}{c_j} \right) + \frac{\mathbf{J}_i}{c_i E_{iM}} =$$

$$= -\frac{1}{R_o T} (\nabla_T \mu_i - \mathbf{F}_i) - \sum_{j=1}^{\nu} \frac{c_j}{cD_{ij}} D_{ij}^T \nabla \ln T , \tag{274}$$

where the augmented diffusion coefficients are defined as

$$E_{iM} = D_{iM} \left(1 + \frac{B_o R_o T}{\eta} \sum_{j=1}^{\nu} \frac{c_j}{D_{jM}} \right) , \tag{275}$$

$$\frac{1}{E_{ij}} = \frac{1}{D_{ij}} + \frac{cB_o R_o T}{\eta E_{iM} D_{jM}} . \tag{276}$$

The characteristic indicator of osmotic flow, namely the term ∇p_{eq}, has now disappeared. The only clue that Eq. (274) refers to a semipermeable membrane and that the corresponding Eq. (267) refers to an open membrane is that the summations in Eq. (274) run over only the permeant components and omit the impermeant ones, whereas the summations in Eq. (267) run over all components.

In summary, the use of the dusty-gas model has enabled the general problem of membrane transport to be handled in a uniform way.

Chapter V

CONCLUDING REMARKS

The purpose of this monograph has been to present the fundamental theory underlying the dusty-gas model, and to show how its scope can be extended beyond the original problem of gas transport in porous media. Such apparently diverse topics as aerosol motion and solution transport through membranes fit naturally into the general theory that has developed from the dusty-gas model.

Experimental results have been discussed only insofar as they provide tests and illustrations of the theory. Similarly, we have only alluded to the many applications to engineering problems, since a review of engineering applications in any depth would be at least as lengthy as this presentation of fundamentals. In our opinion, it would also be somewhat premature, without there first being a critical exposition of the basic theory, which the present work provides. In short, we anticipate that the present work will serve as a firm base for the systematic application of the theory to a number of engineering problems. Some of the general areas of application are as follows: catalysis and heterogeneous kinetics; separations processes ranging from isotope separation by gaseous diffusion to purification of feed streams by ultrafiltration and reverse osmosis; rarefied gas dynamics, particularly problems involving mean free path effects on boundary conditions; aerosol motion, ranging from pollution and entrainment problems to erosion of turbine blades and other parts of rotating machinery; and bioengineering, especially problems involving membranes and aerosols.

It is obvious that this monograph addresses only part of the problems involved in the above-mentioned applications, and certainly does not in itself provide the complete solution to any engineering problem. That is, the transport equations are only part of the equipment needed to solve real problems; one also needs conservation equations, equations of motion, and some knowledge of boundary conditions and of the structure of the medium, among other things. The transport equations are nevertheless an essential part.

The great virtue of the dusty-gas model, and its generalizations and extensions, is that it manages to separate the transport problem from the problem of the structure of the porous medium (or membrane). Although the results

have considerable generality, there are various restrictions and limitations on them. These have been detailed throughout the text, but it is worthwhile to mention them here again. The following list of restrictions is given in increasing order of seriousness:

(1) Low-velocity flow, in particular small Mach number. This restriction is almost never serious.

(2) For rarefied gases, logarithmic terms in the Knudsen number do not appear. Although fundamental kinetic theory indicates that such terms should appear, there is no experimental evidence that they are significant. This theoretical defect in the model is thus largely only cosmetic.

(3) Molecular diameters much smaller than pore sizes. This restriction can be removed fairly easily by just making all the diffusion coefficients purely phenomenological parameters [D5]. However, the result is that the coefficients are then no longer related to one another, as through $D_{ij} = (\varepsilon/q)\mathcal{D}_{ij}$, and more experiments are needed to characterize the system.

(4) Inertial terms must be negligible in the flow, and turbulence must be absent — in other words, only flows at very low Reynolds numbers can be treated. This restriction is more serious because its removal would require rather drastic modifications, which probably would require recoupling the structure of the medium with the transport equations.

(5) A one-dimensional approximation is used in most applications. This provides great simplification, and usually seems to work amazingly well, but is a potential source of error. There is no great difficulty of principle involved in removing this approximation, but the practical mathematical difficulties may increase enormously.

(6) Details of gas-surface interactions are treated only cursorily. In particular, we have indicated (Chapter II) how to treat surface diffusion only in the limiting case of (a) low surface coverage (i.e., the adsorbed species act independently), and (b) no interaction with other transport mechanisms. The work of L. F. Brown et al. strongly indicates that there are cases where such interactions are important [B7, B8, S11]. In particular, the adsorbed layer may change the boundary conditions for transport in the gas phase. Much further work will be required before surface transport is satisfactorily incorporated into the present transport theory.

In view of the capability of the model to treat diverse phenomena in a unified manner, these limitations are not a serious deficiency; the dusty-gas model is now sufficiently mature and useful to be incorporated into engineering practice.

REFERENCES

A1 Alievskii, M. Ya., and Zhdanov, V. M., Soviet Phys.-JETP 28, 116 (1969) [Zh. Eksp. Teor. Fiz. 55, 221 (1968)]. Transport and relaxation phenomena in polyatomic gas mixtures.

A2 Anderson, J. L., and Quinn, J. A., Biophys. J. 14, 130 (1974). Restricted transport in small pores. A model for steric exclusion and hindered particle motion.

A3 Annis, B. K., Phys. Fluids 14, 269 (1971). Stress induced diffusion in monatomic gases and gas suspensions.

A4 Annis, B. K., J. Chem. Phys. 57, 2898 (1972). Thermal creep in gases.

A5 Annis, B. K., and Malinauskas, A. P., J. Chem. Phys. 54, 4763 (1971). Temperature dependence of rotational collision numbers from thermal transpiration.

A6 Annis, B. K., and Mason, E. A., Phys. Fluids 13, 1452 (1970). Slip and creep in polyatomic gas mixtures.

A7 Annis, B. K., and Mason, E. A., J. Aerosol Sci. 6, 105 (1975). Theory of thermodiffusiophoresis of spherical aerosol particles.

A8 Annis, B. K., Malinauskas, A. P., and Mason, E. A., J. Aerosol Sci. 3, 55 (1972). Theory of drag on neutral or charged spherical aerosol particles.

A9 Annis, B. K., Malinauskas, A. P., and Mason E. A., J. Aerosol Sci. 4, 271 (1973). Theory of diffusiophoresis of spherical aerosol particles and of drag in a gas mixture.

A10 Annis, B. K., Malinauskas, A. P., and Yun, K. S. J. Chem. Phys. 52, 1992 (1970). Composition dependence of the thermal diffusion factor of a dusty gas.

A11 Aranow, R. H., Proc. Natl. Acad. Sci. US 50, 1066 (1963). Periodic behavior in charged membranes and its physical and biological implications.

B1 Bakanov, S. P., and Derjaguin, B. V., Disc. Faraday Soc. 30, 130 (1960). The motion of a small particle in a non-uniform gas mixture.

B2 Barrer, R. M., "Diffusion in and through Solids." Cambridge Univ. Press, London, 2nd ed., 1951.

B3 Barrer, R. M., Appl. Mater. Res. 2, 129 (1963). Diffusion in porous media.

B4 Bean, C. P., in "Membranes: A Series of Advances" (G. Eisenman, ed.) Vol. 1, Chap. 1. Marcel Dekker, New York, 1972. The physics of porous membranes — neutral pores.

B5 Bearman, R. J., J. Chem. Phys. 31, 751 (1959). On the linear phenomenological equations. II. The linear statistical mechanical theory.

B6 Bearman, R. J., and Kirkwood, J. G., J. Chem. Phys. 28, 136 (1958). Statistical mechanics of transport processes. XI. Equations of transport in multicomponent systems.

B7 Bell, W. K., and Brown, L. F., J. Chem. Phys. 59, 3566 (1973). Interactions between a mobile adsorbed phase and diffusing gases in porous media — an experimental study.

B8 Bell, W. K., and Brown, L. F., J. Chem. Phys. 61, 609 (1974). Kinetic theory approach to simultaneous gas and surface diffusion in capillaries.

B9 Brenner, H., and Gaydos, L. J., J. Colloid Interface Sci. 58, 312 (1977). The constrained Brownian movement of spherical particles in cylindrical pores of comparable radius. Modes of the diffusive and convective transport of solute molecules in membranes and porous media.

B10 Breton, J.-P., Phys. Fluids 12, 2019 (1969). Interdiffusion of gases through porous media — effect of molecular interactions.

B11 Breton, J.-P., J. Physique 31, 613 (1970). Étude du transport des gaz a travers les milieux poreux.

B12 Breton, J.-P., and Massignon, D., J. Chim. Phys. 60, 294 (1963). Théorie de la séparation des isotopes par diffusion gazeuse a travers un empilement de spheres.

B13 Brock, J. R., J. Colloid Interface Sci. 23, 448 (1967). The thermal force in the transition region.

B14 Brüche, E., and Littwin, W., Z. Physik 52, 318 (1928). Experimentelle Beiträge zur Radiometerfrage.

B15 Butherus, T. F., and Storvick, T. S., J. Chem. Phys. 60, 321 (1974). Rotational collision numbers and the heat conductivity of nitrogen gas from thermal transpiration measurements to 1250 K.

C1 Carman, P. C., "Flow of Gases through Porous Media." Academic Press, New York, 1956.

C2 Cercignani, C., "Mathematical Methods in Kinetic Theory." Plenum Press, New York, 1969.

C3 Cercignani, C., "Theory and Application of the Boltzmann Equation." Elsevier, New York, 1975.

C4 Cercignani, C., and Pagani, C. D., Phys. Fluids 11, 1395 (1968). Flow of a rarefied gas past an axisymmetric body. I. General remarks.

C5 Cercignani, C., Pagani, C. D., and Bassanini, P., Phys. Fluids 11, 1399 (1968). Flow of a rarefied gas past an axisymmetric body. II. Case of a sphere.

C6 Chapman, S., in "Lectures in Theoretical Physics, Vol. 9C: Kinetic Theory" (W. E. Britten, ed.), pp. 1-13. Gordon and Breach, New York, 1967. The kinetic theory of gases fifty years ago.

C7 Chapman, S., and Cowling, T. G., "The Mathematical Theory of Non-Uniform Gases." Cambridge Univ. Press, London, 3rd ed., 1970.

C8 Chen, O. T., and Rinker, R. G., Chem. Eng. Sci. 34, 51 (1979). Modification of the dusty-gas equation to predict mass transfer in general porous media.

C9 Cowling, T. G., "Molecules in Motion." Hutchinson, London, 1950.

C10 Cussler, E. L., "Multicomponent Diffusion." Elsevier, Amsterdam, 1976.

D1 Daneshpajooh, M. H., Mason, E. A., Bresler, E. H., and Wendt, R. P., Biophys. J. 15, 591 (1975). Equations for membrane transport: Experimental and theoretical tests of the frictional model.

D2 Das Gupta, A., and Storvick, T. S., J. Chem. Phys. 52, 742 (1970). Analysis of the heat conductivity data for polar and nonpolar gases using thermal transpiration measurements.

D3 Davson, H., and Danielli, J. F., "The Permeability of Natural Membranes," pp. 56-58 and Appendix A. Cambridge Univ. Press, London, 1943.

D4 de Groot, S. R., and Mazur, P., "Non-Equilibrium Thermodynamics." North-Holland, Amsterdam, 1962.

D5 del Castillo, L. F., and Mason, E. A., Biophys. Chem. 12, 223 (1980). Statistical-mechnical theory of passive transport through partially sieving or leaky membranes.

D6 del Castillo, L. F., Mason, E. A., and Revercomb, H. E., Biophys. Chem. 10, 191 (1979). Statistical-mechanical theory of passive transport through semipermeable membranes.

D7 del Castillo, L. F., Mason, E. A., and Viehland, L. A., Biophys. Chem. 9, 111 (1979). Energy-barrier models for membrane transport.

D8 Deriagin, B. V., and Bakanov, S. P., Soviet Phys. - Doklady 2, 326 (1957) [Dokl. Akad. Nauk. SSSR 115, 267 (1957)]. Theory of gas flow in a porous body near the Knudsen region. Pseudomolecular flow.

D9 Deriagin, B. V., and Bakanov, S. P., Soviet Phys. - Tech. Phys. 2, 1904 (1957) [Zh. Tekh. Fiz. 27, 2056 (1957)]. Theory of the flow of a gas in a porous material in the near-Knudsen region.

D10 Dorfman, J. R., Kuperman, W. A., Sengers, J. V., and McClure, C. F., Phys. Fluids 16, 2347 (1973). Drag coefficients and the generalized Boltzmann equation.

D11 Dorfman, J. R., van Beijeren, H., and McClure, C. F., Arch. Mech. (Warsaw) 28, 333 (1976). Kinetic theory of hydrodynamic flows.

D12 Dullien, F. A. L., Chem. Eng. J. 10, 1 (1975). Single phase flow through porous media and pore structure.

D13 Dullien, F. A. L., and Scott, D. S., Chem. Eng. Sci. 17, 771 (1962). The flux-ratio for binary counterdiffusion of ideal gases.

D14 Dushman, S., "Scientific Foundations of Vacuum Technique," pp. 277-80. Wiley, New York, 2nd ed., 1962.

E1 Evans, J. W., Canad. J. Chem. Eng. 50, 811 (1972). Gas-solid reactions: The viscous flow term.

E2 Evans, J. W., and Song, S., Canad. J. Chem. Eng. 51, 616 (1973). Gas-solid reactions: The viscous flow term (non-equimolar fluxes).

E3 Evans, R. B. III, Love, L. D., and Mason, E. A., J. Chem. Ed. 46, 423 (1969). Graham's Laws: Simple demonstrations of gases in motion. Part II. Experiments.

E4 Evans, R. B. III, Truitt, J., and Watson, G. M., J. Chem. Eng. Data 6, 522 (1961). Interdiffusion of helium and argon in a large-pore graphite.

E5 Evans, R. B. III, Watson, G. M., and Mason, E. A., J. Chem. Phys. 35, 2076 (1961). Gaseous diffusion in porous media at uniform pressure.

E6 Evans, R. B. III, Watson, G. M., and Mason, E. A., J. Chem. Phys. 36, 1984 (1962). Gaseous diffusion in porous media. II. Effect of pressure gradients.

E7 Evans, R. B. III, Watson, G. M., and Truitt, J., J. Appl. Phys. 33, 2682 (1962). Interdiffusion of gases in a low permeability graphite at uniform pressure.

E8 Evans, R. B. III, Watson, G. M., and Truitt, J., J. Appl. Phys. 34, 2020 (1963). Interdiffusion of gases in a low-permeability graphite. II. Influence of pressure gradients.

F1 Feng, C., and Stewart, W. E., Ind. Eng. Chem. (Fund.) 12, 143 (1973). Practical models for isothermal diffusion and flow of gases in porous solids.

F2 Feng, C., Kostrov, V. V., and Stewart, W. E., Ind. Eng. Chem. (Fund.) 13, 5 (1974). Multicomponent diffusion of gases in porous solids. Models and experiments.

F3 Ferziger, J. H., and Kaper, H. G., "Mathematical Theory of Transport Processes in Gases." Elsevier, New York, 1972.

F4 Fick, A., Ann. Physik 94, 59 (1855); Phil. Mag. 10, 30 (1855). On diffusion.

F5 Frankel, S. P., Phys. Rev. 57, 661 (1940). Elementary derivation of thermal diffusion.

G1 Ganzi, G., and Sandler, S. I., J. Chem. Phys. 55, 132 (1971). Determination of thermal transport properties from thermal transpiration measurements.

G2 Graham, T., Quart. J. Sci. 2, 74 (1829). Reprinted in "Chemical and Physical Researches," pp. 28-35. Edinburgh Univ. Press, Edinburgh, 1876. A short account of experimental researches on the diffusion of gases through each other, and their separation by mechanical means.

G3 Graham, T., Phil. Mag. 2, 175, 269, 351 (1833). Reprinted in "Chemical and Physical Researches," pp. 44-70. Edinburgh Univ. Press, Edinburgh, 1876. On the law of the diffusion of gases.

G4 Graham, T., Phil. Trans. Roy. Soc. 136, 573 (1846). Reprinted in "Chemical and Physical Researches," pp. 88-161. Edinburgh Univ. Press, Edinburgh, 1876. On the motion of gases.

G5 Graham, T., Phil. Trans. Roy. Soc. 139, 349 (1849). Reprinted in "Chemical and Physical Researches," pp. 162-210. Edinburgh Univ. Press, Edinburgh, 1876. On the motion of gases — Part II.

G6 Graham, T., Phil. Trans. Roy. Soc. 153, 385 (1863). Reprinted in "Chemical and Physical Researches," pp. 210-234. Edinburgh Univ. Press, Edinburgh, 1876. On the molecular mobility of gases.

G7 Grew, K. E., and Ibbs, T. L., "Thermal Diffusion in Gases." Cambridge Univ. Press, London, 1952.

G8 Gunn, R. D., and King, C. J., A. I. Ch. E. J. 15, 507 (1969). Mass transport in porous materials under combined gradients of composition and pressure.

H1 Hanley, H. J. M., J. Chem. Phys. 43, 1510 (1965). Experimental verification of the "dusty-gas" theory for thermal transpiration.

H2 Hanley, H. J. M., "Transport Phenomena in Fluids." Marcel Dekker, New York, 1969, pp. 427-432.

H3 Hawtin, P., Chem. Eng. Sci. 26, 1783 (1971). Diffusion and flow of gases in porous solids - a comment on Youngquist's recent review.

H4 Hawtin, P., Dawson, R. W., and Roberts, J., Trans. Instn. Chem. Engrs. 47, T109 (1969). The diffusion of gases through graphite.

H5 Healy, R. N., and Storvick, T. S., J. Chem. Phys. 50, 1419 (1969). Rotational collision number and Eucken factors from thermal transpiration measurements.

H6 Hesse, D., and Köder, J., Chem. Eng. Sci. 28, 807 (1973). Multicomponent diffusion in porous media.

H7 Hewitt, G. F., in "Chemistry and Physics of Carbon, Vol. 1" (P. L. Walker, Jr., ed.), Chap. 2, pp. 73-120. Marcel Dekker, New York, 1965. Gaseous mass transport within graphite.

H8 Hewitt, G. F., and Sharratt, E. W., Nature 198, 952 (1963). Gaseous diffusion in porous media with particular reference to graphite.

H9 Hidy, G. M., and Brock, J. R., "The Dynamics of Aerocolloidal Systems," Pergamon Press, Oxford, 1970.

H10 Hirschfelder, J. O., Curtiss, C. F., and Bird, R. B., "Molecular Theory of Gases and Liquids." Wiley, New York, 2nd printing, 1964.

H11 Hogg, J., and Williams, E. J., Proc. Roy. Soc. Edinburgh A70, 197 (1971-72). A kinetic approach to the irreversible thermodynamics of membrane transport.

H12 Hoogschagen, J., J. Chem. Phys. 21, 2096 (1953). Equal pressure diffusion in porous substances.

H13 Hoogschagen, J., Ind. Eng. Chem. 47, 906 (1955). Diffusion in porous catalysts and adsorbents.

H14 Hopfinger, E. J., and Altman, M., J. Chem. Phys. 50, 2417 (1969). Experimental verification of the dusty-gas theory for thermal transpiration through porous media.

H15 Hutcheon, J. M., Longstaff, B., and Warner, R. K., in "Industrial Carbon and Graphite," pp. 259-271. Society of the Chemical Industry, London, 1958. The flow of gases through a fine-pore graphite.

J1 Jackson, R., "Transport in Porous Catalysts." Elsevier, Amsterdam, 1977.

J2 Jacobsen, S., and Brock, J. R., J. Colloid Sci. 20, 544 (1965). The thermal force on spherical sodium chloride aerosols.

J3 Jenkins, R. E., and Mason, E. A., Phys. Fluids 13, 2478 (1970). Thermal effects in rarefied binary gas mixtures.

K1 Katchalsky, A., and Curran, P. F., "Nonequilibrium Thermodynamics in Biophysics," Chap. 10. Harvard Univ. Press, Cambridge, Mass., 1967.

K2 Kedem, O., and Katchalsky, A., Biochim. Biophys. Acta 27, 229 (1958). Thermodynamic analysis of the permeability of biological membranes to non-electrolytes.

K3 Kedem, O., and Katchalsky, A., J. Gen. Physiol. 45, 143 (1961). A physical interpretation of the phenomenological coefficients of membrane permeability.

K4 Kennard, E. H., "Kinetic Theory of Gases," Chap. 8. McGraw-Hill, New York, 1938.

K5 Knudsen, M., "The Kinetic Theory of Gases," pp. 7-11, 21-25, 33-39. Methuen, London, 3rd ed., 1950.

K6 Kramers, H. A., Nuovo Cimento Suppl. 6, 197 (1949). On the behaviour of a gas near a wall.

K7 Kramers, H. A., and Kistemaker, J., Physica 10, 699 (1943). On the slip of a diffusing gas mixture along a wall.

K8 Kundt, A., and Warburg, E., Ann. Physik 155, 337, 525 (1875); Phil. Mag. 50, 53 (1875). On friction and heat-conduction in rarefied gases.

L1 Lang H., and Loyalka, S. K., Phys. Fluids 13, 1871 (1970). An exact expression for the diffusion slip velocity in a binary gas mixture.

L2 Lang, H., and Loyalka, S. K., Z. Naturforsch. 27a, 1307 (1972). Diffusion slip velocity: Theory and experiment.

L3 Liang, S. C., J. Appl. Phys. 22, 148 (1951). Some measurements of thermal transpiration.

L4 Lightfoot, E. N., "Transport Phenomena and Living Systems," Chap. 3. Wiley, New York, 1974.

L5 Loeb, L. B., "The Kinetic Theory of Gases," Chap. 7. Dover, New York, 3rd ed., 1961.

L6 Loschmidt, J., Sitzber. Akad. Wiss. Wien 52, 395 (1866). Zur Grösse der Luftmolecüle.

L7 Loschmidt, J., Sitzber. Akad. Wiss. Wien 61, 367 (1870). Experimental - Untersuchungen über die Diffusion von Gasen ohne poröse Scheidewände.

L8 Loschmidt, J., Sitzber. Akad. Wiss. Wien 62, 468 (1870). Experimental - Untersuchungen über die Diffusion von Gasen ohne poröse Scheidewände.

L9 Loyalka, S. K., J. Chem. Phys. 48, 5432 (1968). Momentum and temperature-slip coefficients with arbitrary accommodation at the surface.

L10 Loyalka, S. K., Phys. Fluids 12, 2301 (1969). Thermal transpiration in a cylindrical tube.

L11 Loyalka, S. K., Phys. Fluids 14, 21 (1971). Slip in the thermal creep flow.

L12 Loyalka, S. K., Z. Naturforsch. 26a, 964 (1971). The slip problems for a simple gas.

L13 Loyalka, S. K., Phys. Fluids 14, 2291 (1971). Approximate method in the kinetic theory.

L14 Loyalka, S. K., J. Chem. Phys. 55, 4497 (1971). Kinetic theory of thermal transpiration and mechanocaloric effect. I.

L15 Loyalka, S. K., Phys. Fluids 14, 2599 (1971). Velocity slip coefficient and the diffusion slip velocity for a multicomponent gas mixture.

L16 Loyalka, S. K., J. Chem. Phys. 63, 4054 (1975). Kinetic theory of thermal transpiration and mechanocaloric effect. II.

L17 Loyalka, S. K., and Cipolla, J. W. Jr., Phys. Fluids 14, 1656 (1971). Thermal creep slip with arbitrary accommodation at the surface.

L18 Loyalka, S. K., and Storvick, T. S., J. Chem. Phys. 71, 339 (1979). Kinetic theory of thermal transpiration and mechanocaloric effect. III. Flow of a polyatomic gas between parallel plates.

L19 Loyalka, S. K., Petrellis, N., and Storvick, T. S., Phys. Fluids 18, 1094 (1975). Some numerical results for the BGK model: Thermal creep and viscous slip problems with arbitrary accommodation at the surface.

L20 Loyalka, S. K., Storvick, T. S., and Park, H. S., J. Vac. Sci. Technol. 13, 1188 (1976). Poiseuille flow and thermal creep flow in long, rectangular channels in the molecular and transition flow regimes.

M1 MacElroy, J. M. D., and Kelly, J. J., in "Developments in Drying." Science Press, Princeton, N.J., 1979. The kinetics of drying of microporous materials.

M2 Mackey, M. C., Biophys. J. 11, 75 (1971). Kinetic theory model for ion movement through biological membranes. I. Field-dependent conductances in the presence of solution symmetry.

M3 Malinauskas, A. P., J. Chem. Phys. 44, 1196 (1966). Thermal transpiration. Rotational relaxation numbers for nitrogen and carbon dioxide.

M4 Malinauskas, A. P., and Mason, E. A., Trans. Faraday Soc. 67, 2243 (1971). Heats of transport of ideal gases and gas mixtures.

M5 Malinauskas, A. P., Annis, B. K. and Fuson, R. E., unpublished data. Thermal transpiration in binary gas mixtures.

M6 Malinauskas, A. P., Gooch, J. W., Jr., Annis, B. K., and Fuson, R. E., J. Chem. Phys. 53, 1317 (1970). Rotational collision numbers of N_2, O_2, CO, and CO_2 from thermal transpiration measurements.

M7 Manning, G. S., J. Chem. Phys. 49, 2668 (1968). Binary diffusion and bulk flow through a potential-energy profile: A kinetic basis for the thermodynamic equations of flow through membranes.

M8 Marrero, T. R., and Mason, E. A., J. Phys. Chem. Ref. Data 1, 3 (1972). Gaseous diffusion coefficients.

M9 Martin S., Sci. Am., June 1971, p. 124. The Amateur Scientist conducted by C. L. Strong. Experiments with salt fountains and related instabilities in water.

M10 Mason, E. A., J. Chem. Phys. 39, 522 (1963). Molecular relaxation times from thermal transpiration measurements.

M11 Mason, E. A., Am. J. Phys. 35, 434 (1967). Equal pressure diffusion and Graham's law.

M12 Mason, E. A., Phil. J., Trans. Roy. Phil. Soc. Glasgow 7, 99 (1970). Thomas Graham and the kinetic theory of gases.

M13 Mason, E. A., and Block, B., Ann. Phys. (N.Y.) 37, 7 (1966). Molecular inelastic collision cross sections from the radiometer force.

M14 Mason, E. A., and Chapman, S., J. Chem. Phys. 36, 627 (1962). Motion of small suspended particles in non-uniform gases.

M15 Mason, E. A., and Evans, R. B. III, J. Chem. Ed. 46, 358 (1969). Graham's laws: Simple demonstrations of gases in motion. Part I. Theory.

M16 Mason, E. A., and Kronstadt, B., J. Chem. Ed. 44, 740 (1967). Graham's laws of diffusion and effusion.

M17 Mason, E. A., and Malinauskas, A. P., J. Chem. Phys. 41, 3815 (1964). Gaseous diffusion in porous media. IV. Thermal diffusion.

M18 Mason, E. A., and Marrero, T. R., Adv. Atom. Mol. Phys. 6, 155 (1970). The diffusion of atoms and molecules.

M19 Mason, E. A., and Viehland, L. A., J. Chem. Phys. 68, 3562 (1978). Statistical-mechanical theory of membrane transport for multicomponent systems: Passive transport through open membranes.

M20 Mason, E. A., and Wright, P. G., Contemp. Phys. 12, 179 (1971). Graham's laws.

M21 Mason, E. A., Evans, R. B. III, and Watson, G. M., J. Chem. Phys. 38, 1808 (1963). Gaseous diffusion in porous media. III. Thermal transpiration.

M22 Mason, E. A., Malinauskas, A. P., and Evans, R. B. III, J. Chem. Phys. 46, 3199 (1967). Flow and diffusion of gases in porous media.

M23 Mason, E. A., Munn, R. J., and Smith, F. J., Adv. Atom. Mol. Phys. 2, 33 (1966). Thermal diffusion in gases.

M24 Mason, E. A., Wendt, R. P., and Bresler, E. H., J. Chem. Soc. Faraday II 68, 1938 (1972). Test of the Onsager relation for ideal gas transport in membranes.

M25 Maxwell, J. C., Phil. Mag. 20, 21 (1860). Reprinted in "Scientific Papers," Vol. 1, pp. 392-409, Dover, New York, 1962. Illustrations of the dynamical theory of gases. Part II. On the process of diffusion of two or more kinds of moving particles among one another.

M26 Maxwell, J. C., Phil. Trans. Roy. Soc. 157, 49 (1867). Reprinted in "Scientific Papers," Vol. 2, pp. 26-78. Dover, New York, 1962. On the dynamical theory of gases.

M27 Maxwell, J. C., Nature 8, 537 (1873). Reprinted in "Scientific Papers," Vol. 2, pp. 343-350. Dover, New York, 1962. On Loschmidt's experiments on diffusion in relation to the kinetic theory of gases.

M28 Maxwell, J. C., Phil. Trans. Roy. Soc. 170, 231 (1879). Reprinted in "Scientific Papers," Vol. 2, pp. 681-712. Dover, New York, 1962. On stresses in rarefied gases arising from inequalities of temperature.

M29 McCarty, K. P., and Mason, E. A., Phys. Fluids 3, 908 (1960). Kirkendall effect in gaseous diffusion.

M30 McConville, G. T., Taylor, W. L., and Watkins, R. A., J. Chem. Phys. 53, 912 (1970). Analysis of the determination of rotational relaxation numbers from thermal transpiration.

M31 Mehta, G. D., Morse, T. F., Mason, E. A., and Daneshpajooh, M. H., J. Chem. Phys. 64, 3917 (1976). Generalized Nernst-Planck and Stefan-Maxwell equations for membrane transport.

M32 Miller, G. A., and Bernstein, R. B., J. Phys. Chem. 63, 710 (1959). Gas-kinetic collision diameters of the halomethanes.

M33 Miller, L., and Carman, P. C., Nature 186, 549 (1960). Analogy to the Kirkendall effect in the gas phase.

M34 Miller, L., Spurling, T. H., and Mason, E. A., Phys. Fluids 10, 1809 (1967). Instabilities in ternary diffusion.

M35 Millikan, R. A., Phys. Rev. 22, 1 (1923). The general law of fall of a small spherical body through a gas, and its bearing upon the nature of molecular reflection from surfaces.

M36 Monchick, L., and Mason, E. A., Phys. Fluids 10, 1377 (1967). Free-flight theory of gas mixtures.

M37 Monchick, L., Munn, R. J., and Mason, E. A., J. Chem. Phys. 45, 3051 (1966); errata 48, 3344 (1968). Thermal diffusion in polyatomic gases: A generalized Stefan-Maxwell equation.

M38 Monchick, L., Pereira, A. N. G., and Mason, E. A., J. Chem. Phys. 42, 3241 (1965). Heat conductivity of polyatomic and polar gases and gas mixtures.

M39 Monchick, L., Sandler, S. I., and Mason, E. A., J. Chem. Phys. 49, 1178 (1968). Thermal diffusion in polyatomic gases: Nonspherical interactions.

M40 Monchick, L., Yun, K. S., and Mason, E. A., J. Chem. Phys. 39, 654 (1963). Formal kinetic theory of transport phenomena in polyatomic gas mixtures.

M41 Muckenfuss, C., J. Chem. Phys. 59, 1747 (1973). Stefan-Maxwell relations for multicomponent diffusion and the Chapman-Enskog solution of the Boltzmann equations.

N1 Noyes, A. A., and Sherrill, M. S., "A Course of Study in Chemical Principles," p. 151. Macmillan, New York, 2nd ed., 1938.

O1 Omata, H., and Brown, L. F., A. I. Ch. E. J. 18, 967 (1972). Using the dusty gas diffusion equation in catalyst pores smaller than 50 Å radius.

P1 Partington, J. R., "An Advanced Treatise on Physical Chemistry. Vol. I: Fundamental Principles. The Properties of Gases," p. 903. Longmans, Green, New York, 1949.

P2 Patel, P. V., and Butt, J. B., Ind. Eng. Chem. (Process Des. Dev.) 14, 298 (1975). Multicomponent diffusion in porous catalysts.

P3 Present, R. D., "Kinetic Theory of Gases," p. x. McGraw-Hill, New York, 1958.

P4 Present, R. D., and de Bethune, A. J., Phys. Rev. 75, 1050 (1949). Separation of a gas mixture flowing through a long tube at low pressure.

R1 Remick, R. R., and Geankoplis, C. J., Ind. Eng. Chem. (Fund.) 12, 214 (1973). Binary diffusion of gases in capillaries in the transition region between Knudsen and molecular diffusion.

R2 Remick, R. R., and Geankoplis, C. J., Chem. Eng. Sci. 29, 1447 (1974). Ternary diffusion of gases in capillaries in the transition region between Knudsen and molecular diffusion.

R3 Reynolds, O., Phil. Trans. Roy. Soc. B170, 727 (1879). On certain dimensional properties of matter in the gaseous state.

R4 Rosenblatt, P., and La Mer, V. K., Phys. Rev. 70, 385 (1946). Motion of a particle in a temperature gradient; thermal repulsion as a radiometer phenomenon.

R5 Rothfeld, L. B., A. I. Ch. E. J. 9, 19 (1963). Gaseous counterdiffusion in catalyst pellets.

R6 Ruckstuhl, A., J. Chem. Ed. 28, 594 (1951). Thomas Graham's study of the diffusion of gases.

S1 Satterfield, C. N., "Mass Transfer in Heterogeneous Catalysis." M.I.T. Press, Cambrige, Mass., 1970.

S2 Schadt, C. F., and Cadle, R. D., J. Phys. Chem. 65, 1689 (1961). Therma forces on aerosol particles.

S3 Schlögl, R., Quart. Rev. Biophys. 2, 305 (1969). Non-linear transport behaviour in very thin membranes.

S4 Schmitt, K. H., Z. Naturforsch. 14a, 870 (1959). Untersuchungen an Schwebstoffteilehen in Temperaturfeld.

S5 Scott, D. S., and Cox, K. E., Canad. J. Chem. Eng. 38, 201 (1960). Temperature dependence of the binary diffusion coefficient of gases.

S6 Scott, D. S., and Dullien, F. A. L., A. I. Ch. E. J. 8, 113 (1962). Diffusion of ideal gases in capillaries and porous solids.

S7 Scott, D. S., and Dullien, F. A. L., A. I. Ch. E. J. 8, 293 (1962). The flow of rarefied gases.

S8 Smith, J. M., "Chemical Engineering Kinetics." McGraw-Hill, New York, 1970.

S9 Snell, F. M., Aranow, R., and Spangler, R. A., J. Chem. Phys. 47, 4959 (1967). Statistical-mechanical derivation of the partial molecular stress tensors in isothermal multicomponent systems.

S10 Sone, Y., Phys. Fluids 15, 1418 (1972). Flow induced by thermal stress in rarefied gas.

S11 Spencer, J. L., and Brown, L. F., J. Chem. Phys. 63, 2882 (1975). Experimental observations of gas phase - adsorbed phase interactions during counterdiffuion in porous media.

S12 Spiegler, K. S., Trans. Faraday Soc. 54, 1408 (1958). Transport processes in ionic membranes.

S13 Spiegler, K. S., and Kedem, O., Desalination 1, 311 (1966). Thermodynamics of hyperfiltration (reverse osmosis): Criteria for efficient membranes.

S14 Sposito, G., Water Resources Res. 14, 474 (1978). The statistical-mechanical theory of water transport through unsaturated soil. 1. The conservation laws.

S15 Sposito, G., Water Resources Res. 14, 479 (1978). The statistical-mechanical theory of water transport through unsaturated soil. 2. Derivation of the Buckingham-Darcy flux law.

S16 Stefan, J., Sitzber. Akad. Wiss. Wien 63, 63 (1871). Über das Gleichgewicht und die Bewegung, insbesondere die Diffusion von Gasgemengen.

S17 Stefan, J., Sitzber. Akad. Wiss. Wien 65, 323 (1872). Über die dynamische Theorie der Diffusion der Gase.

S18 Storvick, T. S., Park, H. S., and Loyalka, S. K., J. Vac. Sci. Technol. 15, 1844 (1978). Thermal transpiration: A comparison of experiment and theory.

S19 Szekely, J., Evans, J. W., and Sohn, H. Y., "Gas-Solid Reactions." Academic Press, New York, 1976.

T1 Tao, J. C., Ganzi, G. C., and Sandler, S. I., J. Chem. Phys. 56, 3789 (1972). Determination of thermal transport properties from thermal transpiration measurements. II.

T2 Tao, J. C., Revelt, W., and Sandler, S. I., J. Chem. Phys. 60, 4475 (1974). Determination of thermal transport properties from thermal transpiration measurements. III. Polar gases.

T3 Thiele, E. W., Am. Sci. 55, 176 (1967). The effect of grain size on catalyst performance.

T4 Turner, J. S., Ann. Rev. Fluid Mech. 6, 37 (1974). Double-diffusive phenomena.

T5 Tyndall, J., Proc. Roy. Inst. 6, 3 (1870). On dust and disease.

V1 Viehland, L. A., and Mason, E. A., J. Aerosol Sci. 8, 381 (1977). Phoresis of spherical particles in multicomponent gas mixtures.

W1 Waldmann, L., Z. Naturforsch. 14a, 589 (1959). Über die Kraft eines inhomogenen Gases auf kleine suspendierte Kugeln.

W2 Waldmann, L., and Schmitt, K. H., Z. Naturforsch. 16a, 1343 (1961). Über das bei der Gasdiffusion auftretende Druckgefälle.

W3 Weber, S., Kgl. Danske Videnskab. Selskab., Mat.-Fys. Medd. 28, No. 2 (1954). Über den Zusammenhang zwischen der Lamineren Strömung der Reinen Gase durch Rohre und dem Selbstdiffusionkoeffizienten. [Transl. by R. Ash and J. B. Sykes, AERE-Trans 946, Harwell (1963).] The connection between the laminar flow of pure gases through tubes and the self-diffusion coefficient.

W4 Weisz, P. B., Science 179, 433 (1973). Diffusion and chemical transformation. An interdisciplinary excursion.

W5 Weisz, P. B., and Prater, C. D., Adv. Catalysis 6, 143 (1954). Interpretation of measurements in experimental catalysis.

W6 Wendt, R. P., Mason, E. A., and Bresler, E. H., Biophys. Chem. 4, 237 (1976). Effect of heteroporosity on flux equations for membranes.

W7 Wheeler, A., Adv. Catalysis 3, 249 (1951). Reaction rates and selectivity in catalyst pores.

W8 Wicke, E., Kolloid Z. 93, 129 (1940). Unterschungen über Ad- und Desorptionsvorgange in körnigen, durchströmten Adsorberschichten.

W9 Wicke, E., and Hugo, P., Z. phys. Chem. 28, 401 (1961). Gleitungserscheinungen bei der Gasdiffusion.

W10 Wicke, E., and Kallenbach, R., Kolloid Z. 97, 135 (1941). Die Oberflächendiffusion von Kohlendioxyd in aktiven Kohlen.

W11 Williams, M. M. R., "Mathematical Methods in Particle Transport Theory," Wiley-Interscience, New York, 1971.

W12 Williams, M. M. R., J. Phys. D6, 759 (1973). On the motion of small spheres in gases. IV. Diffusion coefficient of porous membranes.

W13 Wong, R. L., and Denny, V. E., Chem. Eng. Sci. 30, 709 (1975). Diffusion, flow, and heterogeneous reaction of ternary mixtures in porous catalytic media.

W14 Wong, R. L., Hubbard, G.L., and Denny, V. E., Chem. Eng. Sci. 31, 541 (1976). Effects of temperature and pressure gradients on catalyst pellet effectiveness factors - I. $\Sigma\nu_i = 0$.

W15 Wright, P. G., J. Chem. Soc. Faraday II 68, 1951 (1972). Remarks on the Stefan-Maxwell equations for diffusion in a dusty gas.

W16 Wright, P. G., Ber. Bunsen-Ges. phys. Chem. 79, 210 (1975). Thermal transpiration in a dissociating gas.

Y1 Youngquist, G. R., Ind. Eng. Chem. 62 (No. 8), 52 (1970). Diffusion and flow of gases in porous solids.

Z1 Zhdanov, V. M., Soviet Phys. - Tech. Phys. 12, 134 (1967). [Zh. Tekh. Fiz. 37, 192 (1967)]. Theory of slip at the boundary of a gaseous mixture.

Z2 Zhdanov, V. M., Soviet Phys. - JETP 26, 1187 (1968). [Zh. Eksp. Teor. Fiz. 53, 2099 (1967)]. The kinetic theory of a polyatomic gas.

Z3 Zhdanov, V., Kagan, Yu., and Sazykin, A., Soviet Phys. - JETP 15, 596 (1962). [Zh. Eksp. Teor. Fiz. 42, 857 (1962)]. Effect of viscous transfer of momentum on diffusion in a gas mixture.

Z4 Zwolinski, B. J., Eyring, H., and Reese, C. E., J. Phys. Colloid Chem. 53, 1426 (1949). Diffusion and membrane permeability.

LIST OF SYMBOLS

Special notes: The subscripts i and j usually denote species being transported through a porous medium or membrane, whereas the subscript d denotes "dust." For membrane transport, the subscript M denotes membrane, and the subscripts s and w denote solute and solvent ("water"), respectively.

A - cross sectional area

A_o - mixture Knudsen coefficient, Eq. (159a)

A_1 - mixture transport coefficient, Eq. (159b)

A_2 - mixture transport coefficient, Eq. (159c)

A_{ij}^* - dimensionless ratio of collision integrals

a - numerical constant, Eq. (146a)

a_i - activity of species i, Eq. (242)

a_{ij} - matrix element, Eqs. (184)

a' - radiometer force constant, Eq. (210)

a_i' - dimensionless parameter, Eq. (220)

B_o - viscous flow parameter, Eq. (11)

B_i - thermal diffusion factor parameter, Eq. (193)

B_{ij}^* - dimensionless ratio of collision integrals

b - numerical constant, Eq. (146b)

b_i - thermal diffusion factor parameter, Eq. (191)

b' - radiometer force constant, Eq. (210)

b_i' - dimensionless parameter, Eq. (221)

C_i - parameter defined by Eq. (231)

C_{ij}^* - dimensionless ratio of collision integrals, Eq. (44)

c - total molar concentration

c_i - molar concentration of component i

c_1 - numerical constant, Eq. (146c)

c_2 - numerical constant, Eq. (146d)

c' - radiometer force constant

c_i' - dimensionless parameter, Eq. (222)

$\bar{c}_s$ - average molar concentration of solute

$(\bar{c}_i)_{int}$ - internal specific heat per gram, Eq. (47)

D_i - effective diffusion coefficient, Eq. (29)

D_{ij} - concentration diffusion coefficient for transport in a porous medium, Eq. (20)

D_{iK} - Knudsen diffusion coefficient, Eq. (5) and Eq. (61)

D_{iM} - membrane diffusion coefficient

D_{iS} - surface diffusion coefficient, Eq. (21)

D_{ij}^T - multicomponent thermal diffusion coefficient

$D_{eff}^{(i)}$ - effective multicomponent diffusion coefficient, Eq. (214)

$\langle D_K \rangle$ - average Knudsen diffusion coefficient for a mixture, Eq. (180)

$\mathfrak{D}_{ij}$ - concentration diffusion coefficient in free space, Eqs. (13)

$[\mathfrak{D}_{ij}]_1$ - first approximation for $\mathfrak{D}_{ij}$, Eq. (41)

$(\mathfrak{D}_{ii})_{int}$ - diffusion coefficient for internal energy, Eq. (47)

$\underset{\sim}{d}_i$ - gradient term, Eq. (39)

$\bar{E}_i$ - effective augmented diffusion coefficient, Eq. (134)

E_{ij} - augmented diffusion coefficient, Eq. (126)

E_{iK} - augmented Knudsen diffusion coefficient, Eq. (125)

$\underset{\sim}{F}_i$ - external force on species i

$F_d(ther)$ - thermophoretic force, Eq. (238)

f - fraction of gas molecules scattered elastically and diffusely from a surface, Eq. (65)

f_{ij} - frictional coefficient, Eq. (261)

f_{tr} - translational Eucken factor, Eq. (172)

H_{ik} - determinant element for calculation of the viscosity coefficient Eqs. (53) and (54)

J - total flux

J_K - free molecule or Knudsen flux, Eq. (2)

J_V - volume flux, Eq. (250)

J_D - average relative diffusive flux, Eq. (251)

J_{iD} - diffusive flux of species i, Eqs. (13)

J_{iS} - surface flux, Eq. (21)

J_{rel} - relative diffusive flux, Eq. (136)

J_{visc} - viscous flux, Eq. (11)

$j_i^{(k)}$ - flux of species $\underline{i}$ in a single capillary of type $\underline{k}$, Eq. (89)

K_o - Knudsen flow parameter or permeability coefficient, Eq. (6)

$\bar{K}_i$ - mean permeability coefficient of a pure gas, Eq. (144)

$\bar{K}_{ij}$ - mean permeability coefficient of a binary gas mixture, Eq. (129)

$\bar{K}_{min}$ - Knudsen permeability minimum, Eq. (151)

$[K_o]_1$ - first approximation to K_o, Eq. (82)

k_o - shape factor

k_B - Boltzmann's constant

L - length parameter

L_{ij} - Onsager phenomenological coefficient

L_{eff} - effective length

ℓ - mean free path, Eq. (174)

m - molecular mass

$\bar{m}$ - mean molecular mass, Eq. (40)

$\langle m^n \rangle$ - average n-th power of the mass, Eq. (204)

n - molecular density, Eq. (2)

P_i - diffusive permeability coefficient, Eq. (89)

$P_{\eta i}$ - dimensionless viscous flow factor, Eq. (189)

$\bar{P}_{12}$ - mean mixed diffusion coefficient, Eq. (138)

p - total pressure

p_i - partial pressure of species $\underline{i}$

p_{min} - pressure at Knudsen permeability minimum, Eq. (150)

p_{max} - pressure at maximum Δp

p^* - dimensionless pressure, Eq. (170)

$\bar{p}$ - average pressure

Q_k - flow rate of species $\underline{k}$ through a porous medium, Eq. (110)

Q^* - heat of transport, Eq. (178)

q - tortuosity

R - dust particle radius

R_o - ideal gas constant

R_{ij} - inverse Onsager coefficients of mass transport, Eq. (247)

R_o' - modified Stokes radius, Eq. (206)

$\bar{R}_{12}$ - mean relative diffusive permeability coefficient, Eq. (131)

r - capillary radius or particle radius

S_d - geometric contant characteristic of dust particles, Eq. (64)

s - Sutherland constant

T - absolute temperature

V - flow speed

V_o - mass average velocity of a gas mixture, Eq. (194)

V_d - aerosol velocity, Eq. (211)

V_{gas} - local mass-average velocity of a gas, Eq. (211)

V_{oz} - z-directional component of the mass average velocity

V_d^o - aerosol velocity in a stationary gas, Eq. (212)

$\bar{V}$ - molar volume

$\bar{V}_i$ - partial molar volume, Eq. (242)

$\bar{V}_{iD}$ - average diffusion velocity, Eq. (34)

$V_d^o(coupl)$ - coupled phoresis velocity, Eq. (213)

$V_d^o(diff)$ - diffusiophoresis velocity, Eq. (213)

$V_d^o(ther)$ - thermodiffusiophoresis velocity, Eq. (213)

$\bar{v}$ - mean molecular speed, Eq. (3)

w - probability factor, Eq. (2)

X_j - generalized driving force

x_i - mole fraction

Y - reduced flux, Eq. (98)

Z - particle mobility, Eq. (212)

Z_∞ - high pressure limiting value of Z

z - distance parameter

Greek Symbols

α_i - dimensionless flux variable, Eq. (96)

α_{ij} - thermal diffusion factor

α_{iL} - thermal diffusion factor of a Lorentz gas, Eqs. (69) and (73)

α_{iR} - thermal diffusion factor of a Rayleigh gas, Eqs. (69) and (74)

$\alpha_{12}(\text{eff})$ - effective thermal diffusion factor, Eq. (186)

$\alpha_{12}(\infty)$ - continuum limit of $\alpha_{12}(\text{eff})$, Eq. (190)

$(\alpha_{ij})_{tr}$ - translational component of α_{ij}, Eq. (43)

$(\alpha_{ij})_{int}$ - internal component of α_{ij}, Eq. (43)

β - numerical constant, Eq. (239)

β_i - diffusive drift factor, Eq. (141)

β_i^o - dimensionless permeability coefficient, Eq. (97)

γ_i - relative transport coefficient, Eq. (31)

Δ_{ij} - factor characteristic of higher approximations for $\mathfrak{D}_{ij}$, Eq. (42)

Δ_i^{λ} - correction to $(\lambda_{ii})_{tr}$ due to inelastic collisions, Eq. (47)

δ - correction to $[K_o]_1$, Eq. (82)

δ_i - relative transport coefficient, Eq. (30)

ϵ - porosity, Eq. (75)

ϵ_i - relative transport coefficient, Eq. (135)

ϵ/q - porosity-tortuosity factor, Eq. (20)

ζ_{ii} - collision number for an interchange of internal and translational energy, Eq. (47)

η - viscosity coefficient of gas mixture

η_i - partial viscosity

η_{ii} - viscosity coefficient of pure gas, Eq. (46)

θ_{id} - augmented thermal diffusion factor, Eq. (127)

Λ_i - pressure scale factor, Eq. (217)

Λ_{ik} - determinant element for the calculation of the translational component of thermal conductivity, Eqs. (49) and (50)

λ_{tr} - translational component of the thermal conductivity of a gas mixture, Eq. (45)

λ_{tr}^{∞} - high pressure limiting value of λ_{tr}

$(\lambda_i)_{tr}$ - partial contribution to λ_{tr} by species $\underline{i}$, Eqs. (45) and (48)

$(\lambda_{ii})_{tr}$ - translational thermal conductivity of pure gas i, Eq. (46)

μ_i - chemical potential of species $\underline{i}$, Eq. (240)

μ_{ij} - reduced mass, Eq. (41)

ν - number of species in a gas mixture

ν_k - number of pores of type $\underline{k}$ per unit area, Eq. (90)

ξ_i - gas-surface scattering parameter, Eq. (68)

Π - osmotic pressure

π_g - pressure scale factor for gas-dust thermal diffusion in a pure gas, Eq. (71)

π_i - pressure scale factor for species $\underline{i}$ in a gas mixture, Eq. (71)

π_{Di} - pressure scale factor, Eq. (153b)

$\pi_{\eta i}$ - pressure scale factor, Eq. (147)

π_i' - pressure scale factor similar to π_i, Eq. (72)

π_i^* - reduced pressure scale factor, Eq. (171)

$\langle\pi_\eta\rangle$ - pseudo pure gas pressure scale factor, Eq. (182)

ρ - mass density

σ - entropy production per unit volume, Eq. (248)

σ_r - pore size distribution parameter, Eq. (84)

σ_{ij} - molecular distance parameter, Eq. (41)

σ_{diff} - diffusive slip coefficient, Eq. (195)

σ_{ther} - thermal creep coefficient, Eq. (195)

σ_{visc} - viscous slip coefficient, Eq. (195)

σ'_{ther} - modified thermal creep coefficient, Eq. (201)

σ'_{visc} - modified viscous slip coefficient, Eq. (197)

σ''_{ther} - modified thermal creep coefficient, Eq. (202)

τ - reduced radiometer torque, Eq. (209)

Φ - flux scale factor, Eq. (153a)

$\phi(\alpha_k)$ - dimensionless flux function, Eq. (100)

$\Omega_{ij}^{(m,n)*}$ - transport collision integral, Eq. (41)